Escola d'Enginyeria

Departament d'Enginyeria Química, Biològica i Ambiental

Developing and scaling up a trickle bed reactor for degrading pesticides from agricultural wastewater by fungi

PhD thesis

PhD Program in Environmental Science and Technology

Kaidi Hu

Supervised by:

Dra. Montserrat Sarrà Adroguer & Dra. Glòria Caminal Saperas

Academic tutor:

Dra. Montserrat Sarrà Adroguer

June 2021

Title: Developing and scaling up a trickle bed reactor for degrading pesticides from agricultural wastewater by fungi

Carried out by: Kaidi Hu

Supervised by: Montserrat Sarrà Adroguer and Glòria Caminal Saperas

PhD program in Environmental Science and Technology

Departament d'Enginyeria Química, Biològica i Ambiental

Escola d'Enginyeria

Universitat Autònoma de Barcelona. Bellaterra (Cerdanyola del Vallès), 2021.

MONTSERRAT SARRÀ ADROGUER, associate professor from the Departament d'Enginyeria Química, Biològica i Ambiental of the Universitat Autònoma de Barcelona, and GLÒRIA CAMINAL SAPERAS, scientific researcher from the Institut de Química Avançada de Catalunya (IQAC) of the Consejo Superior de Investigaciones Científicas (CSIC).

CERTIFY:

That the engineer KAIDI HU has carried out under our supervision the research work entitled "Developing and scaling up a trickle bed reactor for degrading pesticides from agricultural wastewater by fungi", which is presented in this report and it constitutes his thesis to obtain the Degree of Doctor in Environmental Science and Technology from the Universitat Autònoma de Barcelona.

To whom it may concern and may record it for the appropriate purposes, we present the aforementioned thesis to the Escola de Doctorat of the Universitat Autònoma de Barcelona, signing this certificate at

Bellaterra (Cerdanyola del Vallès), June 2021

MONTSERRAT SARRA ADROGUER - DNI 40312755B
Firmado digitalmente por MONTSERRAT SARRA ADROGUER - DNI 40312755B
Fecha: 2021.06.14 18:20:33 +02'00'

GLORIA CAMINAL SAPERAS - DNI 46213816P
Firmado digitalmente por GLORIA CAMINAL SAPERAS - DNI 46213816P
Fecha: 2021.06.14 18:25:14 +02'00'

Dra. Montserrat Sarrà Adroguer

Dra. Glòria Caminal Saperas

Abstract

Over the last decades, the pollution of aquatic environment by numerous micropollutants is one of global problems facing humanity. Although those compounds are normally present at low concentrations, they raise considerable toxicological concerns, posing severe threat to ecosystem and human beings. Among micropollutants, pesticides, introduced inadvertently or deliberately into environment resulted from anthropogenic activities, mainly agricultural practice, are widely accepted as the key trigger of water deterioration and a major current challenge for modern societies, since their poor elimination in conventional wastewater treatment plant. Thus, the development of technologies capable of reducing them from water body is urgently needed. The richness and low-substrate specificity features of lignin-degrading enzyme system enable the high potential of white-rot fungi (WRF) in addressing this escalating world concern.

The present thesis aims to develop a pilot plant that is allowed to address pesticides from agricultural wastewater in a long-term treatment by WRF under non-sterile conditions.

Firstly, an optimal candidate was screened out from several ligninolytic fungi using different pesticides, which were frequently detected in two Catalonian agricultural area, as substrates. *Trametes versicolor* was selected for reactors set up owing to its remarked performance. In addition, the degradation characteristics of the targeted pesticides by the chosen alternative were investigated, including enzymatic system and degradation pathway.

Secondly, a lab-scale trickle bed (TBR) was constructed with *T. versicolor* immobilized on pine wood chips. It was employed to treat agriculture water (AW) fortified by selected pesticides, and compared to the well established fluidized bed reactor (FBR) based on different aspects, such as removal efficacy, robustness, and economic cost, etc. Accordingly, TBR emerged as the preferred option in the comparative study. Then, it was subsequently applied for eliminating pesticides from real AW, turned out good results were obtained. Both spiked and real scenarios indicate that the lignocellulosic carrier not only act as nutrient source, but also played a vital role in treatment, through adsorption effect. Besides, our findings suggest that an enhanced demonstration could be achieved by retaining the biomass inside the reactor.

Based on gained experiences and perspectives, a pilot-scale TBR with *T. versicolor* colonized on oak wood chips, was installed and successfully operated for 186 days to deal with spiked AW under non-sterile conditions in continuous mode. Throughout the long-term running period, stable and promising performances were approached. The clogging issue, as a consequence of continuous fungal growth, was effectively tackled by rearrangement of the packing bed, without damaging the biofilm. The scaled-up reactor displayed persistent bioactivity and high robustness.

To sum up, this study sheds light into pesticides-contaminated water bioremediation by WRF. Also, it serves as a proof of the concept that micropollutants in the wastewater can be dismissed by a long-term white-rot fungal treatment.

Resumen

Durante las últimas décadas, la contaminación del medio acuático por numerosos microcontaminantes es uno de los problemas globales a los que se enfrenta la humanidad. Aunque esos compuestos normalmente se detectan en bajas concentraciones, suscitan considerables preocupaciones toxicológicas, lo que representa una grave amenaza para el ecosistema y los seres humanos. Entre los microcontaminantes, los pesticidas, introducidos de forma involuntaria o deliberada en el medio ambiente como resultado de actividades antropogénicas, principalmente prácticas agrícolas, se consideran la contribución clave en el deterioro del agua y un importante desafío para las sociedades modernas, debido a su escasa eliminación en las plantas de tratamiento de aguas residuales convencionales. Por lo tanto, se necesita con urgencia el desarrollo de tecnologías capaces de eliminarlos del agua. La gran variedad y la característica de baja especificidad por el sustrato del sistema de enzimas que degradan la lignina otorgan un alto potencial a los hongos de pudrición blanca (WRF) para abordar esta creciente preocupación mundial.

La presente tesis tiene como objetivo desarrollar una planta piloto que permita eliminar pesticidas de aguas residuales agrícolas con un tratamiento WRF en condiciones no estériles y durante largos periodos sin necesidad de cambiar el biocatalizador.

En primer lugar, se seleccionó un candidato óptimo entre varios hongos ligninolíticos utilizando como sustratos diferentes pesticidas, que se detectaban con frecuencia en dos zonas agrícolas catalanas. Se seleccionó *Trametes versicolor* para ser utilizado en los reactores debido a su mayor rendimiento de degradación. Además, se investigaron las características de degradación de los pesticidas seleccionados por *T. versicolor*, incluido el sistema enzimático y la vía de degradación.

En segundo lugar, se construyó un filtro percolador (TBR) a escala de laboratorio con *T. versicolor* inmovilizado sobre astillas de madera de pino. Se empleó para tratar agua de agricultura (AW) dopada con pesticidas seleccionados, y se comparó con el reactor de lecho fluidizado (FBR) bien establecido en el grupo de investigación, en función de diferentes aspectos, como la eficacia de eliminación, la robustez y el costo económico, etc. En consecuencia, TBR resultó la mejor opción en el estudio comparativo. Posteriormente se

aplicó para eliminar pesticidas de AW reales y se obtuvieron buenos resultados. Tanto los experimentos con aguas reales AW, como con AW dopadas indican que el soporte lignocelulósico no solo actúa como fuente de nutrientes, sino que también desempeña un papel vital en el tratamiento, a través de la adsorción. Además, los resultados demuestran que se podría mejorar el proceso aumentando la cantidad de biomasa en el reactor, por lo que se cambio de soporte, eligiendo uno del hábitat natural de hongo.

Sobre la base los resultados previos, se construyó un TBR a escala piloto con astillas de madera de roble colonizadas por *T. versicolor* y se operó con éxito durante 186 días para tratar el AW dopada, en condiciones no estériles y operando en continuo. Durante el período de tratamiento, se alcanzaron resultados estables y prometedores. El problema de la obstrucción, como consecuencia del crecimiento continuo del hongo, se abordó eficazmente mediante la reorganización del lecho empacado, sin dañar la biopelícula. El reactor ampliado mostró una bioactividad persistente y una gran robustez.

En resumen, este estudio arroja luz sobre la biorremediación de agua contaminada con pesticidas mediante WRF. Además, sirve como prueba de concepto de que los microcontaminantes de las aguas residuales pueden eliminarse mediante un tratamiento prolongado con hongos de podredumbre blanca sin necesidad de adicionar nutrientes ni renovar la biomasa.

Resum

Al llarg de les darreres dècades, la contaminació del medi aquàtic per part de nombrosos micro-contaminants és un dels problemes globals a què s'enfronta la humanitat. Tot i que aquests compostos es detecten a baixes concentracions, susciten considerables preocupacions toxicològiques i representen una greu amenaça pels ecosistemes i els éssers humans. Entre els micro-contaminants, els pesticides, introduïts involuntàriament o deliberadament en el medi ambient com a resultat d'activitats antròpiques, principalment pràctiques agrícoles, es consideren la contribució clau del deteriorament de l'aigua i un desafiament important per a les societats modernes, degut a la seva escassa eliminació en les plantes convencionals de tractament d'aigües residuals. Per tant, es necessita amb urgència el desenvolupament de tecnologies capaces d'eliminar-los de l'aigua. La gran varietat i les característiques de baixa especificitat vers els substrats del sistema enzimàtic degradador de la lignina, permeten als fongs de podridura blanca (WRF) ser una opció per afrontar aquesta creixent preocupació mundial.

La present tesi té com a objectiu desenvolupar una planta pilot que permeti abordar l'eliminació de pesticides de les aigües residuals agrícoles mitjançant un tractament per WRF en condicions no estèrils operant duran períodes llargs de temps sense necessitat de canviar el biocatalitzador.

En primer lloc, es va seleccionar un candidat òptim entre diversos fongs ligninolítics estudiant la degradació de diferents pesticides, que es van detectar amb freqüència en dues zones agrícoles catalanes. *Trametes versicolor* es va seleccionar per a ser utilitzat en els reactors a causa del seu millor rendiment de degradació. A més, es van investigar les característiques de degradació dels pesticides seleccionats, inclosos el sistema enzimàtic involucrat i la via de degradació.

En segon lloc, es va construir un filtre percolador a escala de laboratori (TBR) amb *T. versicolor* immobilitzat sobre estelles de fusta de pi. Es va utilitzar per tractar l'aigua agrícola (AW) dopada amb pesticides seleccionats i es va comparar amb el reactor de llit fluïditzat (FBR), ben establert en el grup de recerca, es van analitzar diferents aspectes, com ara l'eficàcia de l'eliminació, la robustesa i el cost econòmic, etc. TBR va resultar la

millor opció. Després, es va aplicar per eliminar els pesticides de l'AW real, i es van obtenir bons resultats. Tant amb l'aigua real com amb la dopada es va demostrar que el suport lignocel·lulòsic no només actua com a font de nutrients, sinó que també té un paper vital en el tractament, degut a l'adsorció. A més, els resultats suggereixen que es podria aconseguir una millora en el procés amb més biomassa a l'interior del reactor, per la qual cosa es va canviar de suport, escollint un de l'habitat natural del fong.

Basant-se en els resultats previs, es va construir un TBR a escala pilot amb *T. versicolor* colonitzat sobre estelles de fusta de roure i va funcionar amb èxit durant 186 dies tractant AW dopada en condicions no estèrils i en continu. Al llarg del període de funcionament, el reactor es va comportar estable i prometedor. El problema de l'obstrucció, com a conseqüència d'un creixement continu del fong, es va abordar eficaçment mitjançant la reordenació del llit empacat, sense danyar el biofilm. L'escalat del reactor va mostrar una bio-activitat persistent i una alta robustesa.

En resum, aquest estudi aporta llum a la bioremediació d'aigües contaminades per pesticides mitjançant WRF. A més, serveix com a prova del concepte que els micro-contaminants de les aigües residuals poden ser eliminats mitjançant un tractament a llarg termini amb fongs amb podridura blanca.

List of abbreviations

ABTS	2,2'-azino-bis (3-ethylbenzothiazoline-6-sulfonic acid) diammonium salt
ATCC	American Type Culture Collection
AU	Activity unit
AW	Agricultural wastewater
CFU	Colony-forming unit
CL	Confidence level
COD	Chemical oxygen demand
CYP450	Cytochrome P450 system
DGGE	Denaturing gradient gel electrophoresis
DMP	2,6-dymetoxyphenol
DW	Dry weight
EC	European Commission
ED	Endocrine disruptor
ESI	Electrospray ionization
FAO	Food and Agriculture Organization of the United Nations
FBCC	Fungal Biotechnology Culture Collection
FBR	Fluidized bed reactor
HPC	Heterotrophic plate count
HPLC	High-performance liquid chromatography
HRT	Hydraulic residence time
IS	Internal standard
MBR	Membrane bioreactor
MnP	Manganese peroxidase
MS	Mass spectrometry
PBCB	Packed bed channel bioreactor
PCP	Personal care product
PCR	Polymerase chain reaction
PVDF	Polyvinylidene difluoride

PhC	Pharmaceutical compound
PPDB	Pesticide Properties Database
RBC	Rotating biological contactor
RR	Recirculation ratio
SD	Standard deviation
SEM	Scanning electron microscope
TBR	Trickle bed reactor
TOC	Total organic carbon
TP	Transformation product
TSS	Total suspended solid
UPLC	Ultra performance liquid chromatography
VSS	Volatile suspended solid
WRF	White-rot fungi
WWTP	Wastewater treatment plant

Content

Chapter 1

Chapter 2

Chapter 3

Chapter 4

Chapter 7

Chapter 1

Literature review

1.1 Water Risk

As an essential resource for all living organisms, water is at the core of sustainable development. It can affect the livelihoods of billions by flowing through food and energy security, as well as human and environmental health, all of which are the pillars of sustainable development. Water issues have risen in prominence in recent years, scarcity and pollution present as two major concerns we are facing.

1.1.1 Water scarcity

Due to the increasing world population, improving living standards, changing consumption patterns, and expansion of irrigated agriculture, global water use has increased by a factor of six over the past 100 years and continue to grow steadily at a rate of 1% annually (WWAP, 2020). Mekonnen and Hoekstra (2016) pitched a report saying that two-thirds of the global population (4.0 billion people) suffer from severe water scarcity for at least one month per year, and half a billion people face severe water scarcity all year around. Geographically, such stress already affects every continent (Figure 1.1), especially the Middle East area, northwest of India and arid areas (e.g. north of Africa, center of Australia), which puts those countries or communities in an extremely vulnerable position (Mekonnen and Hoekstra, 2016). From the agricultural point of view, 25% of the global croplands encounter with agricultural economic water scarcity. It means these regions are lack of economic or institutional capacity to access available fresh surface and ground water bodies (Rosa et al., 2020).

Furthermore, climate change exacerbates water stress. For example, it leads to accelerating evaporation and melting of glaciers, negatively affecting dry and mountain regions in the long term, respectively (WWAP, 2020). Despite water reuse is gaining momentum as a best solution to address water scarcity, particularly in irrigation, there are some risks brought by untreated or inadequately treated wastewater, such as human health, soil contamination, and groundwater pollution. Besides, globally only a small fraction of wastewater actually undergoes advanced (tertiary) treatments (WWAP, 2017).
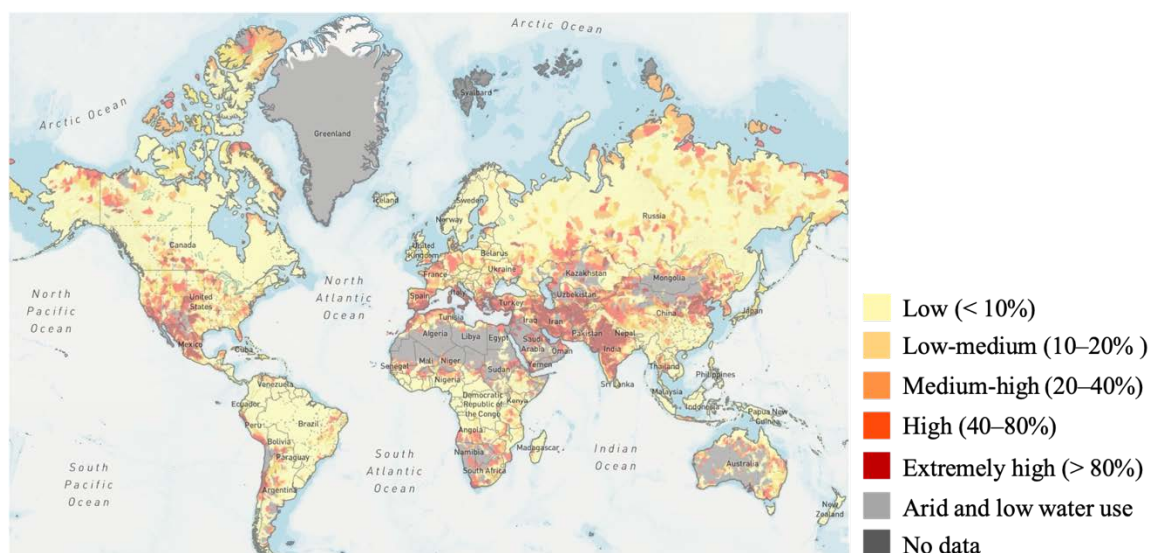
Figure 1.1 Annual baseline water stress around the world. Attribution: Aqueduct Global Maps 3.0 Data (WRI, 2019). Note: Baseline water stress measures the ratio of total water withdrawals to available renewable surface and groundwater supplies. Water withdrawals include domestic, industrial, irrigation, and livestock consumptive and non-consumptive uses. Available renewable water supplies include the impact of upstream consumptive water users and large dams on downstream water availability. Higher values indicate more competition among users.

1.1.2 Water pollution

According to The United Nations World Water Development Report 2017, wastewater is regarded as a combination of one or more of different sources, including domestic effluent, municipal effluent, urban runoff, agricultural runoff, industrial effluent, livestock effluent, aquaculture runoff and stormwater, etc. Municipal, urban, industrial and agricultural activities are the main driving forces for global wastewater production. Even if they can be reused for irrigation, industrial activity, groundwater recharge, etc., still the risks associated with contaminants are pronounced (WWAP, 2017). The typical components in municipal wastewater, urban runoff, industrial wastewater and agricultural runoff are summarized in Table 1.1. Particularly, pharmaceuticals, personal care products, industrial chemicals, endocrine disruptors and pesticides are classified as micropollutants, also termed as emerging contaminants, which can be defined as "*Substances that are present in aquatic environment at trace concentrations ($\leq \mu g\ L^{-1}$) and whose bioaccumulation, persistence as well as toxicity may impose negative effect on ecosystem and/or human health*" (Grandclément et al., 2017; Luo et al., 2014; Sauvé and Desrosiers,

2014; WWAP, 2017). Owing to their diverse properties, micropollutants are inadequately removed in conventional wastewater treatment plants (WWTPs), thereby ending up in the aquatic environment and becoming threats to wildlife and human beings (Luo et al., 2014; Margot et al., 2015; Tran et al., 2018). Besides, 70% of the municipal and industrial wastewater generated in high-income countries can be treated. That proportion drops to 38% in upper middle-income countries and to 28% in lower middle-income countries. Only 8% undergoes treatment in low-income countries since their lack of infrastructure, technical and institutional capacity, and financing (WWAP, 2017). This absolutely adds a risk on degrading global water quality by micropollutants.

Table 1.1 Typical components in some major wastewater (modified from (WWAP, 2017)).

Sources of wastewater	Typical components
Municipal wastewater	Pathogenic microorganisms, nutrients (i.e. carbon, nitrogen and phosphorus), organic matter, heavy metals, pharmaceuticals, personal care products and many other emerging contaminants.
Urban runoff	Incomplete products of combustion (e.g. polycyclic aromatic hydrocarbons and black carbon/soot from fossil fuel combustion), rubber, motor oil, heavy metals, non-degradable/organic trash (especially plastics from roads and parking lots), suspended particulate and fertilizers and pesticides
Industrial wastewater	Contaminants depend on the kind of industry, including pulp and paper, iron and steel, mines and quarries, food industry, brewing, diary, organic chemicals, textiles and energy, etc.
Agricultural runoff	Pathogenic microorganisms, nutrients from fertilizers applied to the soils, and pesticides derived from the agricultural practices

a) Pharmaceutical compounds

As produced to meet therapeutic purpose, pharmaceutical compounds (PhCs) are widely used in medical field and livestock production. They are classified into certain groups, such as antibiotics, analgesics, anti-inflammatories, therapeutic hormones, psychiatric drugs, antipyretics, beta-blockers, etc. Indeed, the PhCs as well as their by-products and metabolites in receiving environmental media are primarily originated from hospital effluent, diagnostic waste, animal waste, research activities and discharge of expired medicine (Tiwari et al., 2017), subsequently compiling in urban wastewater (Michael et al., 2013). But as aforementioned, WWTPs are generally not equipped to deal with complex

pharmaceuticals, thus a large part of them could escape from the barrier and enter into different water bodies, causing disturbance of aquatic flora as well as fauna and risking to human health (De García et al., 2014; de Jesus Gaffney et al., 2015; Frédéric and Yves, 2014; Verlicchi et al., 2012). On the other hand, among those classifications, antibiotics pose the highest risk, partly because they could hinder the activity of beneficial microbes in WWTPs that will further weaken its treatment efficiency, and partly because they may contribute to the development of multiple antibiotic resistant bacteria and the spread of antibiotic resistant genes (Bouki et al., 2013; Michael et al., 2013; Rizzo et al., 2013; Tiwari et al., 2017; Verlicchi et al., 2012).

b) Personal care products

Personal care products (PCPs) consist of a diverse collection of categories, including disinfectants, fragrances, preservatives and UV filters, used in lotions, toothpaste, cosmetic, shampoo, shower gel and sunscreen etc. All of which are applied externally, thus resulting in two main release routes: water recreation activities (e.g. swimming, bathing, floating, water sliding), and domestic activities (e.g. showering or laundering). Unlike PhCs, they do not undergo metabolic alteration and enter the environment directly. To date, it has been widely accepted that various PCPs present in different environmental compartments and chronic exposure to them may pose a risk to humans and wildlife because their inherent ability to induce physiological effects at low doses (Brausch and Rand, 2011; Bu et al., 2013; Ebele et al., 2017; Tran et al., 2018).

c) Industrial chemicals

In the aspect of industrial sectors, manufacturing is the greatest polluter. On the other hand, there are great discrepancies in characteristics of wastewater between different industrial activities, as noted in Table 1.1. For instance, the typical contents in the effluent from pulp and paper plant are chlorinated organic compounds, while the core of wastewater treatment for food industry is to address high level of biochemical oxygen demand (BOD) and suspended solids (SS) concentrations (WWAP, 2017). It is worth remarking that chemical industry is one generator of pesticides and/or pharmaceuticals contaminated wastewater.

d) Endocrine disruptors

Endocrine disruptors (EDs), referring to exogenous compounds that affect health and reproduction in animals and humans by disturbing hormonal regulation and the normal endocrine system, cover natural estrogens and androgens, artificial synthetic estrogens or androgens, phytoestrogens. Apart from those, pesticides, PhCs, industrial chemicals also tend to demonstrate endocrine disrupting properties (Casals-Casas and Desvergne, 2011; Falconer et al., 2006; Liu et al., 2009; Massarsky et al., 2011). Accordingly, it can be supposed that we are surrounded by a wide range of endocrine disrupting chemicals in our daily life, which exist in the air we breathe, water we drink, and the soil where our food is cultivated. There are numerous evidences indicating that endocrine disruptors are responsible for producing negative impacts on ecosystem and human health (Casals-Casas and Desvergne, 2011; Kabir et al., 2015; Liu et al., 2009; Patisaul and Adewale, 2009; Ying et al., 2002).

As another kind of micropollutants, which is also considered as the major trigger of water deterioration, pesticides were comprehensively introduced in the following sections. Also, the work of this thesis targeted at addressing pesticides contamination by using fungal treatment.

1.2 Pesticides

1.2.1 Classification

Pesticides have been defined by Food and Agriculture Organization of the United Nations (FAO) as "*Any substance or mixture of substances intended for preventing, destroying or controlling any pest, including vectors of human or animal disease, unwanted species of plants or animals causing harm during or otherwise interfering with the production, processing, storage, transport or marketing of food, agricultural commodities, wood and wood products or animal feedstuffs, or substances which may be administered to animals for the control of insects, arachnids or other pests in or on their bodies. The term includes substances intended for use as a plant growth regulator, defoliant, desiccant or agent for thinning fruit or preventing the premature fall of fruit, and substances applied to*

crops either before or after harvest to protect the commodity from deterioration during storage and transport" (FAO, 2020). Accordingly, pesticides can be simplified as chemical, or chemical mixtures that increase the yield and efficiency of crops by protecting them from pest, weed and disease. In addition, pesticides can be categorized as insecticides, fungicides, herbicides, rodenticides, acaricides, nematicides, molluscicides, disinfectants, repellents and plant growth regulator etc. on the basis of target organism or activity. Simultaneously, other properties also serve pesticides classification, such as application, chemical nature, mode or time of action; formulation, hazard and half-lives (Table 1.2) (Arias-Estévez et al., 2008; Jayaraj et al., 2016; NPIC; Tiryaki and Temur, 2010; WHO, 2020; Yadav and Devi, 2017).

Table 1.2 Different classifications of pesticides.

Basis	Category
Target organism	Insecticides, fungicides, herbicides, rodenticides, acaricides, nematicides, molluscicides, disinfectants, repellents and plant growth regulator etc.
Application	Agriculture pesticides, public health pesticides, domestic pesticides
Chemical nature	Organochlorines, organophosphates, carbamates, pyrethroids, neonicotinoids, phenyl amides, phenoxy alkonates, trazines and benzoic acid derivatives etc.
Mode or time of action	Contact, eradicant, fumigants, nonselective, post-emergence, pre-emergence, preplant, protectants, selective, soil sterilant, stomach poison, systemic
Formulation	Aerosol, bait, dust, granule, powders, emulsifiable concentrate, flowable, ultra-low-volume concentrates, microencapsulated etc.
Hazard	Extremely hazardous, highly hazardous, moderately hazardous, slightly hazardous and unlikely to present acute hazard
Half-lives	Nonpersistent, moderately persistent, persistent

1.2.2 Emission sources

Pesticides are widely used in agricultural, public health and domestic applications, resulting in their occurrence in agricultural urban runoff (WWAP, 2017). In particular, the agricultural sector holds the largest single share of total usage (> 80%), globally (Atwood and Paisley-Jones, 2017; Zhang et al., 2011). Figure 1.2 depicts the average pesticides applied in agriculture from 1990 to 2018 all over the world. As can be seen, most of

pesticides had been used in Asia, Americas and Europe, aggregately reaching 96.6% of total usage according to FAO Statistics (FAOSTAT, 2019).
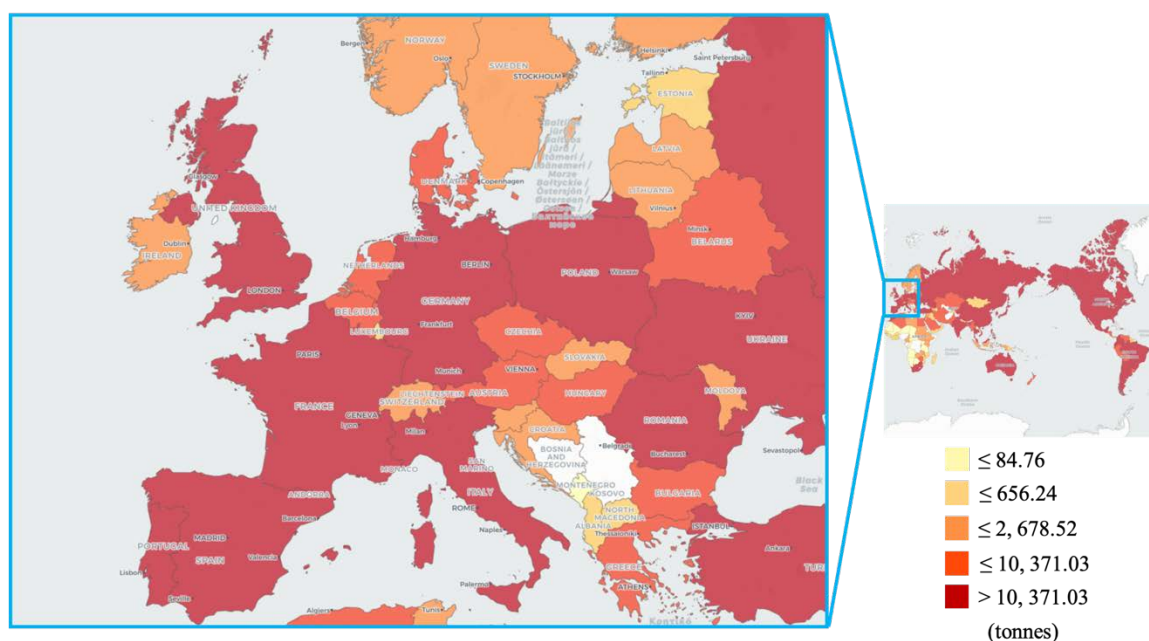
Figure 1.2 Average pesticides usage in agriculture from 1990 to 2018 around the world (FAOSTAT, 2019).

If sights are thrown into statistical data, it is clear that the pesticides consumption shows an increasing trend during last two decades in Spain, EU and the whole world (Table 1.3), ascribed to the increasing population that further demands more food. Unfortunately, only small amounts (< 0.01%) of applied pesticides could reach target pests (Pimentel and Burgess, 2012), and the rest of them will experience different transports and eventually enter the environment. The relevant redistribution is summarized in section 1.2.3.

Table 1.3 Pesticides usage in different areas from 1990 to 2018 (FAOSTAT, 2019).

Year	Agricultural usage (tonnes)		
	World	European Union	Spain
1990	2, 299, 979	370, 799	39, 562
1995	2, 708, 908	335, 338	27, 852
2000	3, 089, 827	343, 521	34, 597
2005	3, 449, 778	351, 001	41, 017
2010	4, 010, 862	313, 190	39, 043
2015	4, 113, 513	343, 415	59, 018
2018	4, 122, 334	348, 493	61, 343

Instead of protecting crops, pesticides, in urban area, are normally employed for lawn,

turf, home garden, structural, indoor and outdoor pests control (Meftaul et al., 2020). The residual pesticides on impermeable surfaces are predicted to be washed off by rain or other sources of water, ending up in surface and underground water. Meanwhile some extent of pesticides adsorbed by soil will redissolve in water through runoff and leaching (Meftaul et al., 2020).

As mentioned above, agrochemical industry is another source of pesticides contamination. Different reports have revealed the occurrence of pesticides in water and sediments surrounding the manufacturing zone, ranging from ng g^{-1} up to mg g^{-1} (Abdel-Halim et al., 2006; Alalm et al., 2015; Syed and Malik, 2011). Last but not least, accidental spills or leaks resulted from inappropriate storage and transport may also contribute to pesticides emission (Damalas and Eleftherohorinos, 2011; Meftaul et al., 2020; Ramakrishnan et al., 2019).

1.2.3 Environmental fate of pesticides

An understanding of the fate of pesticides is beneficial for rational decision and appropriate management strategy, to alleviate or prevent their negative impacts on ecosystem and human health. In fact, less than 0.01% of the pesticides applied to crops could reach the target pest, while pollinators such as bees and butterflies are equally exposed (Hladik et al., 2016; Pimentel and Burgess, 2012). The contaminated leaves, flowers, seeds, pollen and nectar are hazard to other non-target organisms. A great extent of residues will be received by soil, where adsorption and biodegradation are pronounced. Those two routes are governed by various factors, including soil moisture, pH, organic matter content, texture, physical-chemical properties of the pollutant and lock weather conditions etc. (Gavrilescu, 2005; Tiryaki and Temur, 2010). Pesticides remaining in the soil can ultimately move into surface water and groundwater through runoff and leaching respectively, or they may be available for plant uptake. Furthermore, pesticides adsorbed onto soil particles are potentially transported into air by wind. Volatilization and application drift are also engaged in this atmospheric pollution. As a consequence of windy conditions, airborne pesticides may move very long distances and reach non-agriculture landscape, provoking unpredictable risks. Meantime they tend to be removed from the atmosphere

when it rains and end up in surface water. (Arias-Estévez et al., 2008; Fenner et al., 2013; Gavrilescu, 2005; Ramakrishnan et al., 2019; Tiryaki and Temur, 2010). From the point of human health view, the bioaccumulation of pesticides through food chain may pose a serious threat (Aznar-Alemany and Eljarrat, 2020; Chopra et al., 2011; Gupta and Gupta, 2020). Lastly, all pesticides are susceptible to sunlight at different degree, especially those remain on crop and soil surface or in the air (Fenner et al., 2013; Gavrilescu, 2005; Tiryaki and Temur, 2010). Based on above illustrations, a comprehensive transport mechanism is presented as Figure 1.3.
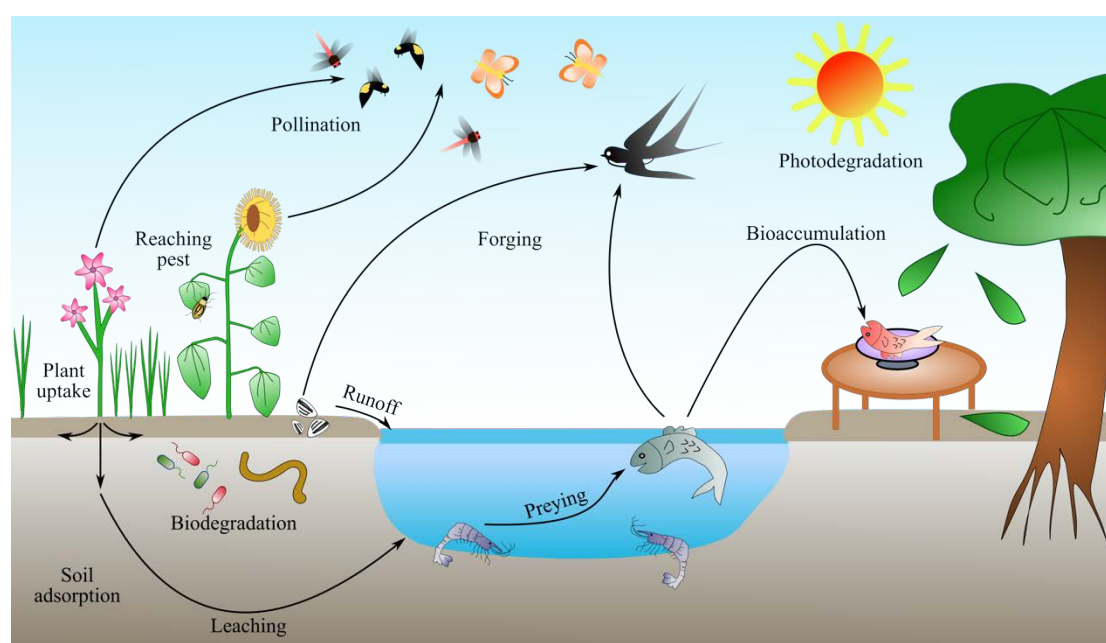
Figure 1.3 Overview of pesticides transport in agriculture landscape (Gavrilescu, 2005).

1.2.4 Residues in the environment

1.2.4.1 Occurrence of pesticides in soil

Soil serves as the sink for applied pesticides that present as the most common contaminants among all xenobiotics in soil (Wołejko et al., 2020). Although attenuation most frequently take place, during which biological metabolization plays a fundamental role, some pesticides are persistent in soil anyway, because of their high recalcitrance to biodegradation and low bioavailability (Arias-Estévez et al., 2008; Curran, 2016; Gavrilescu, 2005; Ren et al., 2018). For example, several organochlorine insecticides were frequently detected in soils worldwide during last ten years, even if they have been banned

by different authorities (Table 1.4). Moreover, due to the long-range atmospheric transport, those recalcitrant pollutants could land in polar regions, leaving a stain on the last piece of pure land (Zhang et al., 2015).

1.2.4.2 Occurrence of pesticides in air

As remarked above, pesticides can contaminate atmosphere through drifting and volatilizing. There are many cases of pesticide residues in air (Table 1.5). Actually, a non-negligible fraction of sprayed dosage could emit into atmospheric environment during application (Van den Berg et al., 1999), governed by technical and environmental factors (Gil and Sinfort, 2005). Likewise, the rate of volatilization is dependent on weather conditions, application techniques, pesticides formulations, etc. (Gavrilescu, 2005). On the other hand, the more persistent contaminants are, the longer aerial transport distance will be (Carratalá et al., 2017). It can be noted that different groups of pesticides exist in air, including insecticides, herbicide and fungicides (Table 1.5). Most of which are currently being used, highlighting the fact that the residues in air tightly related to local applications (Carratalá et al., 2017; Coscollà et al., 2010; Estellano et al., 2015). Some pesticides, such as DDTs, HCHs and endosulfan, were observed across the globe (Table 1.5).

1.2.4.3 Occurrence of pesticides in water

Water behaves pretty much like air in the aspect of pesticides spatial distribution. Water flow can carry either dissolved or sorbed pesticides to anywhere it goes (Gavrilescu, 2005; Tiryaki and Temur, 2010). Consequently, different pesticides were found in surface water, groundwater and even drink water across the world (Table 1.6). To protect freshwater resources, EU established strict regulations and one of which clarifies that the maximum admissible concentration for individual pesticides in drinking water is 0.1 $\mu g\ L^{-1}$ and 0.5 $\mu g\ L^{-1}$ for total pesticides (EC, 1998). Then Priority Substances List and Watching List were successively published and amended (EC 2013, 2018). Another point of concern is that despite WWTPs act as primary barriers against the spread of pesticides in aquatic environment, their removal is poor in there (Köck-Schulmeyer et al., 2013b; Luo et al., 2014; Margot et al., 2015). This problem adds uncertainty to their negative effect on ecosystem, wildlife and human beings (Firouzsalari et al., 2019; Muenze et al., 2017).

Massive amounts of complex pesticides are released by agricultural activity. They will eventually enter aquatic media in the local and surrounding areas, such as irrigation channels and river streams, exhibiting abundant quantities (Calvo et al., 2021; Climent et al., 2019; Glinski et al., 2018; Wang et al., 2021). The cocktail of pesticides (pesticides mixture) in aquatic habitats very likely pose severe toxic and deleterious effect on the native biota (de Souza et al., 2020). This thesis mainly focused on addressing pesticide contamination in the agricultural irrigation waters.

Table 1.4 Pesticides residues in soils worldwide.

Sample type	Country/Region	Pesticides	Concentration (ng g^{-1})	References
Farmland soil	Nepal	DDTs, HCHs, endosulfan, dicofol	1.97–230	Yadav et al., 2016
Urban, suburban and rural area surface soil	India	DDTs, HCHs, endosulfan, chlordane, HCB	0.01–214	Chakraborty et al., 2015
Cropped soil	Tunisia	DDTs, HCHs, chlordane	12.49–310.54	Haddaoui et al., 2016
Arable soil	Czech Republic	Triazines, conazoles, chloroacetanilide, fenpropidin, diflufenican	ND–163	Hvězdová et al., 2018
Surface soil surrounding industrial zone	Pakistan	DDTs, HCHs, dicofol, endrin, heptachlor, dieldrin and endosulfan	ND–1, 811.98	Syed and Malik, 2011
Cropland and vineyard soils	European Union	Glyphosate, DDTs, boscalid, epoxiconazole, tebuconazole, etc.	ND–2050	Silva et al., 2019
Orchard soil	China	Chlorpyrifos, dimethoate, DDTs, HCHs, endosulfan, quintozene, aldrin, dieldrin, fenpropathrin, cypermethrin, deltamethrin triadimefon and buprofezin	ND–400.1	Liu et al., 2016
Cocoa farm soil	Ghana	Lindane, HCHs, dieldrin and DDTs	ND–50	Fosu-Mensah et al., 2016
Cocoa farm soil	Nigeria	Endosulfan, heptachlor, heptachlor epoxide, aldrin, deldrin and HCBs	ND–350, 100	Aiyesanmi and Idowu, 2012

Note: DDT, dichloro-diphenyl-trichloroethane; HCH, hexachlorocyclohexane; HCB, hexachlorobenzene; ND, not detected or below the detection limit.

Table 1.5 Pesticides residues in air worldwide.

Country/Region	Pesticides	Concentration (pg m^{-3})	References
France	Trifluralin, acetochlor, endosulfan, alachlor, chlorothalonil, chlorpyrifos, cyprodinil, fenpropidin, fenpropimorph, HCHs, pendimethalin, spiroxamine etc	100–117, 330	Coscollà et al., 2010
Spain	Chlorpyrifos, triazines, chlortal-dimethyl, pendimethalin, propyzamide, etc	ND–4, 902.4	Carratalá et al., 2017
Italy	Chlorpyrifos, malathion, terbufos, diazinon, dacthal, trifluralin, pendimethalin, chlorothalonil	ND–580	Estellano et al., 2015
China	DDTs, HCHs, endosulfan, HCB	0.03–479	Zhan et al., 2017
Costa Rica and Uganda	Endosulfan, chlordane, DDTs, chlorpyrifos, chlorothalonil, pendimethalin, HCB, heptachlor epoxide, cypermethrin, etc	0.18–82	Wang et al., 2019c
China	Chlorpyrifos, cypermethrin, allethrin, bifenthrin, cyfluthrin, cyhalothrin, dimefluthrin, permethrin and tetramethrin	ND–2, 901	Li et al., 2014
Greece	DDTs, HCB, dicofol, HCHs, dieldrin, endosulfan etc	ND–32.69	Iakovides et al., 2021
USA	Atrazine, glyphosate, propanil, chlorpyrifos, pendimethalin, malathion, metolachlor, etc	ND–16, 100	Majewski et al., 2014

Note: DDT, dichloro-diphenyl-trichloroethane; HCH, hexachlorocyclohexane; HCB, hexachlorobenzene; ND, not detected or below the detection limit.

Table 1.6 Pesticides residues in water worldwide.

Sample type	Country/Region	Pesticides	Concentration (ng L^{-1})	References
River water	Portugal	Atrazines, diuron, imidacloprid, irgarol, isoproturon, carbendazim, simazine, turbuthrin etc	0–45	Gonzalez-Rey et al., 2015
Surface water and groundwater	Spain	Terbuthylazine, fluometuron, ethofumesate, pyrimethanil, tebuconazole, diuron, pirimicarb, atrazine, benalaxyl etc	ND–18, 365	Herrero-Hernández et al., 2013
Groundwater	Greece	Alachlor, metolachlor, atrazines, dicofol, diphenylamine, propanil, propazine, propham, simazine, terbacil, trifluralin, malathion, chlorpyrifos, DDTs, HCH etc	ND–1, 540	Vryzas et al., 2012
River water	China	DDTs, HCHs, chlordane, endosulfans, lindane, dicofol etc	ND–13.0	Tang et al., 2013
Coastal water	Ecuador	Carbendazim, cadusafos, DDT, diuron, linuron, aldrin, chlorpyrifos, malathion, fenpropimoph, heptachlor etc	ND–23, 930	Riascos-Flores et al., 2021
Surface wáter	USA	Bifenthrin, permethrin, imidacloprid, fipronil, carbaryl, malathion, 2,4-D, dicamba, diuron, pendimethalin etc	ND–11, 500	Ensminger et al., 2013
Groundwater and surface water	Netherland	Fluopyram, clothianidine, acetamiprid, thiamethoxam, mandipropamid etc	ND–1, 100	Sjerps et al., 2019
Drinking water	China	Acetamiprid, imidacloprid, clothianidin, thiamethoxam, thiacloprid, dinotefuran, imidaclothiz, nitenpyram, flonicamid	ND–807	Mahai et al., 2021
Surface water and drinking water	Brazil	Atrazine, iprodione, bentazon, diuron, carbofuran, fipronil, azoxystrobin, irgarol, propanil, simazine, trifloxystrobin etc	ND–1, 000	Caldas et al., 2019
Urban stormwater	Australia	Diuron, MCPA, 2,4-D, simazine, triclopyr, metolachlor, hexazinone, fluroxypyr, dichloroprop, carbaryl etc	ND–2, 008	Rippy et al., 2017

Note: DDT, dichloro-diphenyl-trichloroethane; HCH, hexachlorocyclohexane; MCPA, 2-methyl-4-chlorophenoxyacetic acid; ND, not detected or below the detection limit.

1.2.5 Toxicity of pesticides and their impact on environment

The adverse effects of pesticides are multidimensional. In the first, despite soil is essentially a sink retaining pesticide mixtures in which attenuation is very likely occurring, the presence of pesticides mixtures tends to negatively affect terrestrial ecosystems by disturbing and altering microflora as well as enzyme activity, which in turn will reduce the soil sustainability and fertility, further influencing crop production and environmental quality (Imfeld and Vuilleumier, 2012; Riah et al., 2014; Wołejko et al., 2020). Secondly, pesticides contamination in water can produce serious damage to different aquatic organism, from algae to fish, and amphibians, mainly through lowering dissolved oxygen and exhibiting toxicity (de Souza et al., 2020; DeLorenzo et al., 2001; Rani et al., 2020; Relyea, 2003; Ullah and Zorriehzahra, 2015). Thirdly, human beings meet pesticides through both direct and indirect exposures. Apart from drinking water, pesticides are also frequently detected in crops, vegetables, fruits, animal tissues and other raw materials (Alawi et al., 2017; Bempah et al., 2021; Guler et al., 2010; Lehmann et al., 2017; Lozowicka et al., 2014; Pareja et al., 2012; Teló et al., 2015). Mounting reports indicate that pesticides are harmful to human health due to their neurotoxicity (Costa, 2015; Richardson et al., 2019), reproductive toxicity (Mostafalou and Abdollahi, 2017; Nicolopoulou-Stamati et al., 2016), genotoxicity (Graillot et al., 2012; Jacobsen-Pereira et al., 2018), etc. Besides, it has been documented that pesticides attempt to be responsible for various types of health problems, such as cancer, diabetes, respiratory disorders, endocrine disorders, etc. (Meftaul et al., 2020; Rani et al., 2020).

1.2.6 Treatment approaches for pesticides removal from water

Basically, the treatment techniques for removing pesticides from water are grouped into physical (e.g. physisorption or filtration), chemical (e.g. coagulation- flocculation or advanced oxidation process) and biological (e.g. activated sludge or enzyme) methods (Al-Shawabkah et al., 2015; Carra et al., 2016; Doulia et al., 2016; Gao et al., 2014; Marican and Durán-Lara, 2018; Mojiri et al., 2020; Saini and Kumar, 2016). Each treatment has certain limitations and disadvantages in terms of efficiency, operability, cost, reliability and

environmental impact, etc. (Saleh et al., 2020). In comparison with physical and chemical approaches, bioremediation technology received more attention in last decades owing to its satisfying features, i.e. low-cost, efficient and environmental friendly. Bioremediation can be defined as any process that relies on biological mechanisms for the abatement of environmental contamination. Taking into consideration site of application, pesticides-contaminated wastewater bioremediation can be subcategorized into *in-situ* and *ex-situ* techniques. *In-situ* technologies comprise natural attenuation, air sparging, bioaugmentation, biostimulation and phytoremediation, while *ex-situ* bioremediation is commonly accomplished by using bioreactors (Juwarkar et al., 2014). Among those techniques, membrane bioreactor and attached growth treatment emerge as promising alternatives (Goswami et al., 2018; Luo et al., 2014; Zhao et al., 2019).

1.3 Fungal treatment

1.3.1 Pesticides degradation by white-rot fungi and their enzymes

On the theater of bioremediation, white-rot fungi (WRF), mainly belong to Basidiomycota and harbor ability in degrading lignin and its derived substances accompanied with bleaching appearance, are pronounced thanks to the possession of low- or non-substrate specificity extracellular enzymes, including laccase (EC 1.10.3.2, Lac), manganese peroxidase (EC 1.11.1.13, MnP), lignin peroxidase (EC 1.11.1.14, LiP), dye-decolorizing peroxidase (EC 1.11.1.19, DyP), versatile peroxidase (EC 1.11.1.16) etc., and intracellular enzyme cytochrome P450 system (E.C. 1.14.14.1, CYP450s) (Figure 1.4) (Manavalan et al., 2015; Maqbool et al., 2016; Zhuo and Fan, 2021). The rich oxidative enzymatic system renders WRF versatility in degrading a broad spectrum of xenobiotics that are recalcitrant to bacteria, such as pharmaceuticals, dyes, industrial chemicals, personal care products, etc. (Mir-Tutusaus et al., 2018; Zhuo and Fan, 2021). Of course, this superiority also reflects in addressing pesticides contamination. As summarized in Table 1.7, ligninolytic fungi demonstrated efficient degradation capacity towards different pesticides, and most of which were given ligninolytic conditions (Coelho-Moreira et al., 2013; Karas et al., 2011; Mir-Tutusaus et al., 2014; Mori et al., 2017; Rodríguez-Rodríguez

et al., 2017; Torán, 2018).

In parallel, increasing number of applications using ligninolytic enzymes from WRF have been executed to removal pesticides and desirable results were achieved. For instance, Hirai et al. (2004) conducted several treatments towards methoxychlor using partially purified MnP from *Phanerochaete chrysosporium* ME-446 and Lac from *Trametes versicolor* IFO-6482, turned out methoxychlor could be transformed either by MnP-Tween 80 or Lac-1-hydroxybenzotriazole. Complete glyphosate degradation was obtained by a mixture of MnP from *Nematoloma frowardii*, $MnSO_4$ and Tween 80. This mixture could also degrade 22 other pesticides at different rates, ranging from 20% to 100% (Pizzul et al., 2009). Kupski et al. (2019) accomplished an optimization for laccase-mediator system to reduce different pesticides (bentazone, carbofuran, diuron, clomazone, tebuconazole, and pyraclostrobin). Results showed that all the selected pollutants could be sufficiently removed (maximum 53–85%) with 0.95 U mL^{-1} laccase from *Trametes versicolor* and 1.8 mM vanillin. In addition, immobilization has been also employed in ligninolytic enzymes application, in order to enhance the stability and reusability of products (Bilal et al., 2017; Bilal et al., 2019; Voběrková et al., 2018). Chen et al. (2019) carried out the immobilization of laccase on peanut shell and wheat straw, by which nine pesticides, including isoproturon, atrazine, prometryn, mefenacet, penoxsulam, nitenpyram, prochloraz, pyrazosulfuron-ethyl and bensulfuron-methyl, were successfully removed from water. The dissipation of atrazine and prometryn was investigated using Lac immobilized on biodegradable microporous starch. After 7 days treatment, the removal efficiency reached 67% for former and that was 87% for latter one, which were much higher than natural degradation (Chen et al., 2021).
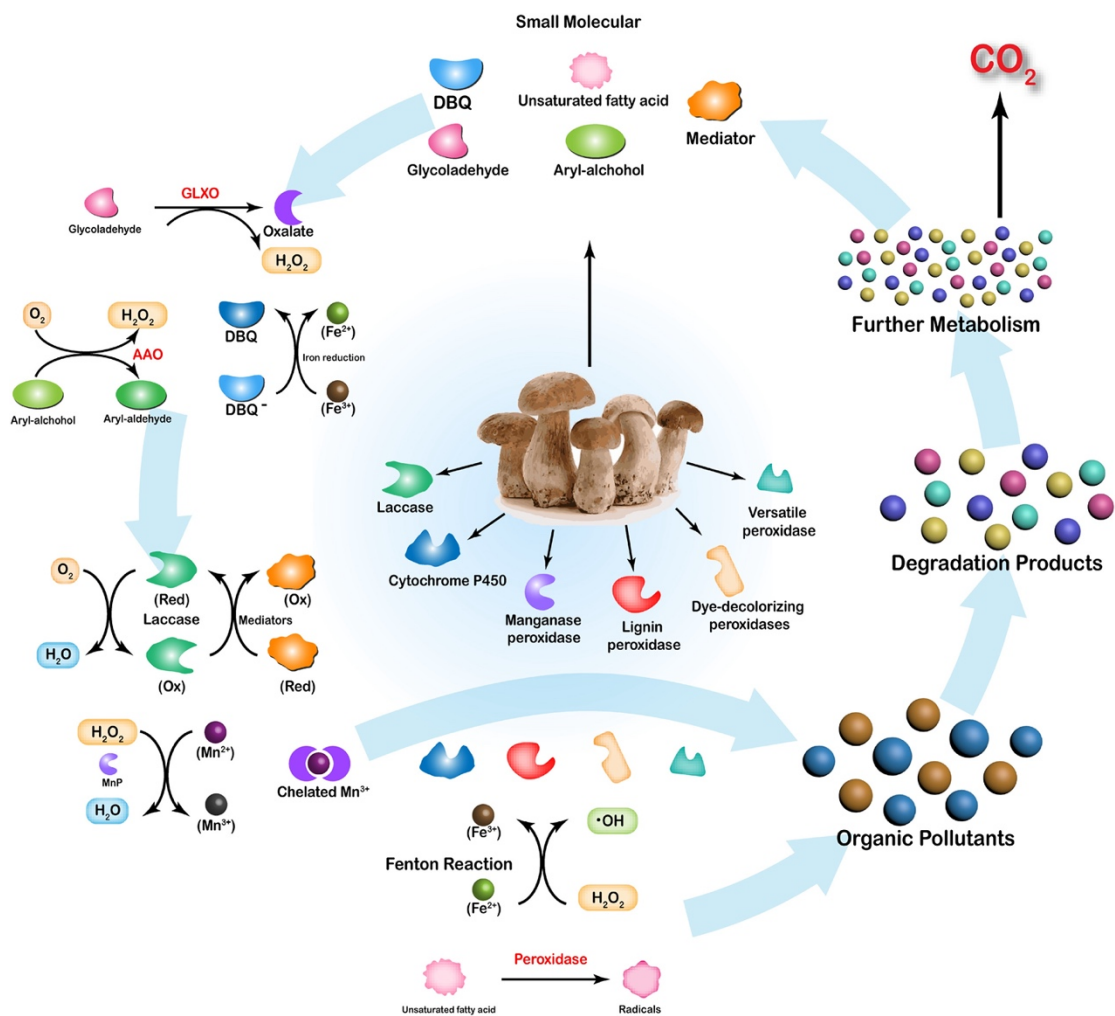
Figure 1.4 Mechanisms of organic pollutants degradation by white-rot fungi (Zhuo and Fan, 2021).

Table 1.7 Pesticides removal by different WRF.

Type	Chemical family	Substance	Time-substrate concentration-removal	WRF strains	Reference
Insecticide	Organochlorine	DDTs	NM-150 µg L^{-1}-> 65%	*Pleurotus ostreatus* OST-1	Sadiq et al., 2015
		Aldrin	14 d-0.25 µmol-72%	*Pleurotus ostreatus* BM9073	Purnomo et al., 2017
		Endosulfan	10 d-10 µM-> 90%	*Trametes hirsuta* IFO4917	Kamei et al., 2011
		Lindane	25 d-0.1 mmol L^{-1}-76%	*Phlebia brevispora* TMIC 34596	Xiao and Kondo, 2020
	Organophosphate	Chlorpyrifos	7 d-5 µg L^{-1}-95%	*Trametes versicolor* ATCC 42530	Torán, 2018
		Parathion	4 h-20 mM-97%	*Pleurotus ostreatus* 7989	Jauregui et al., 2003
		Malathion	12 h- 5 µg L^{-1}-100%	*Trametes versicolor* ATCC 42530	Torán, 2018
	Carbamates	Aldicarb	25 d-15 mg L^{-1}-73%	*Trametes versicolor* ATCC 42530	Rodríguez-Rodríguez et al., 2017
		Methomyl	33 d-15 mg L^{-1}-73%	*Trametes versicolor* ATCC 42530	Rodríguez-Rodríguez et al., 2017
		Methiocarb	30 d-3 mg L^{-1}-100%	*Trametes versicolor* ATCC 42530	Rodríguez-Rodríguez et al., 2017
		Carbofuran	44 d-20 mg L^{-1}-96%	*Trametes versicolor* ATCC 42530	Mir-Tutusaus et al., 2014
	Pyrethroid	Cypermethrin	15 d-10 mg L^{-1}-> 90%	*Trametes versicolor* ATCC 42530	Mir-Tutusaus et al., 2014
	Neonicotinoid	Acetamiprid	15 d-10 µM-45%	*Phanerochaete sordida* YK-624	Wang et al., 2012
		Imidacloprid	28 d-100 µM-100%	*Phanerochaete chrysosporium* ME446	Mori et al., 2021
		Thiacloprid	28 d-100 µM-> 50%	*Phanerochaete chrysosporium* ME446	Mori et al., 2021
		Clothianidin	20 d-100 µM -30%	*Phanerochaete sordida* YK-624	Mori et al., 2017
		Nitenpyram	5 d-100 µM-100%	*Phanerochaete sordida* YK-624	Wang et al., 2019b
		Dinotefuran	20 d-100 µM-31%	*Phanerochaete sordida* YK-624	Wang et al., 2019b
	Phenylpyrazole	Fipronil	9 d-800 µg L^{-1}-97%	*Trametes versicolor* ATCC 42530	Wolfand et al., 2016
Herbicide	Amide	Diflufenican	20 d-NM-> 70%	*Lentinula edodes*	Pinto et al., 2011
	Dinitroaniline	Pendimethalin	28 d-100 mg L^{-1}-95%	*Phanerochaete chrysosporium*	Belal and Elkhateeb, 2014

Note: DDT, dichloro-diphenyl-trichloroethane; NM, not mentioned.

Table 1.7 (cont)

Type	Chemical family	Substance	Time-substrate concentration-removal	WRF strains	Reference
Herbicide	Triazines	Terbuthylazine	10 d-25 mg L^{-1}-26%	*Lentinula edodes* EL1	Pinto et al., 2012
		Irgarol	3 d-5 µg L^{-1}-100%	*Trametes versicolor* ATCC 42530	Torán, 2018
		Simazine	7 d-5 µg L^{-1}-76%	*Trametes versicolor* ATCC 42530	Torán, 2018
	Ureas	Diuron	10 d-70 mg L^{-1}-94%	*Phanerochaete chrysosporium* ATCC 24725	Coelho-Moreira et al., 2013
	Benzothiadiazine	Bentazon	10 d-30 µM-90%	*Ganoderma lucidum*	Coelho et al., 2010b
	Phenoxy	2,4-D	42 d-25 mg L^{-1}-45%	*Phanerochaete chrysosporium* ATCC 34541	Yadav and Reddy, 1993
Fungicide	Triazole	Difenoconazole	10 d-19 mg L^{-1}-13%	*Lentinula edodes* EL1	Pinto et al., 2012
		Tebuconazole	41 d-10 mg L^{-1}-84%	*Trametes versicolor* ATCC 42530	Murillo-Zamora et al., 2017
	Imidazoles	Imazalil	30 d-50 mg L^{-1}-> 50%	*Trametes versicolor* DSMZ 11309	Karas et al., 2011
	Benzimidazole	Thiabendazole	30 d-50 mg L^{-1}-> 50%	*Trametes versicolor* DSMZ 11309	Karas et al., 2011
	Hydroxybiphenyl	2-Phenylphenol	10 d-50 mg L^{-1}-100%	*Trametes versicolor* DSMZ 11309	Karas et al., 2011
	Aniline	Diphenylamine	15 d-50 mg L^{-1}-100%	*Trametes versicolor* DSMZ 11309	Karas et al., 2011
	Phenylamide	Metalaxyl	42 d-10 mg L^{-1}-65%	*Stereum hirsutum* R97 BRE	Bending et al., 2002

Note: DDT, dichloro-diphenyl-trichloroethane; NM, not mentioned.

1.3.2 Fungal reactor

The application of fungal wastewater treatment in term of bioreactor can be achieved by either retaining or immobilizing biomass therein (Mir-Tutusaus and Sarrà, 2020). In the former scenario, adopting pellets formed by self-immobilization presents as a prominent strategy by which operational difficulties usually encountered with dispersed mycelium are available to be mitigated, such as insufficient mixing and volumetric productivity, clogging, adhesion to parts of the reactor, biomass separation, etc. (Espinosa-Ortiz et al., 2016; Mir-Tutusaus and Sarrà, 2020). Stirred tank reactor (STR), airlift reactor (AR), bubble column reactor (BCR) and fluidized bed reactor (FBR) are representative fungal pelleted reactors. Their advantages and limitations have been well discussed by Espinosa-Ortiz et al. (2016). Actually, our group (BioremUAB) has adequate experiences in micropollutants bioremediation using air pulse-fluidized bed reactor inoculated with fungal pellets. Although promising performances were attained under non-sterile conditions through different strategies, including pH adjustment, nutrients supplement at maintenance level (Cruz-Morató et al., 2013), partial biomass renovation and coagulation-flocculation pretreatment to reduce bacteria load (Mir-Tutusaus et al., 2017), economically FBR is an expensive option for long-term treatment. Besides, it will face some practical concern when scaling-up, like biomass separation from liquid phase during empty out. Hence, we keep attempting to seek for alternative candidates displaying high scale-up potential and operational longevity.

Except for fungal pelleted reactor, membrane bioreactor (MBR) and attached growth system treatment process to deal with micropollutants have attracted more attention from scientific community in recent years. Despite MBRs have been deemed as the most recent technology for the treatment of wastewater containing micropollutants, the major drawback of MBRs is fouling, which directly affects their working efficiency (Goswami et al., 2018; Guo et al., 2012; Kanaujiya et al., 2019). As another compelling biological alternative for wastewater treatment, the attached growth system offers advantages in different aspects: 1) high mass transfer; 2) high active biomass concentration; 3) stable performance 4) great flexibility; 5) low operational cost (Luo et al., 2014; Zhao et al., 2019). To our best

knowledge, various types of fungal biofilm reactors have been established and performed under non-sterile conditions, as followings:

a) Trickle bed reactor (TBR)

TBR is widely used to control and reduce fluid pollution, mainly odor abatement (Cohen, 2001; Malhautier et al., 2005; McNevin and Barford, 2000). So far there are several successful relevant examples using immobilized WRF to removal micropollutants. Torán (2018) set up a lab-scale TBR by immobilizing *T. versicolor* on pine wood chips to treat hospital wastewater. Along 49 days operation, ibuprofen, ketoprofen and naproxen were largely removed, while the bacterial contaminations, which presents as an obstacle in the way of full-scale application, was successfully dismissed. Then, she applied this set up into diuron removal from tap water, and a more than 80% yield was obtained. Instead of pine wood, rice husks were served as supporting material for *T. versicolor* too in the scenario of pharmaceuticals remove by TBR (Tormo-Budowski et al., 2021). Křesinová et al. (2018) immobilized *P. ostreatus* on wheat straw pellets with which a lab-scale TBR was filled. It was subsequently utilized to treat fortified WWTP effluent containing different endocrine disruptors (bisphenol A, estrone, 17β-estradiol, estriol, 17α-ethinylestradiol, triclosan and 4-n-nonylphenol), yielding about 95% removal. Afterwards, this configuration was scaled-up and successfully operated for 10 days. The same substrate and fungal species were also tested in lab- and pilot-scale TBR for polychlorinated biphenyls (PCBs) bioremediation. A highest degradation efficiency (87%) was recorded by lab-scale set up at low flow, and the scaled-up system exhibited different removal towards various PCBs during 71-day operation, ranging from 30% to 82%. On the other hand, other materials, such as plastic, sponge, foam, and ceramic coated with Ca-alginate film have been also adopted to immobilize WRF in the regime of TBR (Karimi et al., 2009; Novotný et al., 2011; Palli et al., 2016; Pocedič et al., 2009; Ruggeri and Sassi, 2003; Tavčar et al., 2006). However, the addition of lignocellulosic substrate is able to simulate natural fungal habitat wherein they may demonstrate sufficiently.

In this thesis, TBR was employed for addressing pesticides-contaminated wastewater in Chapter 5 and 6.

b) Packed bed channel bioreactor (PBCB)

Unlike TBR, PBCBs are constructed horizontally, which allows them to be more easily installed for *in-situ* treatment. A lab-scale PBCB was developed by Torán (2018), in which *T. versicolor* was immobilized on pine wood chips. Diuron removals from spiked tap water and agricultural wastewater were assessed successively by using the established reactor in a long-term continuous operation mode. Specifically, averagely up to 89% of spiked diuron was removed from tap water, while a little bit higher mean yield as 94% was reached when it comes to agricultural wastewater, possibly ascribed to the contribution from indigenous microorganism (Torán, 2018).

c) Rotating biological contactors (RBCs)

There are different demonstrations in this group. Beltrán-Flores et al. (2020) proposed an automatic agricultural wastewater treatment process by using a rotating drum bioreactor (RDB), which consists of an open channel and an internal tube. The internal tube was filled fungal colonized (*T. versicolor*) pine wood chips and equipped with electric motor that helped the drum rotate to ensure that all the wood chips were able to contact with water body. Therefore, this reactor is essentially an upgraded version from PBCB, and both of which belong to fixed bed bioreactors. During 16-day continuous operation, an effective average diuron elimination (61%) was gained. Cruz del Álamo et al. (2020) kept *T. versicolor* adhere on rotating polypropylene discs by operating with malt extract in fed-batch mode for 30 days. Then the growth medium was substituted by a synthetic urban wastewater during 20-day acclimation stage. Finally, the reactor was subjected to treat real urban WWTPs effluents under continuous mode. It is noteworthy that the authors introduced advanced bio-oxidation promoters to their process, which means it was a hybrid treatment. Anyway, this type of technique achieved remarkable reductions (70–75%) of the total organic carbon (TOC). Another reactor inspired by RBC is rotating suspension cartridge reactor that possesses meshed cartridges filled with polyurethane foam cubes covered by *P. chrysosporium*. The reactor was continuously operated for 160 days during which more than 50% of spiked carbamazepine was removed from synthetic wastewater. The highest efficiency (91%) was reached within Day 31–74 after one month adaptation

period (Li et al., 2016). Remarkably, immobilized biomass was intermittently submerged in the liquid phase regarding all those applications.

d) Moving bed bioreactor (MBB)

Moving packed bed reactor is another category of attached growth system, but the major discrepancy comes from the fact that biomass is grown on small carrier elements for which internal water stream of reactor facilitates fluidizing movement (Kermani et al., 2008). Some good WRF-based MBB examples have been documented. Park et al. (2011) investigated a pilot-scale dyeing wastewater treatment process where two aerobic MBBRs in series were comprised. Bardi et al. (2019) performed tannic acid removal tests in continuously fed, bench-scale, packed-bed reactor. All of them embedded ligninolytic fungi onto polyurethane foam (Bardi et al., 2019) or its modified material (Park et al., 2011).

e) Countercurrent seepage bioreactor (CSB)

A countercurrent seepage bioreactor is another option for WRF. Li et al. (2015) installed a WRF film reactor by immobilizing it on Chinese fir (*Cunninghamia lanceolata*) flakes. The reactor continuously operated in a countercurrent seepage mode for almost half a year, during which both naproxen and carbamazepine were considerably removed.

Chapter 2

Objectives

The main goal of the present thesis is to develop a pilot plant to treat agricultural wastewater by white-rot fungi under non-sterile conditions. In order to achieve this goal, the following specific objectives were formulated:

- To screen out one optimum fungus harboring the ability in degrading different pesticides, accompanied with identification of involved enzymatic system and transformation products.

- To set up a lab-scale trickle bed reactor with selected fungus immobilized on lignocellulosic carrier for spiked agricultural wastewater treatment under non-sterile conditions and compare its performance to the well established fluidized bed reactor.

- To apply the installed lab-scale TBR in pesticides elimination from real wastewater

- To scale-up the established configuration for continuously treating spiked agricultural wastewater under non-sterile conditions

Based on above aims, a technical route is drawn out as Figure 2.1.
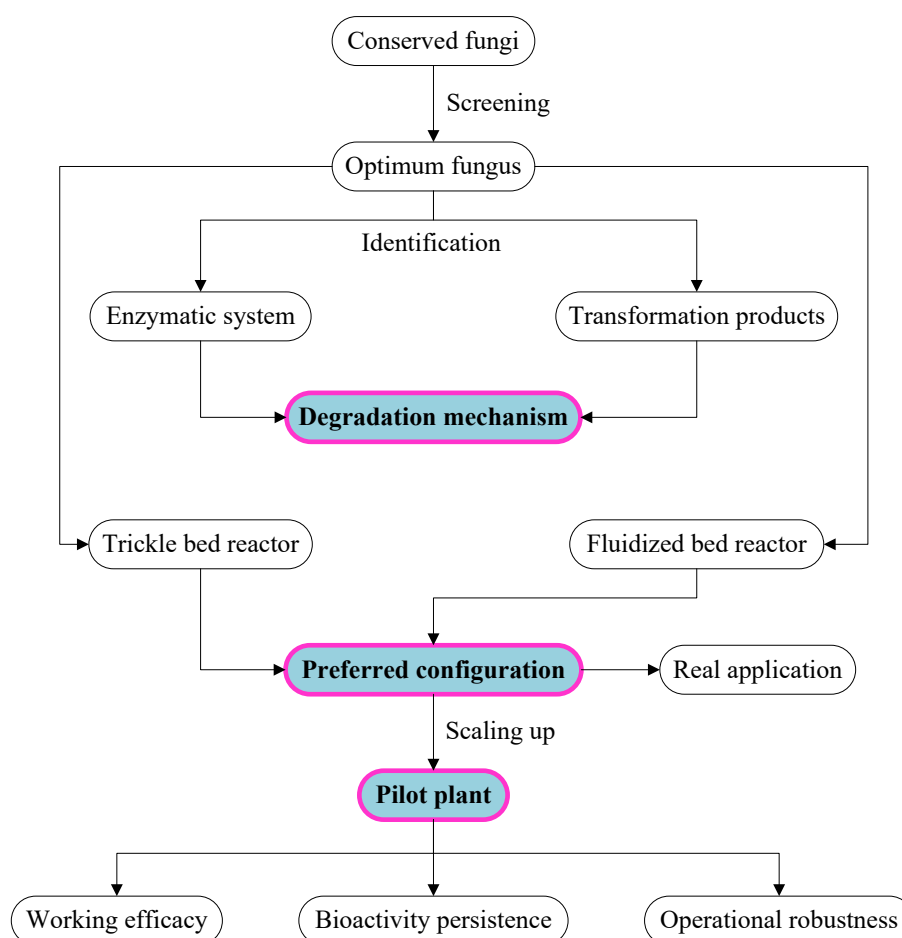
Figure 2.1 Technical route of the thesis.

Chapter 3

Materials and methods

3.1 Microorganisms and culture conditions

3.1.1 Fungal strain

Trametes versicolor ATCC 42530 was acquired from the American Type Culture Collection, *Ganoderma lucidum* (Leysser) Karsten FP-58537-Sp was kindly provided by Dr. C.A. Reddy, from the United States Department of Agriculture Forest Products Laboratory, *Gymnopilus luteofolius* FBCC 466 and *Stropharia rugosoannulata* FBCC 475 were obtained from the Fungal Biotechnology Culture Collection (FBCC) of the University of Helsinki (Finland), and *Pleurotus ostreatus* was isolated from a fruiting body collected from rotting wood (Palli et al., 2014) and preserved in our laboratory. Fungal strains were maintained by subculturing every 30 days on malt extract agar plates (pH 4.5) at 25 °C.

Blended mycelial suspension of each fungus was prepared according to a previously described method (Font et al., 2003). In brief, four agar plugs (1 cm^2) from grown Petri dish were transferred into 500 mL Erlenmeyer flasks containing 150 mL fresh malt extract medium. Then the culture was incubated at 25 ºC on an orbital shaker (135 rpm). After 6 days of incubation, the dense mycelial biomass was harvested by a strainer and subsequently homogenized using a T25 digital ULTRA-TURRAX® dispersers (IKA GmbH, Germany) in 0.85% (w/v) NaCl solution at a ratio of 1:1 (v/v). The resultant blended suspension could be immediately used for inoculation or stored at 4 ºC.

3.1.2 Pellets preparation

As described by Blánquez et al. (2004), pellets were produced in 1 L Erlenmeyer flask by inoculating 1 mL of the mycelial suspension into 250 mL of fresh malt extract medium (pH = 4.5). After 6 days of incubation under shaking condition (135 rpm) at 25 ºC, the pellets were collected with a strainer and washed with distilled water. They could be conserved in 0.85% (w/v) NaCl solution at 4 ºC for one month.

3.1.3 Fungal immobilization

Likewise, the immobilized fungal culture was also prepared by using mycelial suspension as inoculum. Briefly, after crushing and sieving, the obtained lignocellulosic

material ($3 \times 2 \times 0.5$ cm) was subjected to autoclave (121 ºC, 30 min). Then, the solid phase was separated using a strainer and inoculated according to the relation reported by Torán et al. (2017), as 3 mL inoculum per 10 g of lignocellulosic substrates. The incubation was performed statically in a polyvinyl chloride box at 25 ºC (Torán, 2018).

A diagram depicting above process is provided (Figure 3.1). All the manipulations were conducted aseptically.
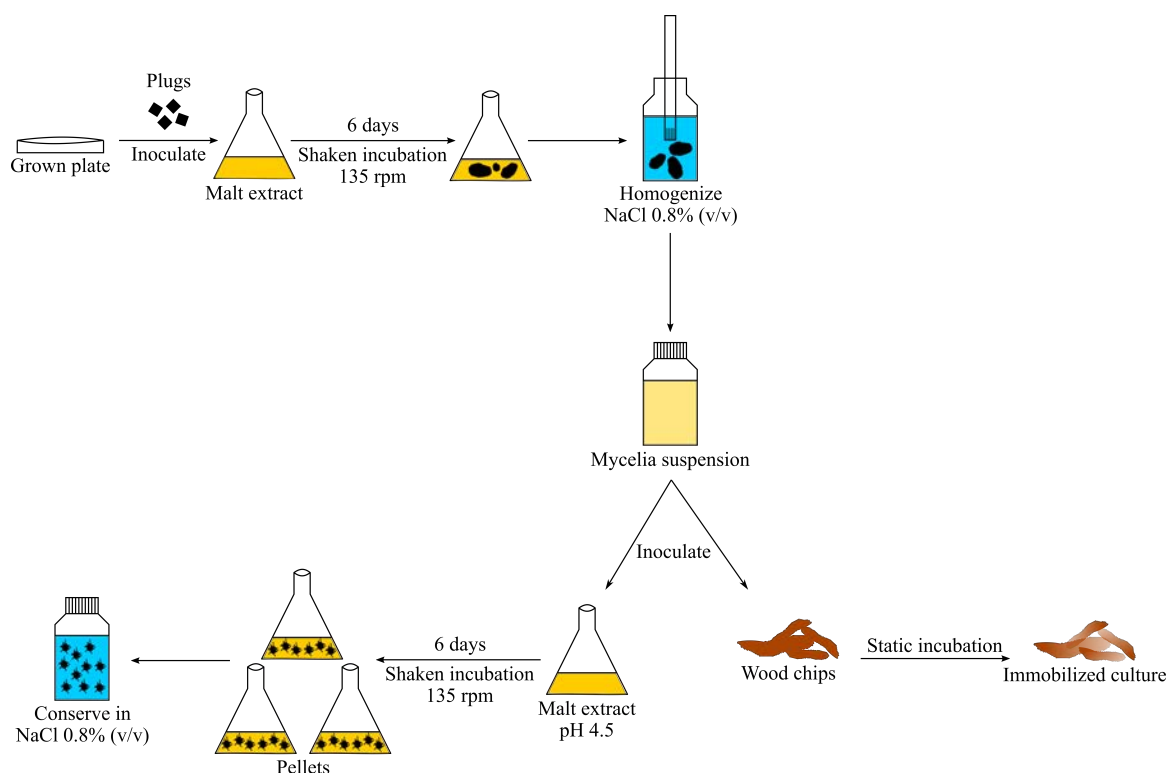
Figure 3.1 Scheme of methodology to obtain pellets and immobilized fungal culture.

3.1.4 Media

The concentration of malt extract medium used for agar plates, mycelial suspensions and pellets growth was 20 g L^{-1}.

The defined medium used in the batch experiments was modified from Kirk et al. (1978), consisting of (per liter) 8 g glucose, 3.3 g ammonium tartrate, 1.68 g dimethyl succinate, 10 mL micronutrients, and 100 mL macronutrients. pH was adjusted to 4.5 using HCl (1 M) and NaOH (1 M). The detailed compositions of micronutrients and macronutrients are given in Table 3.1.

All the media were autoclaved for 30 min at 121 ºC prior to use.

Table 3.1 Composition of micronutrients and macronutrients in defined medium.

Micronutrients	Concentration (g L^{-1})	Macronutrients	Concentration (g L^{-1})
Nitrile triacetic acidic	1.5	KH_2PO_4	20
$MgSO_4 \cdot 7H_2O$	3	$MgSO_4 \cdot 7H_2O$	5
$MnSO_4 \cdot H_2O$	0.5	$CaCl_2$	1
NaCl	1		
$FeSO_4 \cdot 7H_2O$	0.1		
$CoSO_4$	0.1		
$ZnSO_4 \cdot 7H_2O$	0.1		
$CaCl_2 \cdot 2H_2O$	0.1		
$CuSO_4 \cdot 5H_2O$	0.01		
$AlK(SO_4)_2 \cdot 12H_2O$	0.01		
H_3BO_3	0.01		
Na_2MoO_4	0.01		

3.2 Chemicals and regents

3.2.1 Pesticides

Diuron (purity, $\geq 98\%$) and analytical standards ($\geq 98\%$) of other pesticides, including bentazon, acetamiprid, imidacloprid, dicofol, chlorpyrifos and malathion, were purchased from Sigma-Aldrich (Barcelona, Spain). Diuron-d_6 was acquired from Toronto Research Chemicals (Ontario, Canada). Bentazone-d_7, acetamiprid-d_3, imidacloprid-d_5, malathion-d_{10}, d_{10}-chlorpyrifos and d_7-oxadiazon were obtained from Sigma-Aldrich (Barcelona, Spain). Those isotopically labeled analogs were utilized as internal standards (IS) for quantification purposes. Commercial herbicide KAOS-B (bentazon, 48%), used for spiking in reactors, was purchased from SAPEC AGRO (Barcelona, Spain). Stock solutions (10 mg mL^{-1}) of pesticides to be used for fungal treatment were prepared by appropriate dilution of the compounds in ethanol, while those for analytical purposes, e.g., TPs analysis, standard solutions were prepared in methanol at a concentration of 10 mg L^{-1}, except d_{10}-chlorpyrifos and d_7-oxadiazon that of 100 mg L^{-1}. All stock and working standard solutions were stored in the dark at $-20\ ^{\circ}C$ until use.

3.2.2 Other chemical compounds and regents

Commercial laccase purified from *T. versicolor* (20 AU mg^{-1}), laccase mediator 2,2'-azino-bis (3-ethylbenzothiazoline-6-sulfonic acid) diammonium salt (ABTS, 98%), 2,6-

dymetoxyphenol (DMP, 99%), cytochrome P450 inhibitor 1-aminobenzotriazole (98%) and ergosterol (> 95%) were purchased from Sigma-Aldrich (Barcelona, Spain). Microtox bioassay kit was supplied by Strategic Diagnostics Inc. (Newark, USA). Chromatographic grade acetonitrile was purchased from Carlo Erba Reagents S.A.S (Barcelona, Spain). High-performance liquid chromatography (HPLC)-grade water and methanol, formic acid ($\geq$ 98%) used as a mobile phase modifier, nitric acid ($\geq$ 69%) and ferric chloride were obtained from Merck (Darmstadt, Germany). PROSEDIM CS 209 was acquired from Degrémont Iberia (Spain). D(+)-Glucose was purchased from Acros Organics (New Jersey, USA). Ammonium chloride was obtained from Scharlau (Barcelona, Spain). Cyclohexane was purchased from labkem (Barcelona, Spain). All other chemicals used were of analytical grade and acquired from Sigma-Aldrich (Barcelona, Spain).

3.3 Lignocellulosic substrates and agricultural wastewater

a) Lignocellulosic substrate

Two different lignocellulosic substrates were employed in present work. They were pine wood (*Pinus* sp.) and oak wood (*Quercus ilex*). The origins of pine wood were different. The one used in screening step (Chapter 4) was kindly provided by Timgad S.A. (Polinyà, Barcelona, Spain), and another one adopted in Chapter 5 for lab-scale reactor was a generous gift from Embalatges Casajuana (Vidreres, Girona, Spain). The oak wood employed in Chapter 5 and 6 was collected from the forest located at Vidreres (Girona, Spain). All of them are waste products. They were stored at room temperature until use.

b) Agricultural wastewater

Agricultural wastewater (AW) was freshly collected from the irrigation channels located in Gavà (Parc Agrari Baix Llobregat, northeast of Catalonia, Spain) and Ebro River Delta area (southernmost of Catalonia, Spain) (Figure 3.2). The collected AW was stored at 4 °C until use.

Figure 3.2 Agricultural wastewater collection spots for fungal reactor experiments. a. Gavà (41°16'36.0"N 2°01'10.5"E); b. Ebro River Delta (40°42'05.08"N 0°45'47.44"E).

The collection date, location and other information are summarized in Table 3.2. All the AWs were fortified with diuron and bentazon except AW II, reaching a final concentration of 10 mg L^{-1} for both pollutants. It is also worthy to remark that the water collected from July to August 2020 (AW III and IV) required a coagulation-flocculation pretreatment due to the emerging algae biomass. Coagulant ferric chloride and flocculant PROSEDIM CS 209 were employed in this process, during which 2 min of coagulation at 200 rpm, 15 min of flocculation at 20 rpm and 30 min of settling were performed. Specifically, AW III and IV were pretreated with 40 mg L^{-1} of coagulant and 2 mg L^{-1} of flocculant, respectively.

Table 3.2 Agricultural wastewater information.

AW ID	Date of collection	Location	Experiment	Physicochemical characteristics	Spiking
AW I	05/02/2019	Gavà	Chapter 5	Table 5.1	Yes
AW II	18/06/2019	Ebro River Delta	Chapter 5	Table 5.3	No
AW III	09/07/2020	Gavà	Chapter 6	Table 5.2	Yes
AW IV	07/08/2020	Gavà	Chapter 5 and 6		
AW V	06/10/2020	Gavà	Chapter 6	Table 6.2	Yes
AW VI	09/12/2020				

3.4 Fungal reactors

There were in total three different reactors enlisted in this thesis, namely fluidized bed reactor, lab-scale trickle bed reactor and pilot-scale trickle bed reactor. The detailed configurations are as follow:

a) Fluidized bed reactor

A glass fluidized reactor was designed with a cylindrical vertical central body connected with a diametrically wider head (Figure 3.3). The useful volume was 1.5 L. The pH of liquid phase was controlled at a constant value of 4.5 by the addition of 1 M HCl or 1 M NaOH through several ports at the top. Air was introduced from the bottom using an electrovalve through which the fluidized condition (1 s air pulse every 4 s) in the central body was sustained. The aeration rate was approximately 0.8 L min^{-1}. FBR was employed in the screening process (Chapter 4) and comparative study (Chapter 5).
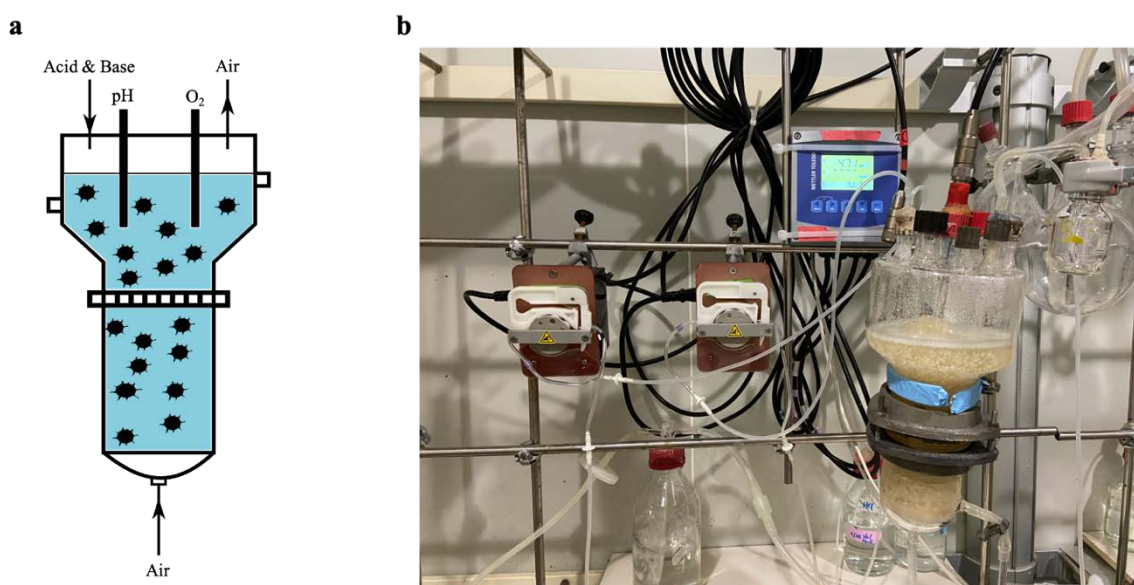
Figure 3.3 Air-pulsed fluidized bed reactor. a. schematic representation; b. actual configuration.

b) Lab-scale trickle bed reactor

As shown in Figure 3.4, a lab-scale trickle bed reactor essentially consists of a vertical cylindrical fixed bed, a liquid recirculation system and pH maintenance facility. After incubation, the fungal colonized wood chips were transferred into a methacrylate tube (Ø 8.3 cm, H 59 cm) and supported by a mesh, achieving an approximate working volume of 2.5 L and a porosity of 60%. The water was loaded into the packing bed from the top of the reactor through a rotary distributor and then collected by the reservoir tank placed at the bottom. The collected water was mixed by a magnetic stirrer, and its pH was maintained at 4.5 by adding either 1 M HCl or 1 M NaOH. An external bottom-to-top recirculation loop was provided, by which the collected water was continuously fed into the packing bed.

Simultaneously, an identical reactor filled with non-colonized chips was operated in parallel to assess the adsorption from the lignocellulosic supporting material. Lab-scale TBR was employed in Chapter 5 and running in sequencing batch mode.
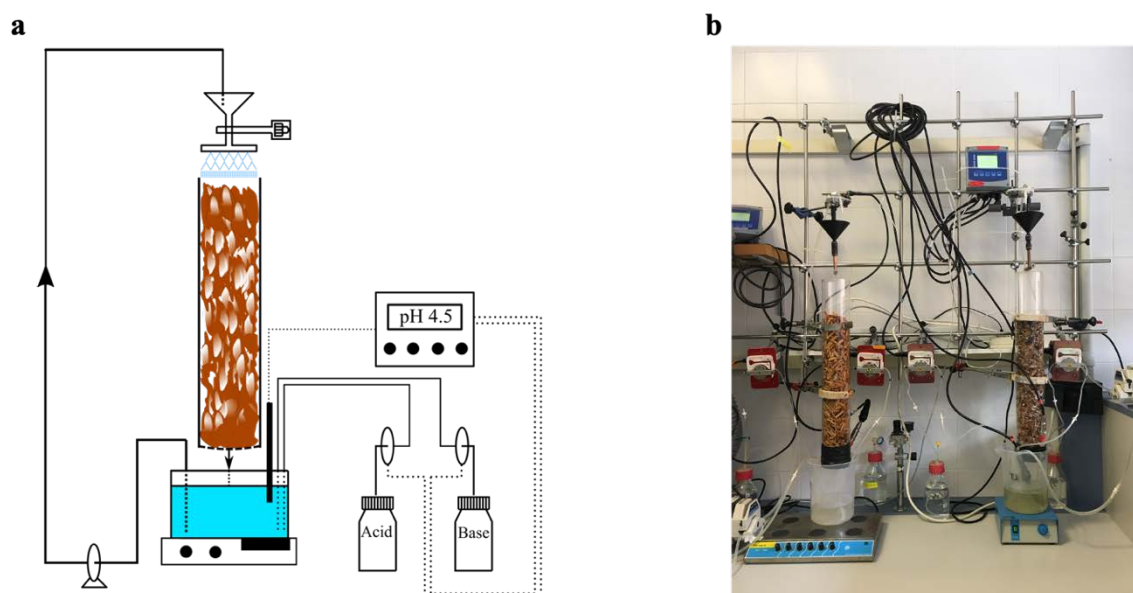
Figure 3.4 Lab-scale trickle bed reactor. a. schematic representation; b. actual configuration (Height: 1.1 m; packed bed length: 46 cm).

c) Pilot-scale trickle bed reactor

A scaled-up trickle bed reactor was constructed in Chapter 6 by joining four identical cylindrical methacrylate columns (Ø 11.7 cm, L 50 cm) filled with fungal solid culture (Figure 3.5). Each section was provided with a metal mesh that supported the filtering material. The total height, from reservoir to distributor, was 2.65 m. The working volume of the packing bed was approximately 17.2 L, with a same porosity of 60%. New spiked AW was fed into the external bottom-to-top recirculation loop through a peristaltic pump, while the effluent stream was drained by overflow through the outlet of the reservoir, reaching a continuous process. The collected water was mixed by an agitator, and its pH was kept at 4.5 as described above. Air was introduced from the bottom of the reactor, providing an aeration rate at approximately 0.5 L min^{-1}. Similarly, an identical reactor filled with non-colonized chips was operated simultaneously, to evaluate the removal contribution from the carrier adsorption.
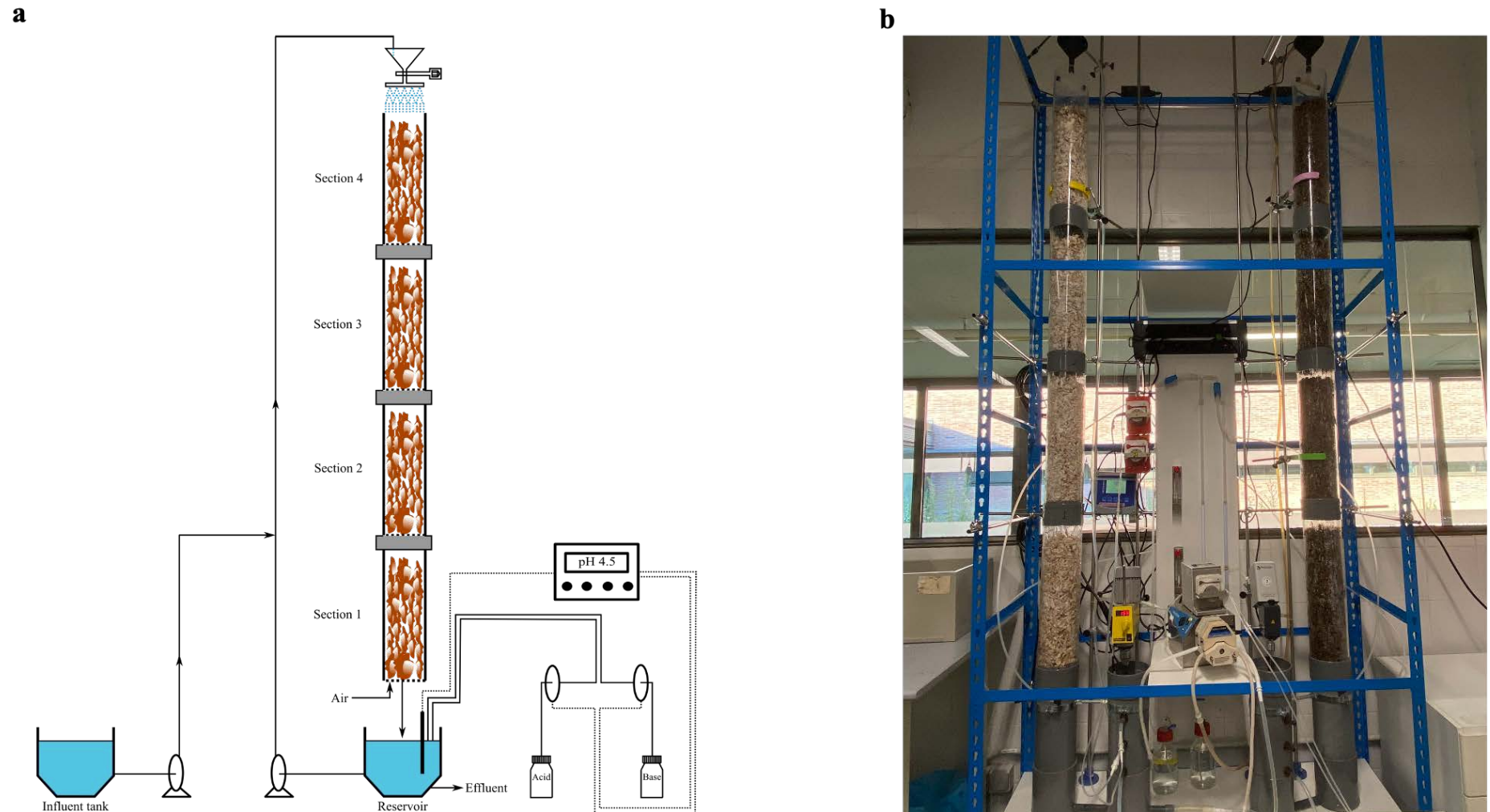
Figure 3.5 Pilot-scale trickle bed reactor. a. schematic representation; b. actual configuration (Height: 2.65 m; packed bed length: 1.6 m; treating capacity: 1.2 L d^{-1}).

3.5 Analytical methods

3.5.1 Diuron and bentazon residues

Samples were firstly filtrated using a Millipore Millex-GV unit equipped with a polyvinylidene difluoride (PVDF) membrane (0.22 μm). Then the residual diuron and bentazon concentrations were determined through HPLC (Ultimate 3000, Dionex, USA) equipped with a UV detector. Chromatographic separation was carried out with a mobile phase consisting of 0.01% (v/v) formic acid in water (A) and acetonitrile (B) at a flow rate of 0.9 mL min^{-1}, and a C18 reversed-phase column (Phenomenex®, Kinetex® EVO C18 100 Å, 4.6 mm × 150 mm, 5 μm) set at 30 °C. A gradient elution program was performed as follows: the percentage of B was 35% from 0 min to 0.5 min, then linearly increased to 45% from 0.51 min to 12 min, followed by dropping back to 35% in 1 min and maintaining at 35% for 2 min. The injection volume was 40 μL. The detection wavelength was set at 254 nm, and a limit of detection as 0.5 mg L^{-1} can be accomplished by using this analysis condition.

3.5.2 Laccase and manganese peroxidase activity

The extracellular enzymatic activities were measured as bioindicators of fungal activity and to assess the possible mechanisms of biodegradation. After filtration by 0.22 μm hydrophilic polypropylene syringe filter (Scharlau, Barcelona, Spain), laccase and manganese peroxidase (MnP) activity through the oxidation of DMP, depending on the fungal species. Laccase was merely measured for *T. versicolor*, where the DMP was oxidized in the absence of cofactor. By contrast, both Mn^{2+} (20 mM) and H$_2$O$_2$ (4 mM) were added in MnP analysis as described by Wariishi et al. (1992). The changes in the absorbance at 468 nm were monitored for 2 min on a Varian Cary 3 UV/Vis spectrophotometer at 30 °C. Activity units per liter (AU L^{-1}) are defined as the amount of DMP in μM which is oxidized in one minute. The molar extinction coefficient of DMP was 24.8 mM^{-1} cm^{-1} (Wariishi et al., 1992).

3.5.3 Biomass

3.5.3.1 Dry weight determination

Biomass in terms of pellets was determined by the dry weight, obtained after filtrating the culture and drying the residue at 105 °C to a constant weight.

3.5.3.2 Ergosterol extraction and quantification

The immobilized biomass in lignocellulosic culture was quantified adopting a modified method documented by Novotný et al. (1999). Specifically, after triturating by an analytical mill (A 11 basic, IKA GmbH, Germany), 0.5 g homogeneously mixed sample was transferred into a test tube, together with 1 mL cyclohexane and 3 mL KOH-methanol solution (10%, w/v). The mixture was subsequently sent to ultrasonication for 15 min (50/60 Hz, 360 W), followed by heating at 70 °C for 90 min. Then, 1 mL distilled water and 2 mL cyclohexane were added, before vortexing for 30 s and centrifuging at 3, 500 rpm for 5 min. The upper organic phase was collected while the aqueous phase was washed twice with 2 mL cyclohexane. The organic phases were pooled and evaporated to dryness by N_2 under moderate stream. The residue was re-dissolved in 1 mL methanol at 40 °C for 15 min. Afterwards, it was vortexed for 30 s and centrifuged at 6, 000 rpm for 3 min. The resultant solution was kept in 2 mL amber vial at − 20 °C prior to analysis. The quantification was achieved through HPLC (Ultimate 3000, Dionex, USA) equipped with a UV detector at 282 nm, using a C18 reverse phase column (Phenomenex®, Kinetex® EVO C18 100 Å, 4.6 mm × 150 mm, 5 µm). The isocratic elution was performed by acetonitrile (100%) at 1 mL min^{-1} with oven temperature of 35 °C, under which the retention time was 7.593 min. The injection volume was 40 µL.

3.5.4 Glucose concentration

The glucose concentration was measured using a biochemistry analyzer (2700 select, Yellow Springs Instrument, USA) after filtrating the sample with a Millipore Millex-GV PVDF syringe filter (0.22 µm).

3.5.5 Water characterization

The absorbance at 650 nm was determined by a UNICAM 8625 UV/VIS spectrometer, and the conductivity was monitored by a CRISON MicroCM 2100 conductometer. The total suspended solids (TSSs) and volatile suspended solids (VSSs) were measured according to the standard methods 2540 D and 2540 E (Baird et al., 2017), respectively. The total organic carbon (TOC) was determined using an Analytik Jena multi N/C 2100S/1 analyzer. The heterotrophic plate counts (HPCs) results were reported as the logarithm of colony-forming units (CFU) per mL [lg (CFU mL^{-1})] using the spread-plate method with a plate count agar (PCA) following the standard method 9215 (Baird et al., 2017). The N-NH_4^+ concentration and the chemical oxygen demand (COD) were analyzed by using the commercial kits LCK 303 and LCK 314 or LCK 114 or LCK 014 (Hach Lange, Germany). Chloride, sulfate, nitrite and nitrate anions were quantified by a Dionex ICS-2000 inorganic chromatograph equipped with a Dionex IonPac AS18-HC column (250 mm x 4 mm), which was eluted at 1 mL min^{-1} with a 13 mM KOH aqueous solution.

3.5.6 Pesticide residues extraction from wood chips and quantification

The extraction was performed by a modified method of Köck-Schulmeyer et al. (2013a) using one PSE extractor (Applied Separations, USA). Wood chips were firstly dried inside a fume hood at room temperature for 48 h and then triturated until homogenization by the A 11 basic analytical mill (IKA GmbH, Germany). 2 g wood powder was mixed with 0.5 g diatomaceous earth and loaded into a 22 mL cell. A mixture of acetone and dichloromethane (1:1, v/v) containing 1% (v/v) formic acid was used as extraction solvent. Temperature and pressure were settled at 100 °C and 100 bar, respectively. After 2 cycles with 5 min static time extraction, the obtained extracts were evaporated under nitrogen to dryness and the residue was reconstituted with 10 mL of methanol, followed by filtration (0.22 μm, PVDF) prior to analysis. The pesticide concentration was determined by using aforementioned HPLC-UV method.

3.5.7 Microbial community analysis

The analysis was conducted by the lab of Dr. Maira Martínez-Alonso and Dr. Núria Gaju,

from the Environmental Microbiology Group, Department of Genetics and Microbiology, Universitat Autónoma de Barcelona (Bellaterra, Spain). The methodology is clarified in Annex A.

Chapter 4

Pesticides degradation by fungi and their TPs

4.1 Introduction

To evaluate the occurrence and fate of pesticides in two agriculture-impacted Catalonian areas, i.e., Llobregat River Basin and Ebro River Delta, several sampling campaigns were performed in February and June 2017. Analysis results showed that diuron, dicofol, chlorpyrifos and malathion were frequently detected in Llobregat River Basin (Barbieri et al., 2020; Peris and Eljarrat, 2021), where diuron was the most ubiquitous pesticide (detection frequency of 100%) and imidacloprid was found at concentration above the acceptable method detection limits (Barbieri et al., 2020). In the scenario of Ebro River Delta, bentazon could be highlighted since it not only was one of the most widely distributed pesticides (detection frequency of 100%), but also found at the highest concentration of 18×10^4 ng L^{-1} (maximum). Apart from bentazon, chlorpyrifos can be also classified among the most ubiquitous pesticides in the investigated area, whereas imidacloprid and acetamiprid correspond to most abundant pesticides (Barbieri et al., 2021).

Specifically, diuron [3-(3,4-dichlorophenyl)-1,1-dimethylurea], a phenylurea herbicide, is used to control pre- and post- emergence weeds (Liu, 2014), and also available for mildew, algae and mosses (Barbieri et al., 2020; Giacomazzi and Cochet, 2004). Bentazon [3-isopropyl-1H-2,1,3-benzothiadiazin-4(3H)-one 2,2-dioxide] is a thiadiazine herbicide and used for address of broadleaf weeds as well as sedges (Gillespie et al., 2011). Dicofol [1,1-bis(chlorophenyl)-2,2,2-trichloroethanol], trade name Kelthane, as a structurally similar substitute for dichlorodiphenyltrichloroethane (DDT), is an organochlorine acaricide (Clark, 1990). Chlorpyrifos [O,O-diethyl O-3,5,6-trichloropyridin-2-yl phosphorothioate] which was first sold in 1975, is a chlorinated organophosphorus insecticide. It is also employed for ectoparasite control (Koshlukova and Reed, 2014). Likewise, malathion [diethyl 2-dimethoxyphosphinothioyl sulfanylbutanedioate] is an organophosphate insecticide, too (Reed and Rubin, 2014). It was first registered in the United States in 1956. Acetamiprid [(E)-N-(6-chloro-3-pyridylmethyl-N'-cyano-N-methylacetamidine] and imidacloprid [(E)-1-(6-chloro-3-pyridylmethyl-N-nitroimidazolidin-2-ylideneamine] are classified as neonicotinoids, the former is targeted at sucking-type insects (Wallace, 2014), whilst the latter is registered to control insect pests, as well as for grubs, termites, fleas and

ticks control (Sheets, 2014). All of them are extensively consumed in agriculture but also in industrial and urban environments.

However, growing evidence has shown that those pesticides are harmful to ecosystem and human health in several aspects (Anderson et al., 2015; Bonmatin et al., 2015; Giacomazzi and Cochet, 2004; Guyton et al., 2015; Huang et al., 2020; Koshlukova and Reed, 2014; Liu, 2014; Macedo et al., 2008; Reed and Rubin, 2014; Sheets, 2014; Turcant et al., 2003; UNEP, 2016; Wallace, 2014). Moreover, some of them can be degraded to products exhibiting higher toxicity or mobility than their parent compounds, such as diuron (Giacomazzi and Cochet, 2004), chlorpyrifos (Huang et al., 2020), acetamiprid and imidacloprid (Anderson et al., 2015). The last three plus malathion are indeed rated as moderately (acetamiprid) or highly (chlorpyrifos, imidacloprid and malathion) toxic for bees (MDA, 2020). Their exposure has been appointed as one of the causes of global pollinator decline, which represents a severe threat to biodiversity conservation and the maintenance of ecosystem services (Huang et al., 2020; Newhart, 2006; Sánchez-Bayo, 2014; Wang et al., 2020). Therefore, the co-occurrence of those pesticides in two investigated areas most likely deteriorates the water quality and poses a serious hazard for aquatic non-target organisms, further threatening the health of residents. Besides, those pesticides were repeatedly detected in Llobregat River Basin (Köck-Schulmeyer et al., 2012; Masiá et al., 2015) and Ebro River Delta (Ccanccapa et al., 2016; Köck-Schulmeyer et al., 2019; Köck et al., 2010) during last decade, ascribed either to their massive usage or to powerful persistence (Anderson et al., 2015; Giacomazzi and Cochet, 2004; Huang et al., 2020).

In this chapter, an optimal candidate was screened out from five different ligninolytic fungi (*T. versicolor*, *G. lucidum*, *S. rugosoannulata*, *G. luteofolius* and *P. ostreatus*) for pesticides-contaminated wastewater fungal treatment, by assessing the ability in degrading diuron, acetamiprid and imidacloprid, and the colonization performance on lignocellulosic substrate. Then, the degradation capacity of the optimum fungus towards bentazon was explored, together with the investigation of its enzymatic system involving in acetamiprid, imidacloprid and bentazon degradation. Finally, the fungal transformation products of target pesticides were identified, including diuron, bentazon, acetamiprid, imidacloprid,

dicofol, chlorpyrifos and malathion.

4.2 Specific methods in this chapter

4.2.1 Fungal selection for diuron removal

To select the best fungal species for diuron removal, degradation experiments were performed in 250 mL Erlenmeyer flasks containing 50 mL of defined medium fortified with diuron at a final concentration of 10 mg L^{-1}. Pellets of each fungus were transferred into flasks as inoculum, thereby achieving a mean concentration of approximately 3.1 g dry weight (DW) L^{-1}. Then the cultures were incubated at 25 °C under continuous orbital-shaking (135 rpm) for 7 days. To obviate the influence of photodegradation, the incubation was performed in the dark. Abiotic (uninoculated) and heat-killed culture (121 °C for 30 min) were used as controls. Each set was tested in triplicate. Aliquots were taken at specific time intervals during incubation to measure diuron and glucose concentrations.

4.2.2 Fungal selection for acetamiprid and imidacloprid removal

Degradation experiments for acetamiprid and imidacloprid were conducted in 1 L mL Erlenmeyer flasks and 1.5 L air pulsed fluidized bed reactor (FBR), successively. The Erlenmeyer contained 200 mL of defined medium, while the reactor carried 1.3 L. Even if an equal biomass as around 2 g DW L^{-1} was inoculated into both sets, there was discrepancy in pesticides fortification. Acetamiprid and imidacloprid were spiked simultaneously into the same Erlenmeyer flask culture, whereas there were treated individually by bioreactor. Meantime, the concentration of each pesticide was 10 mg L^{-1} in Erlenmeyer initially while it was brought down to 4 mg L^{-1} for reactor. Abiotic and heat-killed culture were prepared as described in 4.2.1, and each Erlenmeyer experiment was conducted in triplicate and incubated under the same conditions. The reactor was operated in the dark at 25 ºC for 7 days at a constant pH value of 4.5. Throughout the operation, glucose was regularly monitored and added to a concentration of 4 g L^{-1} before it was completely consumed. Two mL samples were withdrawn periodically for the analysis of the residual pesticide concentration, laccase activity and glucose concentration.

4.2.3 Fungal selection for colonizing on pine wood chips

Taking into account that our further objective is to establish a lab-scale trickle bed reactor immobilized with selected fungus on pine wood chips, therefore the colonization capacity on this particular lignocellulosic carrier by all the species were assessed except *T. versicolor*, since it has been already confirmed by Torán et al. (2017). Specifically, mycelial suspension of each fungus was inoculated on autoclaved (121 ºC, 30 min) pine wood chips according to the protocol in Chapter 3. The cultures were performed in 250 mL Schott bottles as described by Torán et al. (2017). The inoculation and incubation were processed aseptically. After incubating at 25 ºC for 20 days, samples were withdrawn and subjected to ergosterol measurement.

4.2.4 Degradation of bentazon by *T. versicolor*

Despite the bentazon degradation experiments by *T. versicolor* were roughly analogous to those on diuron degradation (4.2.1), some differences should be pointed out. Firstly, the concentration of pelleted inoculum was around 2.5 g DW L^{-1}. Secondly, samples were taken at specific intervals during incubation for measuring bentazon residues, laccase activity and glucose concentration.

4.2.5 Identification of enzymatic system involved in acetamiprid, imidacloprid and bentazon degradation

The degradation ability of four different pesticides by *T. versicolor* has been explored in above experiments, including diuron, acetamiprid, imidacloprid and bentazon. In order to better understand the degradation mechanisms, the enzymatic system participating the biodegradation process was subsequently investigated. The related research regarding diuron had been performed by Torán (2018), so present work focused on the remained three compounds.

a) Laccase

Laccase-mediated *in vitro* degradation experiments towards acetamiprid and imidacloprid were conducted in 250 mL Erlenmeyer flasks containing 20 mL laccase-

sodium malonate dibasic monohydrate solution (250 mM, pH 4.5) at a final enzyme activity of 1000 AU L^{-1}, and a pesticide concentration of 10 mg L^{-1}. The effect of having the laccase mediator ABTS (0.8 mM) in the system was evaluated by comparing with the results of culture where the mediator was not present (Marco-Urrea et al., 2009). Abiotic conditions (only the pesticide) were also explored. All experiments were run in triplicate. The flasks were incubated for 24 h on an orbital shaker (135 rpm) at 25 °C. At designated times, one mL aliquots were collected and mixed with 100 μL of 1 M HCl to stop the reaction, for determining acetamiprid and imidacloprid residues.

In the case of bentazon, all conditions were exactly the same except that the buffer solution was replaced by 50 mL dimethyl succinate solution (1.68 g L^{-1}, pH 4.5), owing to the adverse effect of malonate dibasic monohydrate on HPLC analysis. After 24 h, 1 mL more of the culture was withdrawn from the laccase control to measure the laccase activity. In addition to commercial laccase, the identification was also accomplished using broth. Briefly, pellets were transferred into 250 mL Erlenmeyer flasks containing 50 mL of defined medium, thereby achieving a concentration of approximately 2.5 g DW L^{-1}. Then, the culture was incubated at 25 °C under continuous orbital-shaking (135 rpm) for 3 or 4 days, and the pellets were sacrificed when there was no glucose in the medium. The resultant broth from centrifugation (10, 000 rpm, 15 min) was subsequently fortified with bentazon at 10 mg L^{-1}, followed by continuous incubation under the same conditions for 3 days, during which 2 mL sample was taken daily to determine bentazon concentration and laccase activity.

b) Cytochrome P450

For the involvement evaluation of cytochrome P450 (CYP50) system during the degradation process, *in vivo* experiments were carried out in the presence and the absence of 1-aminobenzotriazole, an inhibitor of the P450 system (Marco-Urrea et al., 2009). However, the degradation experiments were performed in FBR in the case of acetamiprid and imidacloprid, which is different from the referred report, and 4 mM of the inhibitor was introduced. Other conditions such as inoculation and operational parameters were identical to 4.2.2.

With regard to bentazon, *in vivo* degradation experiments were moved back to Erlenmeyer flasks, as conducted by Marco-Urrea et al. (2009), containing 2.5 g DW L^{-1} of fungal pellets and 5 mM of 1-aminobenzotriazole. Both inhibitor and inhibitor-free groups were prepared in triplicate and incubated for 42 h at 25 °C under continuous orbital-shaking (135 rpm).

One mL aliquots were collected at designated times during incubation period to analyze the residual pesticide concentration.

4.2.6 Identification of selected pesticides transformation products by *T. versicolor*

Biodegradation experiments for TPs identification of selected pesticides were all carried out in 500 mL Erlenmeyer flasks containing 100 mL of fresh defined medium, except acetamiprid and imidacloprid, where 1.5 L FBR with 1.3 L defined medium was employed. All the pesticides were spiked at 1 mg L^{-1} and *T. versicolor* pellets were averagely inoculated at 2.5 g DW L^{-1}. Cultures were incubated as described above, together with abiotic and heat-killed controls. In the scenario of bentazon, another control merely containing pellets was used to detect potential artifacts generated by fungus. Each experiment was conducted in triplicate. Samples were taken at specific intervals during incubation and then subjected to different pretreatments according to their physical-chemical properties as compiled in Table 4.1 (PAN Pesticides Database, 2020; PPDB, 2016).

Table 4.1 The physical-chemical properties of the investigated pesticides.

Group	Pesticides	CAS number	Solubility	Log K_{ow}	K_{oc}
Hydrophobic	Dicofol	115-32-2	0.8	4.3	6, 064
	Chlorpyrifos	2921-88-2	1.05	4.7	5, 509
Hydrophilic	Malathion	121-75-5	148	2.75	1, 800
	Diuron	330-54-1	35.6	2.87	680
	Acetamiprid	135410-20-7	2, 950	0.80	200
	Imidacloprid	138261-41-3	610	0.57	262
	Bentazon	25057-89-0	7, 112	$-$ 0.46	55.3

a) Hydrophobic

Each Erlenmeyer flask was totally sacrificed and the culture was firstly filtrated with Whatman^{TM} glass microfiber filter (GF/A, 47 mm). 20 mL of obtained filtrate was then mixed with 50 μL of internal standard (IS) methanol solution (d$_{10}$-chlorpyrifos or d$_7$-oxadiazon, 100 mg L^{-1}), followed by adding filtrate up to 50 mL. Afterward, samples were kept at $-$ 20 °C prior to analysis.

b) Hydrophilic

4 mL of the culture was withdrawn and centrifuged (10, 000 rpm, 4 min) at room temperature. Then, 1.5 mL of the supernatant was transferred into a 2-mL amber vial that contained 0.75 μg of the corresponding deuterium-labeled pesticide that was used as IS. The samples were kept at $-$ 20 °C until analysis.

4.2.7 Analytical methods

4.2.7.1 Acetamiprid and imidacloprid concentrations

Residual concentrations of acetamiprid and imidacloprid were determined using HPLC-UV method (Ultimate 3000, Dionex, USA). HPLC analysis was performed with a mobile phase consisting of 0.01% (v/v) formic acid in water and acetonitrile (60:40, v/v) at a flow rate of 0.7 mL min^{-1}, and a C18 reversed-phase column (Phenomenex$^®$, Kinetex$^®$ EVO C18 100 Å, 4.6 mm × 150 mm, 5 μm) set at 30 °C. The injection volume was 40 μL. The detection wavelengths for acetamiprid and imidacloprid were 242 and 270 nm, respectively.

4.2.7.2 Evaluation and identification of TPs

The identification was conducted by Water, Environmental and Food Chemistry Unit

(ENFOCHEM) from Institute of Environmental Assessment and Water Research (IDAEA-CSIC) according to the following methodology. Specifically, TPs of hydrophobic pesticides were analyzed by the group of Dr. Ethel Eljarrat, and the group led by Miren López de Alda was responsible for hydrophilic pesticides.

a) Hydrophobic

The sample from dicofol and chlorpyrifos degradation experiments were subjected to separation by an Acquity ultra performance liquid chromatography (UPLC) system (Waters, USA) equipped with a Purospher® STAR RP-18 endacapped Hibar® HR (150 × 2.1 mm, 2 µm) UPLC column (Merck, Germany). Methanol and water both containing 0.1% (v/v) formic acid were used as mobile phases A and B, respectively. A gradient elution program was started with 80% (v/v) B from 0 min to 1 min, decreasing to 5% at 8 min and held until 13 min. Then, the percentage of B was further reverted to 80% by 13.5 min and maintained it until 15 min. The follow rate was 0.2 mL min^{-1} with an injection volume of 10 µL. The UPLC system was coupled to a hybrid quadrupole-Orbitrap mass spectrometer Q-Exactive (Thermo Fisher Scientific, USA) equipped with a heated-electrospray ionization source HESI II, which was operated in positive ionization mode under the following conditions: spray voltage, + 3.0 kV; sheath gas, 40 arbitrary units; auxiliary gas, 10 arbitrary units; sweep gas, 2 arbitrary units; capillary temperature, 350 °C and vaporizer temperature, 300 °C. Nitrogen (> 99.98%) was employed as sheath, auxiliary and sweep gas. The mass spectrometer performed a Fourier Transform Mass Spectrometry (FTMS) scan event of 50–700 m/z at a resolution of 70, 000 and a subsequent MS/MS scan event acquired at a resolution of 35, 000. Xcalibur software (Thermo Fisher Scientific, USA) was employed for instrumental control and data processing.

In the case of post-acquisition MS data processing, the total ion current (TIC) chromatograms acquired at different sampling time were compared using Compound Discoverer (Thermo Fisher Scientific, USA), which allows performing differential analysis among selected sets of samples comparing simultaneously thousands of MS spectra, to identify all potential TPs. Accurate mass of the potential TPs was then extracted in Xcalibur to confirm their presence. Identification of the potential TPs was based on their accurate

mass, mass error, molecular formula and degree of unsaturation of the parent ion and product ions.

b) Hydrophilic

The TPs of hydrophilic pesticides formed during the degradation process were evaluated using UPLC-high resolution mass spectrometry (HRMS) system Acquity (Waters, USA) coupled to a hybrid quadrupole-Orbitrap mass spectrometer (Q-Exactive) (Thermo Fisher Scientific, USA), equipped with a heated electrospray ionization source (HESI). Chromatographic separation was achieved with a Purospher® STAR RP-18 endcapped Hibar® HR (150 × 2.1 mm, 2 µm) column (Merck, Germany) and a linear gradient of the organic constituent of the mobile phase. Two chromatographic runs were performed to analyse independently the samples under the electrospray positive ionization (ESI+) and negative ionization (ESI–) modes unless otherwise specified. The mobile phase used for ESI+ analyses consisted of water with and methanol, both with 0.1% of formic acid at a flow rate of 0.2 mL min^{-1}. In the ESI– analyses, a mobile phase consisting of water and acetonitrile at a flow rate of 0.3 mL min^{-1} was used. The linear organic gradient used was as follows: 5% for 1 min, increased to 20% in 2 min, to 80% in next 3 min, and to 100% in 1 more min. Pure organic conditions were maintained for 2 min and then decreased to the initial conditions (5%) in 0.5 min, held for 4.5 min for column re-equilibration. The injection volume was 10 µL.

The ESI interface was operated in all cases using the following specific conditions unless otherwise specified: spray voltage, 3.0 kV; sheath gas flow rate, 40 arbitrary units; auxiliary gas, 10 arbitrary units; capillary temperature, 350 ºC, and vaporizer temperature, 400 ºC. Nitrogen (> 99.98%) was employed as sheath, auxiliary and sweep gas. Accurate mass detection was conducted in data-dependent acquisition (DDA) mode. First, a full MS scan was done within the m/z range 70–1, 000 at 70, 000 full width at half maximum (FWHM) resolution (at m/z 200). Then, data-dependent MS/MS scan events (17, 500 FWHM resolution at m/z 200) were recorded for the five most intense ions (> 10e^5) detected in each scan, with a normalized collision energy of 40%. Data acquisition was controlled by Xcalibur software (Thermo Fisher Scientific, USA).

Malathion was analyzed in the positive ionization mode and quantified using the full scan response of its molecular ion $[M + H]^+$. The quantification of malathion residual concentrations in the samples was performed by the internal standard method using its deuterated analogue (malthion-d_{10}), and a 6-point solvent-based calibration curve. Bentazon was analyzed in the negative mode with the capillary voltage at $-2.5\,kV$, adopting an organic gradient of a mobile phase consisting of water with 20 mM of ammonium acetate (A) and acetonitrile (B) at a constant flow rate of $0.3\,mL\,min^{-1}$. The m/z range for full MS scan covered from 70 to 600.

The acquired UPLC-HRMS data were processed using Compound Discover 3.1 software (Thermo Fisher Scientific, USA). Experimental samples collected intermediately were compared with samples at t = 0 as well as controls to identify newly formed peaks or features. After peak alignment and deconvolution (using a retention time window of 2 min and 5 ppm of mass tolerance), the features (m/z ions) detected were grouped and plausible elemental compositions were assigned to each peak. In parallel, a search by molecular formula or exact mass was performed in various MS libraries and compound databases (ChemSpider, mzCloud, mzVault) to assign a potential compound identity to each peak. Then, the list of potential candidates generated was manually filtered to identify TPs, i.e., those peaks that were only present in samples collected intermediately during degradation, and evaluate the molecular structures proposed by the software. The latter was done using the elemental composition of the molecular and fragment ions, logical fragment rationalization, and considering the presence of isotopic patterns.

4.2.7.3 Microtox Test

The acute toxicity of sample was measured using a Microtox bioluminescence assay. This assay allows monitoring the natural emission (in the range of the visible light, with a maximum intensity at 490 nm) of the marine bioluminescent bacterium *Vibrio fischeri* after exposure to selected samples. Toxicity data, corresponding to the 50% effective concentration (EC_{50}), were based on 5 and 15 min incubation of bacteria with filtered diluted samples (pH 7) at 25 °C. Toxicity was expressed as toxicity units (TU), calculated by $TU = 100/EC_{50}$.

4.3 Results and discussions

Prior to present the results, it is necessary to point out that all the experiments included in present chapter were conducted in Department of Chemical, Biological and Environmental Engineering at Escola d'Enginyeria (UAB) except TPs identification analysis (Section 4.3.4), which was responsible by IDAEA-CSIC (Barcelona, Spain) and some relevant results are presented in Annex B.

4.3.1 Fungal screening

4.3.1.1 Diuron

The screening step was conducted using diuron as substrate in the first place, and Figure 4.1 depicts the degradation ability of different white-rote fungi. As can be seen, diuron in abiotic controls showed high chemical stability during 7 days of incubation, which means that any removal obtained in experimental setups must be exclusively attributed to fungal sorption and biodegradation mechanisms. The five tested microorganisms demonstrated different diuron elimination efficiencies, ranging from 18% to 100%. Although there were small differences, the variation patterns of diuron concentration in each heat-killed fungal culture were essentially similar, showing an initial fast drop due to sorption onto the biomass, after which concentration remined stable. Thus, adsorption contributed to diuron removal at some level. This matches well with the findings reported by Lucas et al. (2018) where pharmaceuticals were eliminated by different WRF. The global adsorption was 13% on average and it's more than double than that acquired towards other xenobiotics possessing similar or higher hydrophobicity than diuron (Log K_{ow} 2.87), i.e., venlafaxine (Log K_{ow} 3.28) and carbamazepine (Log K_{ow} 2.45) (Lucas et al., 2018). Therefore, it is fair to suppose that the adsorption of compound onto biomass may be governed by other physical-chemical characteristics (e.g., pK_a, or water solubility). In addition, there is possibility that active transport participated in the sorption process by living cells, while it was inactive in killed control.
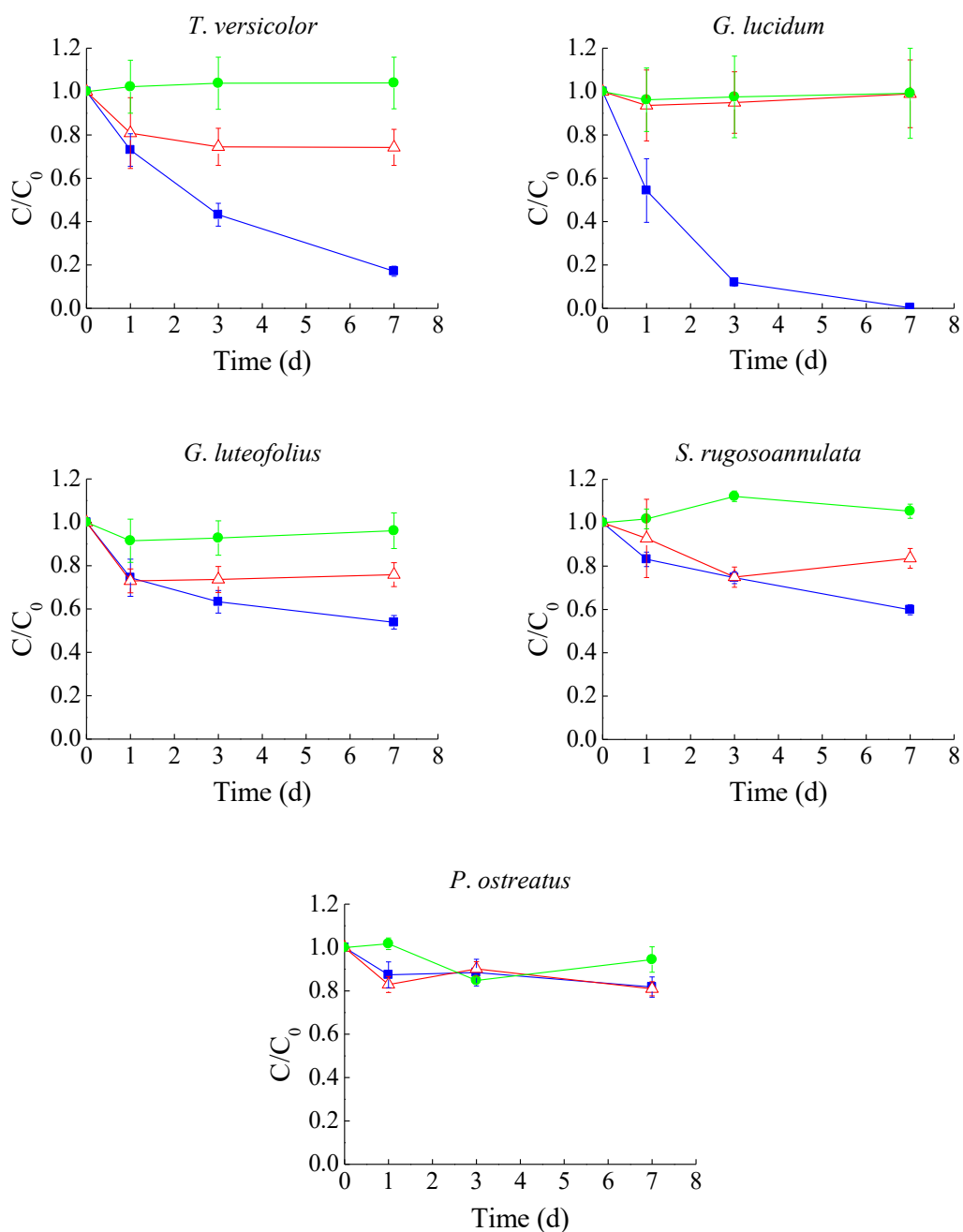
Figure 4.1 Time-course degradation of diuron by different fungi. C represents the residual concentration of diuron in the sample (mg L^{-1}), and C$_0$ corresponds to the initial concentration of diuron in the sample (mg L^{-1}); *Blue lines with filled squares*, experimental; *red lines with empty triangles*, killed control; *green lines with filled circles*, abiotic. Average values of three replicates with the corresponding standard deviations are shown.

With respect to glucose, its concentration plunged to almost zero in the culture of *T. versicolor*, *G. lucidum*, *G. luteofolius*, and *S. rugosoannulata* after one week (Table 4.2). Despite the capability of *P. ostratus* in degrading different contaminants such as plastic, organochlorine pesticides, and polycyclic aromatic hydrocarbons has been well evidenced

(Bhattacharya et al., 2014; da Luz et al., 2013; Purnomo et al., 2010; Purnomo et al., 2017), an exceptional scenario was depicted in diuron degradation, as it presented a much lower consumption of glucose than the other investigated fungi, with a final concentration of 4.85 g L^{-1}. This is indicative of a lower metabolism of this fungal strain as compared to the others, which results in nearly no biodegradation (Figure 4.1). A similar observation was reported regarding the degradation of venlafaxine by this species in an analogous medium (Llorca et al., 2019), in spite that it showed excellent performance for the removal of other pharmaceuticals, namely, diclofenac, ketoprofen, and atenolol, in sterile hospital wastewater (Palli et al., 2017). Hence, further research is needed to address the mechanisms behind this selective performance.

Table 4.2 Variations of glucose concentration (g L^{-1}) in the fungal cultures during diuron degradation.

Fungus	Incubation time (d)			
	0	1	3	7
T. versicolor	7.00 ± 0.13	5.35 ± 0.16	1.83 ± 0.40	< 0.01
G. lucidum	6.26 ± 0.43	4.92 ± 0.10	0.96 ± 0.01	0.02 ± 0.00
G. luteofolius	6.63 ± 0.10	4.77 ± 0.02	0.54 ± 0.29	< 0.01
S. rugosoannulata	7.02 ± 0.13	4.34 ± 0.02	< 0.01	ND
P. ostreatus	7.01 ± 0.12	6.21 ± 0.09	5.67 ± 0.05	4.85 ± 0.10

Note: Each value of glucose concentration represents the mean of triplicate measurements ± standard deviation (SD). ND: no detected.

This is the first proof that shows the potential of *S. rugosoannulata* to degrade diuron, thus enriching the diuron-degrading microbe pool. Given that notable higher removal yields observed from *T. versicolor* and *G. lucidum* in comparison with other investigated species, they were selected as candidates for further screening.

4.3.1.2 Acetamiprid and imidacloprid

The screening was subsequently proceeded through targeting acetamiprid and imidacloprid degradation by those two candidates, owing to the fact that both can be categorized into the most abundant pesticides in Ebro River Delta (Barbieri et al., 2021) and they are frequently found in aquatic environment around the world (Anderson et al., 2015; Hladik et al., 2014; Klarich et al., 2017). In addition, they are included in European Union Watch List (Pietrzak et al., 2019). The profiles of acetamiprid and imidacloprid

removals in biotic, heat-killed, and abiotic experiments using Erlenmeyer flasks are presented in Figure 4.2. It is observed that the fortified pollutants were only slightly removed (11% in average), even though glucose was substantially consumed by the end of experiment (Table 4.3). This is probably due to the effect of the low pH (pH < 4 after 3 d) generated from the acid secretion by the fungi that further hindered their metabolism, which was worse in the culture of *G. lucidum* (Table 4.3) and it reflected in poor removal (7% in average). Besides, simultaneously spiking two pesticides possibly caused high toxic effect to fungus.
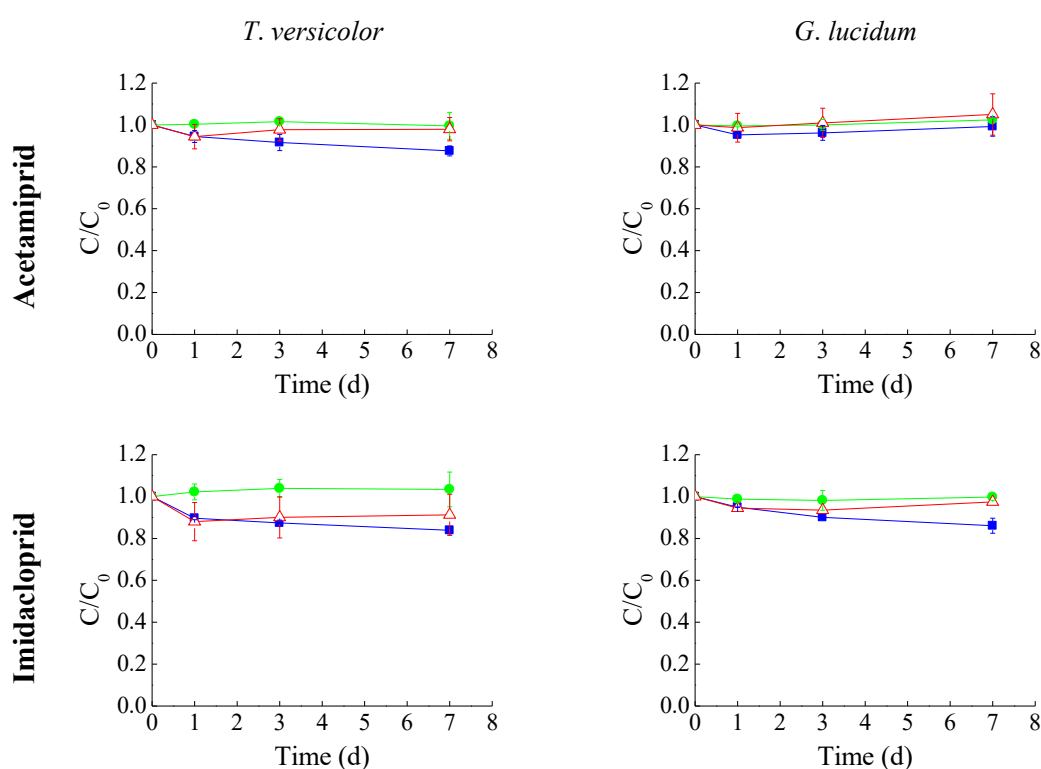
Figure 4.2 Time-course of neonicotinoids degradation by different fungi in Erlenmeyer flask. C represents the residual concentration of the pesticide in the sample (mg L^{-1}), and C_0 corresponds to the initial concentration of the pesticide in the sample (mg L^{-1}); *Blue lines with filled squares*, experimental reactor; *red lines with empty triangles*, killed control; *green lines with filled circles*, abiotic control; *purple lines with inverted filled triangles*, laccase activity in the experimental reactor.

Table 4.3 Variations of glucose concentration and pH in the fungal cultures during neonicotinoids degradation.

Fungi	Incubation time (d)	Glucose concentration (g L^{-1})	pH
T. versicolor	1	4.35 ± 0.32	4.48 ± 0.08
	2	< 0.01	4.14 ± 0.10
	3	< 0.01	3.84 ± 0.04
G. lucidum	1	5.94 ± 0.03	4.32 ± 0.05
	2	4.00 ± 0.16	3.87 ± 0.02
	3	0.24 ± 0.33	3.57 ± 0.05

Note: Each value of glucose concentration and pH represents the mean of triplicate measurements ± SD.

Thus, air-pulsed fluidized bed reactor equipped with a pH controller was subsequently employed, in which less pesticides (4 mg L^{-1}) were individually spiked. In this scenario, *T. versicolor* was able to degrade 20% and 65% of acetamiprid and imidacloprid, respectively, whereas yields were 10% and 15% respectively when it comes to *G. lucidum* (Figure 4.3). On the other hand, significantly higher laccase activities were measured using *T. versicolor* compared to *G. lucidum*. In the regime of WRF, so far only *Phanerochaete* spp. have been reported to harbor the capacity to degrade acetamiprid (Wang et al., 2012) and imidaclorprid (Mori et al., 2021; Xie et al., 2020). Now *T. versicolor* and *G. lucidum* appear as another two ligninolytic fungi candidates that can be used in bioremediation treatment.
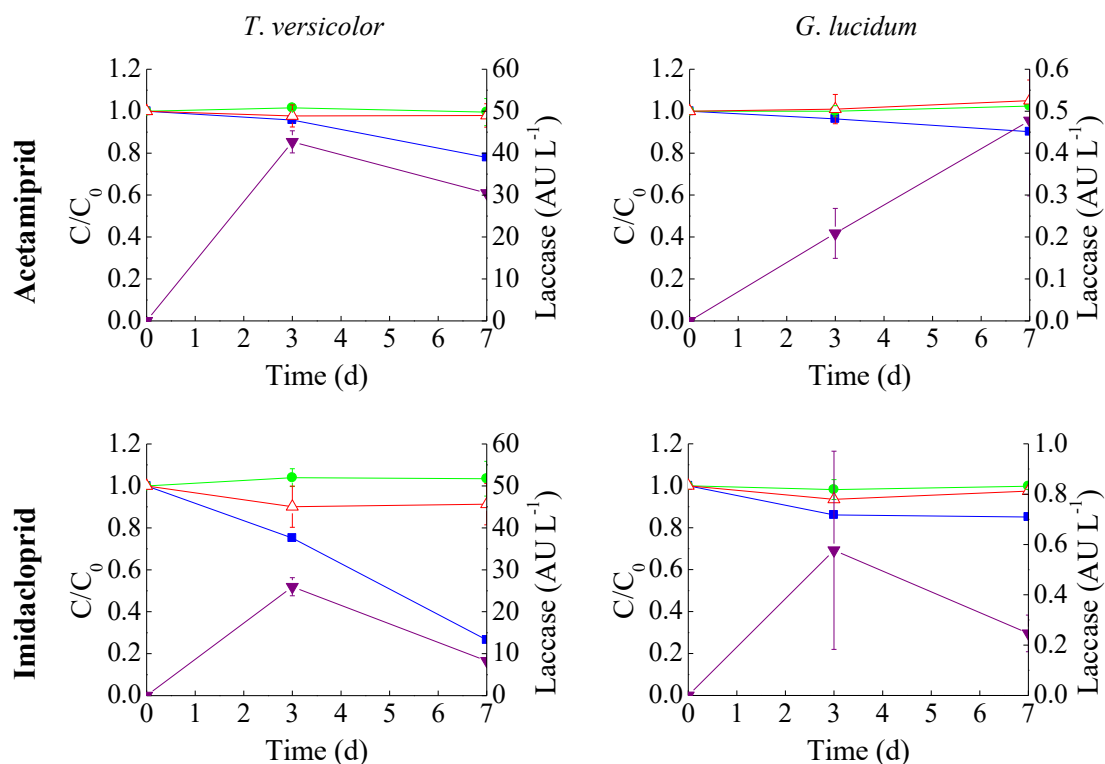
Figure 4.3 Time-course of neonicotinoids degradation by different fungi in fluidized bed reactor. C represents the residual concentration of the pesticide in the sample (mg L^{-1}), and C_0 corresponds to the initial concentration of the pesticide in the sample (mg L^{-1}); *Blue lines with filled squares*, experimental reactor; *red lines with empty triangles*, killed control; *green lines with filled circles*, abiotic control; *purple lines with inverted filled triangles*, laccase activity in the experimental reactor.

4.3.1.3 Fungal colonization on pine wood chips

As a crucial criterion in assessing performance of fixed bed bioreactor, the attachment of biomass governs its removal efficacy. Hence, the colonization of different fungi on pine wood chips was also evaluated. Results reveals that the use of pine wood is more beneficial for *G. lucidum* growth than other three species (Table 4.4), however *T. versicolor* is a profitable alternative since a biomass amount as 0.031 ± 0.002 mg g^{-1} DW^{-1} was obtained by only 9 days (Torán et al., 2017).

Table 4.4 Evaluation of fungal colonization on pine wood after 20 days incubation.

Fungi	Ergosterol (mg g^{-1} DW^{-1})
G. lucidum	0.039 ± 0.004
S. rugosoannulata	0.030 ± 0.005
P. ostreatus	0.034 ± 0.001
G. luteofolius	0.014 ± 0.009

Note: Each value of ergosterol content represents the mean of triplicate ± SD.

To sum up, *T. versicolor* was ultimately chosen for subsequent research because of its most outstanding performances in pesticides degradation and lignocellulosic substrate colonization among all tested fungi.

4.3.2 Bentazon degradation by *T. versicolor*

As mentioned before another point of concern is that bentazon demonstrates the highest ubiquity and residual level among the detected pesticides in Ebro River Delta (Barbieri et al., 2021). Like diuron, bentazon has been included in the priority substance list by the European Commission (EC, 2008) and it widespreadly emerges in different water bodies around the Europe (Hedegaard et al., 2020; Papadakis et al., 2018). Besides, its low affinity to soil (K_{oc} = 55.3) and high solubility in water (7, 112 mg L^{-1}) (PPDB, 2016) render bentazon high mobility, threatening the aquatic environment. So, the ability of *T. versicolor* in degrading this contaminant was further explored. Figure 4.4 depicts its removal in Erlenmeyer flasks under different conditions. Apparently, *T. versicolor* could deplete bentazon in an efficient way, displaying as complete removal 10 mg L^{-1} of it within 3 days. Comparing with the abiotic control, 9% decay in bentazon concentration occurred in heat-killed culture, which could be ascribed to adsorption of the contaminant onto biomass. A maximum laccase activity (9 AU L^{-1}) was also reached on the third incubation day and then declined. Concerning glucose, it was almost completely utilized after 3 days. To our knowledge, this is the first time that *T. versicolor* has been applied in the bentazon elimination.

Figure 4.4 Time-course of bentazon degradation by *T. versicolor*. C represents the residual concentration of the bentazon in the sample (mg L^{-1}), and C$_0$ corresponds to the initial concentration of bentazon in the sample (mg L^{-1}); *Blue lines with filled squares*, experimental; *red lines with empty triangles*, killed control; *green lines with filled circles*, abiotic control; *purple lines with inverted filled triangles*, laccase activity in the experimental.

4.3.3 Role of laccase and cytochrome P450 enzymatic systems in the degradation of selected pesticides.

Several *in vitro* experiments were carried out to examine whether laccase and laccase-mediator systems are involved in acetamiprid, imidacloprid and bentazon degradation. In fact, although laccase activity was detected to some extent during degradation experiments of acetamiprid and imidacloprid using *T. versicolor* as aforementioned (Figure 4.3), there was no pollutants removal using commercial laccase in the absence and presence of the laccase mediator. This behavior keeps in line with diuron case (Torán, 2018), indicating that laccase is not involved in their degradation. But another extracellular enzyme MnP possibly joined the biotransformation mechanisms because its enzymatic activity was captured at low levels in the culture of *G. lucidum*, ranging from 0.03 to 1.60 AU L^{-1}. On the contrary, bentazon completely disappeared in the laccase-ABTS system after 1 h incubation, during which only 11% of the spiked substrate was degraded in the absence of ABTS and this figure did not improve within the rest of treatment period (Table 4.5), but eventually laccase was still active (100 AU L^{-1}).

Table 4.5 Bentazon degradation by commercial laccase in the presence and absence of ABTS.

Time	C/C$_0$		
	Abiotic control	Laccase	ABTS
0 h	1	1	1
30 min	0.97 ± 0.039	0.88 ± 0.039	0.07 ± 0.008
1 h	0.96 ± 0.037	0.89 ± 0.037	0
2 h	0.98 ± 0.041	0.89 ± 0.038	0
4 h	0.98 ± 0.039	0.88 ± 0.039	0
6 h	0.98 ± 0.041	0.91 ± 0.013	0
10 h	0.97 ± 0.042	0.89 ± 0.037	0
24 h	0.98 ± 0.041	0.88 ± 0.024	0

Note: Each value represents the mean of triplicate measurements ± SD. C represents the residual concentration of the bentazon in the sample (mg L^{-1}), and C$_0$ corresponds to the initial concentration of bentazon in the sample (mg L^{-1}).

Furthermore, the results of degradation experiment using fungal broth show that up to 90% of fortified bentazon (10 mg L^{-1}) was decomposed after 48 h (Figure 4.5). The initial and final laccase activities were 13 and 6 AU L^{-1}, respectively. These findings suggest that laccase mediates bentazon metabolization by *T. versicolor*, which has been reported by Knauber et al. (2000), and a less pure broth possibly contains natural mediators generated by *T. versicolor* that may increase the efficiency of degradation (Hultberg et al., 2020). Apart from laccase, both MnP and lignin peroxidase were also found to be involved in bentazon degradation (Coelho et al., 2010b; del Pilar Castillo et al., 2000), which needs to be confirmed in the further work using *T. versicolor*. On the other side, no firm connection between biodegradation and laccase can be proposed based on above results. Similar behaviors have been observed when dealing with other contaminants (Blánquez et al., 2004; Mir-Tutusaus et al., 2014). But in any case, laccase was routinely monitored as an indicator of bioactivity for this particular fungus.
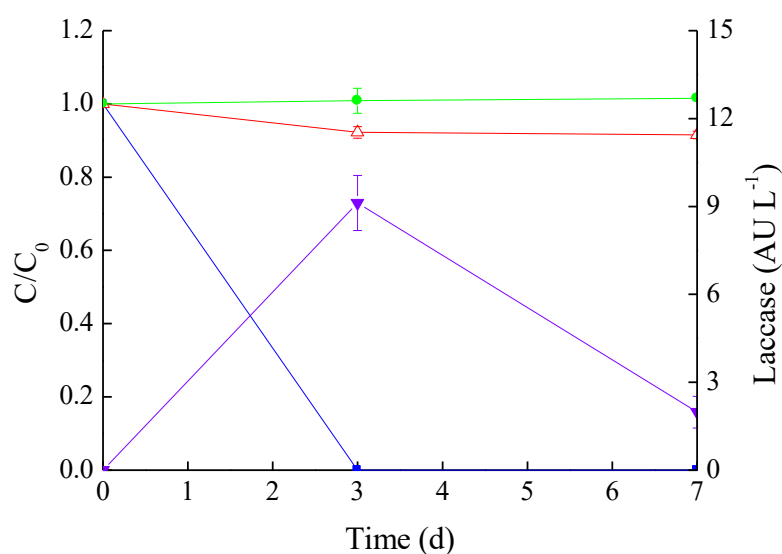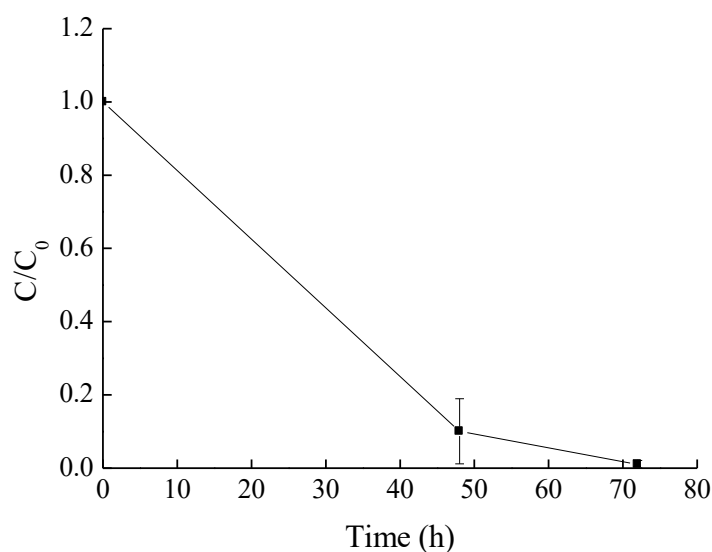
Figure 4.5 Time-course of bentazon degradation by the broth of *T. versicolor*. C represents the residual concentration of the bentazon in the sample (mg L^{-1}), and C$_0$ corresponds to the initial concentration of bentazon in the sample (mg L^{-1}).

Hydroxylation, catalyzed by CYP450, is the first detoxification step in eukaryotes and mammals towards a wide range of contaminants (Črešnar and Petrič, 2011; McDonnell and Dang, 2013). This particular intracellular enzymatic system has been proved to involve in degrading different xenobiotics by *T. versicolor*, and diuron is one of them (Marco-Urrea et al., 2009; Mir-Tutusaus et al., 2014; Torán, 2018). Thence, its participation in acetamiprid, imidacloprid and bentazon degradation was also assessed through *in vivo* experiments. The results are presented in Table 4.6. Obviously, the degradation rate was considerably slowed down by the addition of CYP450 inhibitor 1-aminobenzotriazole. This observation is indicative of the indispensable contribution of CYP450 to the substrate depletion, and it is in agreement with previous reports regarding acetamiprid (Wang et al., 2012; Wang et al., 2019a) and imidacloprid (Mori et al., 2021; Wu et al., 2020). Meanwhile, it's the first evidence for the involvement of CYP450 in bentazon microbial degradation.

Table 4.6 Degradation kinetics parameters of acetamiprid, imidacloprid and bentazon by *T. versicolor* under the effect of cytochrome P450 inhibitor 1-aminobenzotriazole.

Pesticide	Treatment	Regression equation	$T_{1/2}$ (d)	K_d [mg (L d)$^{-1}$]	R^2
Acetamiprid	With inhibitor	ln S = − 0.012 t + 1.372	57.8	0.012	0.92
	Inhibitor-free	ln S = − 0.047 t + 1.637	14.8	0.047	0.96
Imidacloprid	With inhibitor	ln S = − 0.008 t + 1.011	86.6	0.008	0.87
	Inhibitor-free	ln S = − 0.049 t + 1.273	14.2	0.049	0.94
Bentazon	With inhibitor	ln S= − 0.006 t + 1.897	4.8	0.144	0.86
	Inhibitor-free	ln S= − 0.147 t + 2.363	0.2	3.523	0.95

4.3.4 TPs generated during the degradation of different pesticides by *T. versicolor*

Previous work has evidenced the degradation capacity of *T. versicolor* towards dicofol, chlorpyrifos, diuron and malathion (Torán, 2018). The present work assigns a higher value to this capacity by covering acetamiprid, imidacloprid and bentazon. However, their degradation pathways are still unclear. Attention in this section is given to TPs identification and the results presentation are also subdivided into two parts, namely hydrophobic group and hydrophilic group (Table 4.1).

4.3.4.1 Metabolites of hydrophobic pesticides by T. versicolor

a) Dicofol

One compound benzaldehyde was captured and identified as metabolite of dicofol within 7 d incubation according to the results of UPLC-MS/MS analysis. Its chromatographic characteristics are provided in Table 4.7. Considering our result and previous findings (Bumpus and Aust, 1987; Bumpus et al., 1993), we speculated that dichlorination occurred firstly during dissipation process of dicofol, transforming it into 2,2-dichloro-1,1-bis-(4-chlorophenyl)-ethanol (FW-152). FW-152 was then subject to successive reductive dichlorinations and oxidative cleavage, resulting in formation of 4,4'-dichlorobenzophenone, which was further degraded into benzaldehyde through ring cleavage reaction probably because of the role of lignin-degrading system (Bumpus and Aust, 1987).

Table 4.7 Chromatographic characteristics of the TP of dicofol by *T. versicolor*.

Identified TP	Nominal mass	Retention time (min)	Measured mass (m/z)	Mass error (ppm)	Molecular formula	RDB
Benzaldehyde	107	7.47	107.0495	3.537	C_7H_7O	4.5
	91		91.0547	5.307	C_7H_7	4.5
	81		81.0341	8.005	C_5H_5O	3.5
	79		79.0548	7.630	C_6H_7	3.5
	77		77.0392	8.350	C_6H_5	4.5

b) Chlorpyrifos

By contrast, two TPs were found from chlorpyrifos culture. They are O,O-diethyl thiophosphate and diethyl phosphate (Table 4.8), indicating that hydrolyzation occurred in degradation process of chlorpyrifos by *T. versicolor*, which agrees with most cases described to date (Aswathi et al., 2019; Chen et al., 2012; Singh et al., 2004). And it is always the first reaction that also play an irreplaceable role in detoxification of other organophosphorus (Singh and Walker, 2006).

Table 4.8 Chromatographic characteristics of the TPs of chlorpyrifos by *T. versicolor*.

Identified TP	Nominal mass	Retention time (min)	Measured mass (m/z)	Mass error (ppm)	Molecular formula	RDB
O,O-Diethyl thiophosphate	171	4.21	171.0239	− 0.280	$C_4H_{12}O_3PS$	− 0.5
	115		114.9616	2.716	H_4O_3PS	− 0.5
	143		142.9928	1.134	$C_2H_8O_3PS$	− 0.5
	97		96.9510	2.238	H_2O_2PS	0.5
	81		80.9741	6.089	H_2O_3P	0.5
Diethyl phosphate	155	3.10	155.0467	− 0.528	$C_4H_{12}O_4P$	− 0.5
	127		127.0156	1.325	$C_2H_8O_4P$	− 0.5
	99		98.9846	4.732	H_4O_4P	− 0.5
	81		80.9740	4.360	H_2O_3P	0.5

4.3.4.2 Metabolites of hydrophilic pesticides by T. versicolor

a) Malathion

The TPs identified during the degradation of malathion by *T. versicolor* are summarized in Table 4.9. A total of seven compounds were identified including TP172 (diethyl maleate), TP174 (diethyl succinate), TP128 (ethyl (2E)-4-oxo-2-butenoate), TP144 (monoethyl maleate), TP118 (succinic acid), TP132 (monoethyl succinate), and TP160 (ethyl methyl succinate). However, as chemical structures are not confirmed with analytical standards, a

confidence level of 3 was only propose for five of them, accompanied with logical tentative structures, and the others fit Level 5 because no MS^2 data was acquired, according to the Schymanski scale (2014). All cases were found to be present after 7 days of treatment showing an increasing trend by the end of the experiment, except TP132, which could be considered as an intermediate byproduct that was further degraded (Figure B.1).

Given the obtained formulae, we speculate that C-S bond cleavage was the first step in the presence of a proton donor (a base or a reductase), generating diethyl maleate and diethyl succinate, respectively (Figure 4.6). Subsequently, diethyl maleate underwent reduction or hydrolyzation, yielding ethyl (2E)-4-oxo-2-butenoate or monoethyl maleate, which could be further converted into maleic acid, although the last one has not been identified as TP. Meanwhile, diethyl succinate either underwent serial hydrolysis or got through a demethylation process followed by hydrolyzation, until it transformed into succinic acid. The hydrolysis of the phospho-ester bond has been reported as the first and also the most significant step in detoxification of organophosphorus pesticides (i.e., chlorpyrifos, glyphosate, and malathion, etc.) by either bacteria or fungi (Singh et al., 2014; Singh and Walker, 2006) as aforementioned. Our findings point at the cleavage of the S-C bond as the main step. This pathway has been also documented by Paris et al. (1975) using heterogeneous bacterial populations consisting of *F. meningosepticum*, *Xanthomonas* sp., *C. terrigeri,* and *P. cepacia*. On the other hand, the hydrolysis of the carboxylic ester bonds, probably by carboxylesterases, resulted in the mono- and diacid metabolites, and considerably contributed to malathion degradation. This is also in agreement with previous reports (Singh et al., 2012; Zeinat Kamal et al., 2008). Although demethylation has been reported in malathion detoxification using two fungi species including *A. niger* and *P. rotatum* (Mostafa et al., 1972), in our study demethylation takes place on diethyl succinate, rather than on the dimethyl dithiophosphoric acid moiety, leading to the formation of ethyl methyl succinate which is reported for the first time. Identification of the circumstances behind this different pathway would require further research.

Table 4.9 Transformation products formed during the degradation of malathion by *T. versicolor*.

Number	t_R (min)	HESI mode	Full Scan				MS/MS				Suspect identity	Confidence level
			m/z	Formula	RDB	Δm (ppm)	m/z	Formula	RDB	Δm (ppm)		
TP172	6.9	+	173.0816	$C_8H_{13}O_4$	2.5	4.2	129.0552	$C_6H_9O_3$	2.5	4.5	Diethyl maleate	CL3
TP174	7.5	+	175.0971	$C_8H_{15}O_4$	1.5	3.68	143.0708	$C_7H_{11}O_3$	2.5	4.0	Diethyl succinate	CL3
							115.0761	$C_6H_{11}O_2$	1.5	6.2		
TP128	7.5	+	129.0552	$C_6H_9O_3$	2.5	4.9	101.0605	$C_5H_9O_2$	1.5	8.4	Ethyl (2E)-4-oxo-2-bute--noate	CL3
TP144	6.2	+	145.0501	$C_6H_9O_4$	2.5	3.9	145.0501	$C_6H_9O_4$	2.5	3.9	Monoethyl maleate	CL3
							99.0449	$C_5H_7O_2$	2.5	8.0		
							71.0500	C_4H_7O	1.5	12.4		
TP160	7.5	+	161.0814	$C_7H_{13}O_4$	1.5	3.5	115.0761	$C_6H_{11}O_2$	1.5	6.3	Ethyl methyl succinate	CL3
							101.0605	$C_5H_9O_2$	1.5	8.2		
TP132	3.9	–	131.0331	$C_5H_7O_4$	2.5	– 6.4	n.i.				Monoethyl succinate	CL5
TP118	3.6	+	119.0346	$C_4H_7O_4$	1.5	6.0	n.i.				Succinic acid	CL5

Note: t_R, chromatographic retention time; HESI, heated-electrospray ionization; Δm, mass measurement error; RDB, ring and double bond equivalents; n.i., no fragments with plausible formula identified.
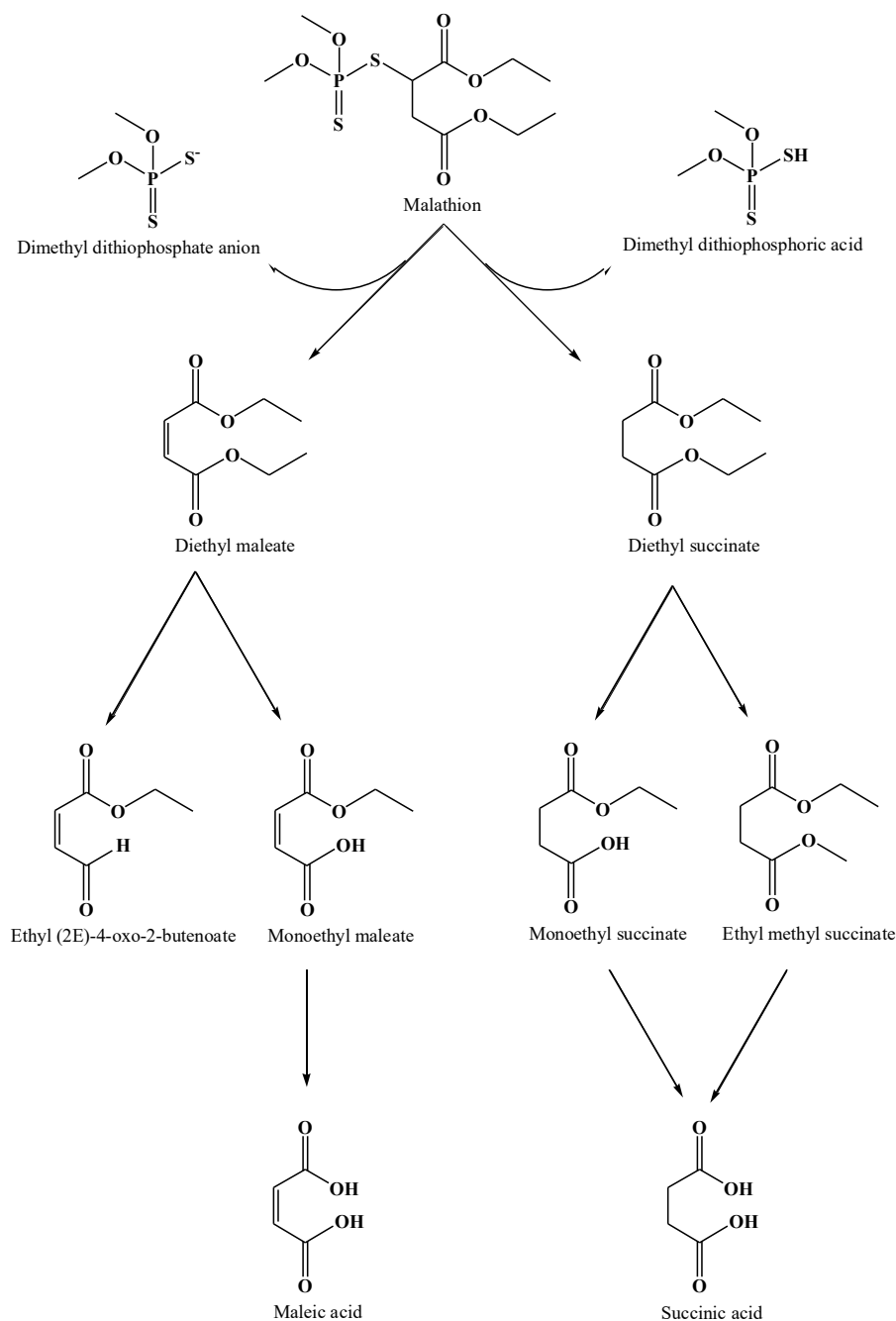
Figure 4.6 Proposed pathway of malathion degradation by *T. versicolor*.

b) Diuron

As for diuron, five ions were detected among which three harvested logical tentative structure (Table 4.10). The remaining two TPs were appointed as "unequivocal molecular formulae" (identification confidence level of 4), as no sufficient evidence existed to propose possible structures (Schymanski et al., 2014). The CL3 TPs were TP248 3-(3,4-dichlorophenyl)-1-hydroxymethyl-1-methylurea (DCPHMU), TP218 3-(3,4-dichlorophenyl)-1-methylurea (DCPMU), and TP204 3,4-dichlorophenylurea (DCPU).

TP218 (DCPMU) and TP204 (DCPU) have been previously reported as aerobic degradation by-products of diuron regardless of the organism (bacteria or fungi) used for its degradation. They are formed after successive N-demethylations reactions of diuron (Badawi et al., 2009; Coelho-Moreira et al., 2013, 2018; Ellegaard-Jensen et al., 2014; Sørensen et al., 2008). Demethylation of diuron may occur intracellularly, as diuron and these demethylated metabolites were found to be present in mycelial extracts of *G. lucidum* (Coelho-Moreira et al., 2018). This matches well with the fact that none decline in diuron concentration was observed in laccase-mediators *in vitro* degradation experiments (Torán, 2018). All identified TPs remained in solution after 7 days of treatment; however, TP204 (DCPU), TP137 and TP195 were the ones that presented an increasing trend by the end of the experiment (Figure B.2). Thus, TP248 (DCPHMU) and TP218 (DCPMU) can be considered as intermediate byproducts that further degraded in contact with the fungus. TP248 is believed to be formed after carbon hydroxylation at the tertiary amine moiety. This reaction may be mediated by the cytochrome P450 system, according to the results reported by Torán (2018) and to a previous study on the detoxification of chlortoluron by the grass weed *A. myosuroides* (Hall et al., 1995). This is the first report of the formation of TP248 during microbial degradation of diuron.

3,4-Dichloroaniline (3,4-DCA) has been widely reported to be a diuron TP that could be generated after the amide bond hydrolysis of DCPU. Likewise, it possesses high toxicity and exhibits persistence in soils (Giacomazzi and Cochet, 2004; Tasca and Fletcher, 2018). The ability of *T. versicolor* to degrade this TP has been already confirmed in previous work, yielding 100% removal towards 10 mg L^{-1} 3,4-DCA in less than 24 h (Torán, 2018). This may explain why 3,4-DCA was not detected in the experimental culture media in this study. In any word, a pathway of diuron degradation by *T. versicolor* is proposed in Figure 4.7; however, further investigation is still needed to understand the entire metabolic pathway.

Table 4.10 Transformation products formed during diuron degradation by *T. versicolor*.

Number	t_R (min)	HESI mode	Full Scan				MS/MS				Suspect identity	Confidence level
			m/z	Formula	RDB	Δm (ppm)	m/z	Formula	RDB	Δm (ppm)		
TP248	6.7	–	247.0030	$C_9H_9O_2N_2Cl_2$	5.5	– 2.1	159.9708	$C_6H_4NCl_2$	4.5	– 4.6	DCPHMU	CL3
TP218	8.6	+	219.0093	$C_8H_9Cl_2ON_2$	4.5	3.3	161.9876	$C_6H_6Cl_2N$	3.5	3.8	DCPMU	CL3
TP204	8.5	+	204.9937	$C_7H_6Cl_2N_2O$	4.5	3.5	161.9877	$C_6H_6Cl_2N$	3.5	3.4	DCPU	CL3
							159.9728	$C_6H_4Cl_2N$	4.5	8.2		
							92.0503	C_6H_6N	4.5	8.5		
TP137	2.9	+	138.0556	C_7H_8O2N	4.5	4.4	110.0608	C_6H_8ON	3.5	7.1	n.s.	CL4
TP195	4.3	+	196.0612	$C_9H_{10}O_4N$	5.5	4.0	178.0508	$C_9H_8O_3N$	6.5	3.6	n.s.	CL4
							150.0556	$C_8H_8O_2N$	5.5	4.5		

Note: t_R, chromatographic retention time; HESI, heated-electrospray ionization; Δm, mass measurement error; RDB, ring and double-bound equivalents; n.s.: no possible structure.
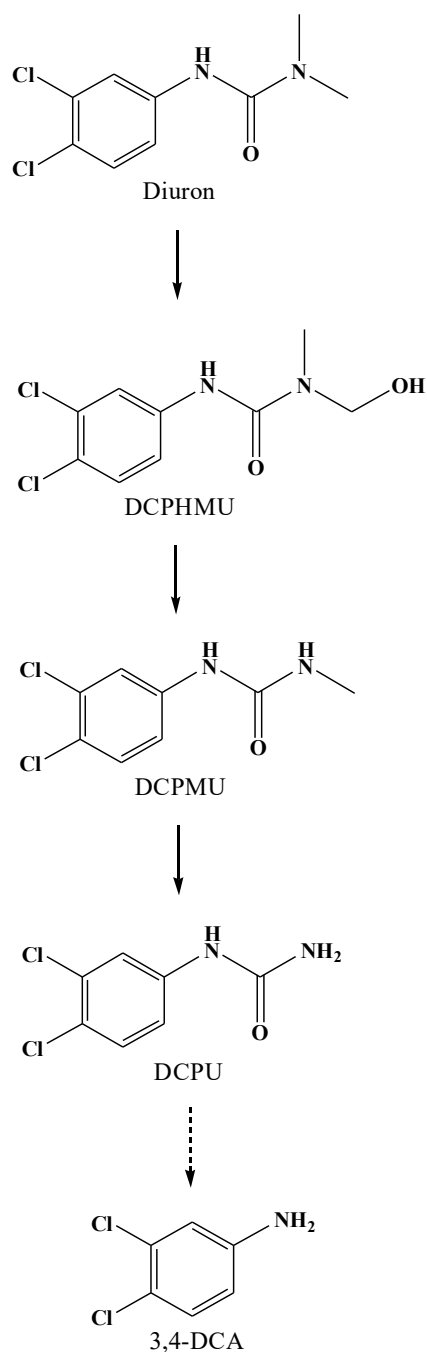
Figure 4.7 Proposed pathway of diuron degradation by *T. versicolor*. *Full lines*, the reactions observed in this study; *dashed lines*, the reaction described in the literature.

c) Acetamiprid and imidacloprid

Concerning acetamiprid and imidacloprid, two compounds TP157 (6-chloronicotinic acid) and TP271 (hydroxyl-imidacloprid) were identified as TPs with a confidence level of 3 (Table 4.11).

Table 4.11 Transformation products formed during acetamiprid and imidacloprid degradation by *T. versicolor*.

Pesticides	Number	t_R (min)	HESI mode	Full Scan				MS/MS				Suspect identity (Confidence level)
				m/z	Formula	RDB	Δm (ppm)	m/z	Formula	RDB	Δm (ppm)	
Acetamiprid	TP157	7.6	+	158.0009	$C_6H_5O_2NCl$	4.5	3.5	122.0234	$C_6H_4O_2N$	5.5	-2.1	6-Chloronicotinic acid (CL3)
								78.0346	C_5H_4N	4.5	9.3	
Imidacloprid	TP271	7.0	+	272.0551	$C_9H_{11}O_3N_5Cl$	6.5	2.3	228.0540	$C_9H_{11}O_2N_3Cl$	5.5	2.5	Hydroxyl-imidacloprid (CL3)
								225.0544	$C_9H_{10}ON_4Cl$	6.5	2.8	
								126.0111	C_6H_5NCl	4.5	3.9	
								144.0216	C_6H_7ONCl	3.5	3.6	
	TP157	7.7	+	158.0010	$C_6H_5O_2NCl$	4.5	4.10	n.a.				6-Chloronicotinic acid (CL5)

Note: t_R, chromatographic retention time, HESI, heated-electrospray ionization; Δm, mass measurement error; RDB, ring and double bond equivalents; n.a., MS^2 data were not acquired for this ion, and m/z ions for fragments were thus not available.

Both metabolites were found to be present after 7 days of treatment, showing an increasing trend by the end of incubation (Figure B.3). The TP157 was generated during the degradation of both pesticides, which is consistent with the degradation experiments conducted with *Mycobacterium* sp. isolated from soil (Kandil et al., 2015). Likewise, Mori et al. (2021) reported that *P. chrysosporium* metabolized chloropyridinyl-type neonicotinoid insecticides through an N-dealkylation reaction catalyzed by cytochrome P450s, generating 6-chloronicotinic acid, which seems to be a common TP of neonicotinoids that contain a pyridinyl ring (Casida, 2011). In the case of imidacloprid, another hydroxylated byproduct was generated, possibly mediated by cytochrome P450 (Casida, 2011). However, it is interesting to point that MS^2 data revealed that the hydroxylation occurred in the pyridinyl ring (Figure 4.8) instead of in the heterocyclic spacer as previously documented (Casida, 2011; Liu et al., 2013; Ma et al., 2014; Sharma et al., 2014).
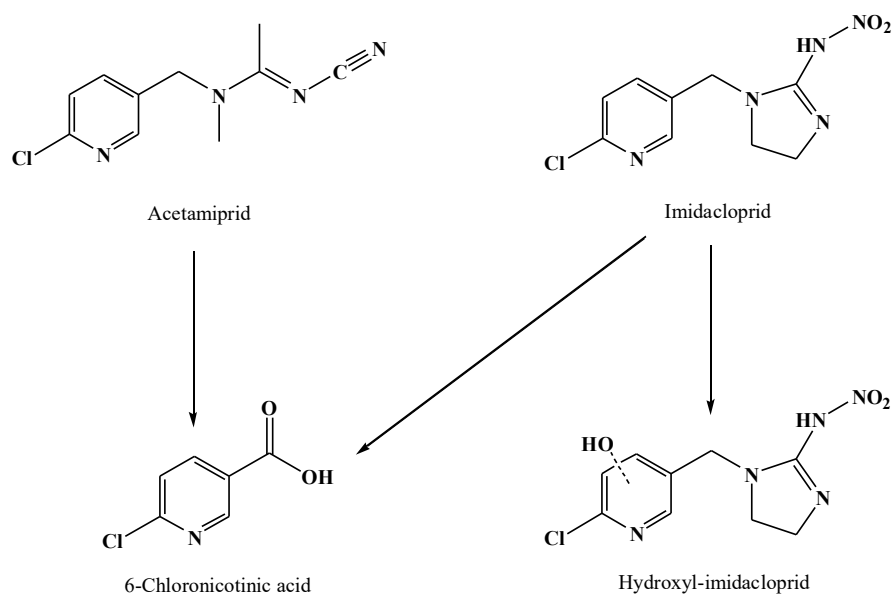
Figure 4.8 Proposed pathways of neonicotinoid pesticides degradation by *T. versicolor*.

d) Bentazon

In the scenario of bentazon, 19 molecular ions were revealed by UPLC-HRMS, but only 8 of them could tentatively gained a chemical structure. They are listed in Table 4.12, and the rest of detected TPs go to Annex B (Table B.1). The time-evaluation of all the TPs is shown in Figure B.4. As a common bentazon TP found in the environment, N-methyl-

bentazon was not caught during fungal degradation process, which contrasts the study by Knauber et al. (2000) and European Food Safety Authority (EFSA, 2015). However, its aldehyde and carboxyl derivatives were captured, namely TP268 (N-aldehyde-bentazon) and TP284a (N-carboxyl-bentazon). It indicates that N-methyl-bentazon went through two successive oxidation steps, possibly catalyzed by CYP450 (Guengerich, 2001; Heitz et al., 2012) that also contributed to the formation of TP256 hydroxyl-bentazon (EFSA, 2015; Knauber et al., 2000). It seems more likely that TP284a generated from TP268 since it appeared at a later stage than the latter. Unlike reported cases, it is not available to locate hydroxyl moiety of TP256 based on the structural information obtained, therefore it could be 6-OH, 8-OH-bentazon, or isopropyl-OH-bentazon (EFSA, 2015; Hedegaard et al., 2018; Huber and Otto, 1994; Knauber et al., 2000). Similar to TP284a, the carboxylation could also occur at the isopropyl moiety, yielding 3-N-isopropyl acid-bentazon (TP284b) which was also identified as the TP of bentazon in microcosm experiments with filter sand (Hedegaard et al., 2019). This phenomenon actually supports the metabolisms of two successive oxidation steps. TP285 could result from introducing N-nitrosation (Adjei et al., 2006). And the generation of TP258 5-Hydroxy-2-isopropyl-2H,7H-benzo[e][1,3,2,4]oxathiadiazin-7-one 3,3-dioxide (HIBOD) seemed to be mediated by laccase, taking into consideration that its catalytic mechanism consists of the abstraction of an electron from a substrate, likely hydroxyl derivative, to produce free radicals during which an iminoquinone intermediate could be produced (Kudanga et al., 2017). Subsequently, HIBOD was further transformed into TP286 3-(8-Hydroxy-2,2-dioxido-6-oxo-3H,6H-benzo[e][1,3,4]oxathiazin-3-yl)butanal (HDOBOB) by the addition of hydroxyl-methyl group. Accordingly, a pathway of bentazon degradation by *T. versicolor* is figured out, as depicted in Figure 4.9. It's also worth noting that hydroxyl-bentazon could further undergo aromatic ring cleavage and decarboxylation reactions as reported by Hedegaard et al. (2019).

Table 4.12 Transformation products formed during bentazon degradation by *T. versicolor* that possess logical tentative structure.

Number	t_R (min)	HESI mode	Full Scan				MS/MS				Suspect identity	Confidence level
			m/z	Formula	RDB	Δm (ppm)	m/z	Formula	RDB	Δm (ppm)		
TP256	4.6	–	255.0439	$C_{10}H_{11}N_2O_4S$	6.5	– 2.4	197.0015	$C_7H_5N_2O_3S$	6.5	– 0.7	Hydroxyl bentazon	CL3
							191.0814	$C_{10}H_{11}N_2O_2$	6.5	– 5.7		
							132.0314	$C_7H_4N_2O$	7.0	– 3.9		
							79.9557	O_3S	1.0	– 21.2		
TP268	5.3	–	267.0440	$C_{11}H_{11}N_2O_4S$	7.5	2.4	224.9967	$C_8H_5N_2O_4S$	7.5	1.0	N-aldehyde-bentazon	CL3
							203.0815	$C_{11}H_{11}N_2O_2$	7.5	0.1		
							160.0265	$C_8H_4N_2O_2$	8.0	– 1.7		
TP285	5.8	–	284.0342	$C_{10}H_{10}N_3O_5S$	7.5	– 1.5	241.9869	$C_7H_4N_3O_5S$	7.5	– 3.4	N-nitroso-bentazon	CL3
							220.0719	$C_{10}H_{10}N_3O_3$	7.5	– 4.4		
							197.0014	$C_7H_5N_2O_3S$	6.5	– 0.7		
							177.0169	$C_7H_3N_3O_3$	8.0	– 6.2		
							132.0311	$C_7H_4N_2O$	7.0	– 3.9		
TP284a	2.8	–	283.0389	$C_{11}H_{11}N_2O_5S$	7.5	– 1.9	240.9915	$C_8H_5N_2O_5S$	7.5	– 3.5	N-carboxyl-bentazon	CL3
							239.0485	$C_{10}H_{11}N_2O_3S$	6.5	– 4.5		
							219.0765	$C_{11}H_{11}N_2O_3$	7.5	– 4.7		
							197.0014	$C_7H_5N_2O_3S$	6.5	– 0.7		
							177.0286	$C_8H_5N_2O_3$	7.5	– 11.3		
							176.0210	$C_8H_4N_2O_3$	8	– 10.0		

Note: t_R, chromatographic retention time; HESI, heated-electrospray ionization; Δm, mass measurement error; RDB, ring and double bond equivalents; n.a., MS^2 data were not acquired for this ion, and m/z ions for fragments were thus not available.

Table 4.12 (cont)

Number	t_R (min)	HESI mode	Full Scan				MS/MS				Suspect identity	Confidence level
			m/z	Formula	RDB	Δm (ppm)	m/z	Formula	RDB	Δm (ppm)		
TP284b	5.7	–	283.0388	$C_{10}H_{11}N_2O_4S$	7.5	– 2.1	239.0487	$C_{10}H_{11}N_2O_3S$	6.5	– 3.9	3-N-isopropyl acid-bentazon	CL3
							197.0014	$C_7H_5N_2O_3S$	6.5	– 0.7		
							175.0863	$C_{10}H_{11}N_2O$	6.5	– 1.7		
							133.0393	$C_7H_5N_2O$	6.5	– 10.7		
							132.0313	$C_7H_4N_2O$	7.0	– 12.6		
							59.0115	$C_2H_3O_2$	1.5	– 39.2		
TP286	4.6	–	285.0182	$C_{10}H_9N_2O_6S$	7.5	2.2	257.0232	$C_9H_9N_2O_5S$	6.5	1.9	HDOBOB	CL3
							214.9759	$C_6H_3N_2O_5S$	6.5	1.0		
							193.0610	$C_9H_9N_2O_3$	6.5	1.3		
							151.0136	$C_6H_3N_2O_2$	6.5	– 1.1		
							150.0055	$C_6H_2N_2O_2$	7.0	– 3.1		
							135.0182	$C_6H_2N_2O_2$	6.5	– 5.2		
							77.9638	NO_2S	1.5	– 7.7		
TP258	5.4	–	257.0230	$C_9H_9N_2O_5S$	6.5	0.75	214.9756	$C_6H_3N_2O_5S$	6.5	– 0.6	HIBOD	CL3
							193.0604	$C_9H_9N_2O_3$	6.5	– 0.5		
							151.0134	$C_6H_3N_2O_2$	6.5	– 2.8		
							134.0105	$C_6H_2N_2O_2$	7.0	– 3.8		
TP494	5.6	–	493.0856	$C_{20}H_{21}N_4O_7S_2$	12.5	– 0.2	n.a.				Dimer	CL5

Note: t_R, chromatographic retention time; HESI, heated-electrospray ionization; Δm, mass measurement error; RDB, ring and double bond equivalents; n.a., MS^2 data were not acquired for this ion, and m/z ions for fragments were thus not available.
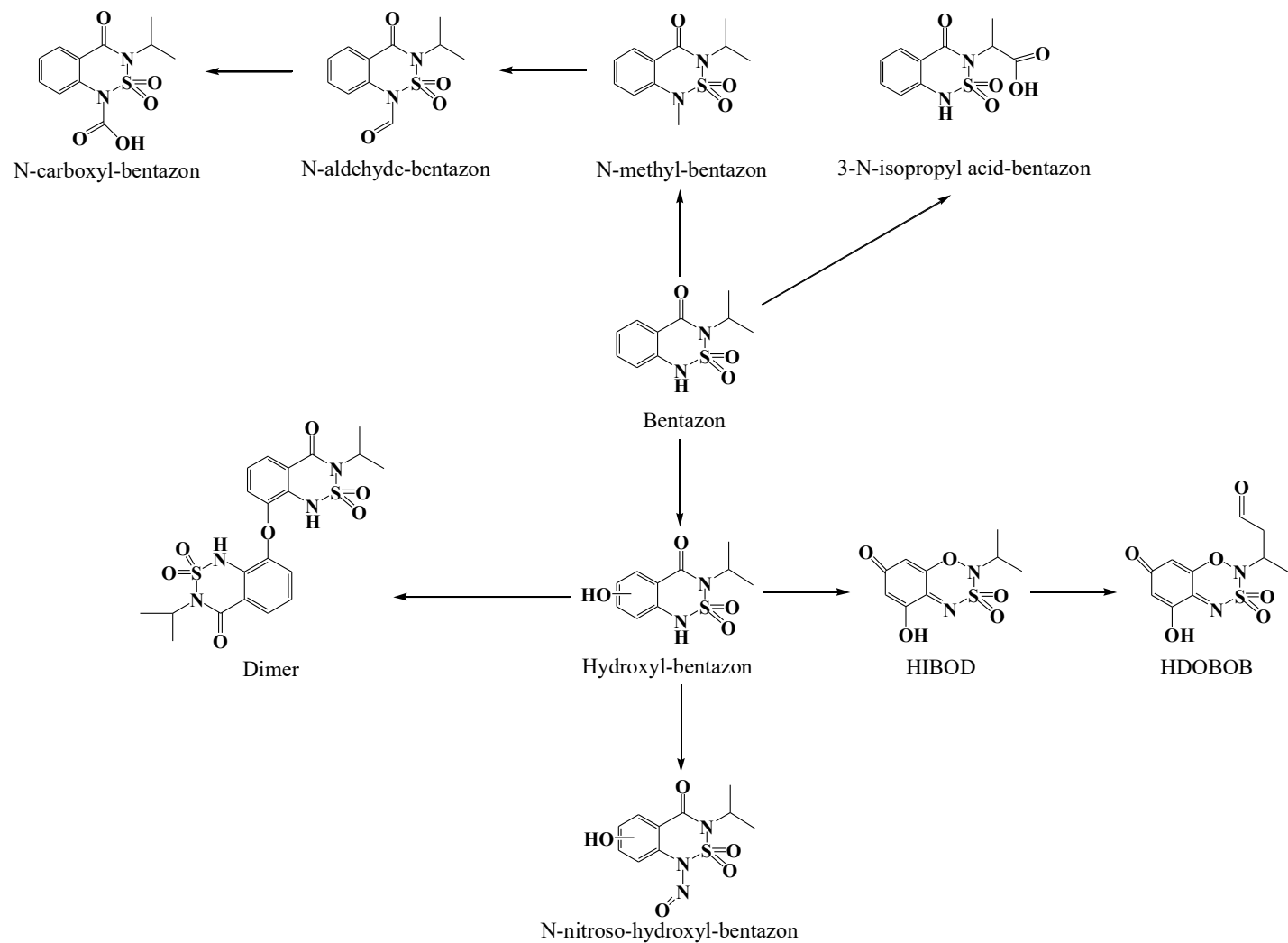
Figure 4.9 Proposed pathway of bentazon degradation by *T. versicolor*.

4.3.5 Toxicity assessment

The aforementioned results showed that some TPs accumulated during incubation period of malathion, diuron, acetamiprid and imidacloprid (Figure B.1-A.3), posing a non-negligible concern since the risk of their existences in the environment is unclear. Thus, toxicity assessments were implemented for all those cultures except diuron, since *T. versicolor* demonstrated efficient degradation capacity towards one of its major metabolites (Torán, 2018), which essentially alleviates this concern.

Toxicity data obtained from the Microtox test performed on the 7-day-culture samples using the *Vibrio fischeri* bacterium showed a general increase of TU in the experimental culture in comparison to the abiotic control. A nearly double effect on TU value was observed in the case of malathion and its degradation products, increasing from 0.65 to 1.27. Although both values were lower than the wastewater discharge limit (25) set in Catalonia industrial areas (DOGC, 2003), the results indicate that some of the metabolites generated in the biotransformation process are more toxic than malathion.

Similar results were observed in the case of imidacloprid and acetamiprid, where TU values increased from 0.54 to 3, and 0 to 0.86, respectively, which supports previously published results indicating that the TP157 (6-chloronicotinic acid) possesses higher toxicity than its parent compounds imidacloprid and acetamiprid (Anderson et al., 2015). In any case, the maximum discharge limit was not achieved, plus the initial pesticide concentration in these experiments was dramatically higher than the environmental levels (normally in the ng or µg L^{-1} range). These results suggest that *Trametes versicolor*-based bioremediation can be a useful tool for the treatment of waters contaminated with malathion, acetamiprid and imidacloprid.

4.4 Conclusions

➢ *T. versicolor* was the most outstanding candidate among five ligninolytic fungi, with degradation efficiency towards different pesticides, including diuron, acetamiprid, imidacloprid and bentazon, and superior performance on lignocellulosic substrate colonization.

➢ The pesticides degraders *T. versicolor* (acetamiprid, imidacloprid and bentazon), *G. lucidum* (acetamiprid and imidacloprid) and *S. rugosoannulata* (diuron) were confirmed for the first time, enriching the microbe pool.

➢ The cytochrome P450 system of *T. versicolor* considerably involved in acetamiprid, imidacloprid and bentazon degradation process. Bentazon degradation was also mediated by laccase.

➢ Hydrolyzation and oxidation, especially hydroxylation, played irreplaceable roles during metabolization of target pesticides by *T. versicolor*.

Chapter 5

Agricultural wastewater treatment by lab-scale fungal reactor

5.1 Introduction

The need for nutrient addition and the competition with autochthonous microorganisms constitute two main drawbacks amid white-rot fungal practical application for addressing micropollutants in wastewater (Mir-Tutusaus et al., 2018). So, searching for a tailored and robust reactor configuration is of great importance. Torán (2018) constructed a fungal trickle bed reactor (TBR) by immobilizing *T. versicolor* on pine wood chips. This system provided favorable growth and biodegradation conditions for the fungal candidate to treat real hospital wastewater. Throughout 49 days operation under non-sterile conditions, bacterial contamination was successfully dismissed, accompanied with satisfying pharmaceuticals elimination. Although its subsequent practice targeting at pesticides ended up with spiked tap water, the optimization results suggested that the removal efficacy is governed by the contact time between the immobilized biomass and the pollutant, which enforces the idea that fungal treatments require high hydraulic residence times (HRTs) (Mir-Tutusaus et al., 2018).

The degradation capacity of *T. versicolor* to diuron and bentazon, the most representative residual pesticide in Llobregat River Basin and Ebro River Delta areas respectively (Barbieri et al., 2020; Barbieri et al., 2021), has been examined in Chapter 4. It turned out that *T. versicolor* could sufficiently degrade these two pollutants. To better understand and evaluate the application of fungal TBR in wastewater treatment for pesticides removal, a comparative study was implemented in this chapter. Two lab-scale reactors were set up, one is trickle bed reactor with *T. versicolor* immobilized on pine wood and another one is fluidized bed reactor (FBR) inoculated with *T. versicolor* pellets. Both reactors were running to remove diuron and bentazon from actual wastewater in sequencing batch mode under non-sterile conditions. Then, the assess for each system was processed based on different aspects, including pesticides removal, feasibility, robustness, economical cost, etc., in order to propose a preferred option for scaling-up and long-term treatment. Prior to the comparison, three different methodologies were adopted to estimate the contact time of the established TBR. Finally, a lab-scale TBR with *T. versicolor* colonized on oak wood was employed to treat real agricultural wastewater without spiking, during which the evolution

of microbial community structure was investigated.

5.2 Specific methods in this chapter

5.2.1 Contact time determination for the trickle bed reactor

Taking into account that the contact time between the immobilized fungi and the water has been suggested to play a vital role in the regime of a TBR (Torán, 2018), its determination is important for the employed reactor. In this work, the contact time was determined using control reactor (non-inoculated) through three different techniques: (1) Volumetric quantification. After the wood was soaked with water, the pump was switched on for a certain time, and all the introduced distilled water was collected at the outlet. The time corresponding to collecting a 10 mL aliquot was recorded. (2) Pulse tracer injection. After injecting 3 mL of 3 M KCl at the top of the reactor, the effluent was collected every 15 s, and the conductivity was measured. (3) Step tracer input. The influent was changed to a KCl solution (46 mM) at a certain point, and then, the samples were collected and analyzed analogously to the pulse input strategy. A flow rate of 70 mL min^{-1} was employed in all experiments, and each kind of test was conducted in duplicate.

5.2.2 Removing selected pesticides by the two different reactors in sequencing batch mode

5.2.2.1 Removing selected pesticides by the trickle bed reactor

After 4 weeks static incubation, the immobilized culture was packed into the methacrylate tube. Multiple runs were implemented in sequencing batch mode at room temperature, and a 3-day cycle was fixed. Two different recirculation flow rates (F_r) were adopted, to explore the effect of different recirculation ratios (RRs) on the removal efficiency. Specifically, F_r of 70 mL min^{-1} was selected for the first 10 batches, whereas it was accelerated to 140 mL min^{-1} was during the following 9 cycles. 1 L of the spiked agricultural wastewater (AW) I (physicochemical characteristics seen in Table 5.1) was treated in every cycle. Samples were taken from the tank after each batch to measure laccase, pesticide concentration, HPCs and COD, and then, the wastewater was totally

replenished.

Table 5.1 Physicochemical characterization of the agricultural wastewater used for the trickle bed reactor.

Parameter	AW I
pH	7.67 ± 0.04
Absorbance at 655 nm	0.05 ± 0.00
Conductivity (mS cm^{-1})	2.25 ± 0.07
TSS (mg L^{-1})	6.33 ± 1.36
VSS (mg L^{-1})	4.27 ± 1.50
TOC (mg L^{-1})	16.23 ± 0.81
HPC [lg (CFU mL^{-1})]	4.68 ± 4.43
Ammonia	ND
COD (mg L^{-1})	31.85 ± 0.78
Chloride (mg Cl$^-$ L^{-1})	570.50 ± 3.76
Sulfate (mg SO$_4^{2-}$ L^{-1})	51.24 ± 0.06
Nitrite (mg NO$_2^-$ L^{-1})	2.78 ± 0.06
Nitrate (mg NO$_3^-$ L^{-1})	0.08 ± 0.01

Note: Mean value and standard deviation of triplicate measurements are shown. ND, not detected.

5.2.2.2 Removing selected pesticides by the fluidized bed reactor

Pellets were transferred into air-pulsed fluidized bed reactor, achieving the same biomass in terms of dry weight as that in the TBR. The reactor carried 1 L of the spiked AW IV, and it was operated in sequencing batch mode with a 3-day cycle at 25 °C. Nutrients including glucose and NH$_4$Cl were fed with a molar C/N ratio of 7.5 based on the glucose consumption rate of *T. versicolor* (Mir-Tutusaus et al., 2017). At the end of each batch, samples were withdrawn for laccase, pesticide concentration, HPCs, COD and glucose analyses, and then, pellets were harvested and reinoculated to replenished wastewater.

A coagulation-flocculation pretreatment was conducted for the AW IV to erase the algae. Table 5.2 shows the physicochemical characteristics before and after the pretreatment. As can be seen, apart from TSS and VSS, mainly contributed by algal biomass, bacteria were also somewhat reduced.

Table 5.2 Physicochemical characterization of the agricultural wastewater used for the fluidized bed reactor.

Parameter	Before pretreated	After pretreated
pH	7.27 ± 0.08	6.65 ± 0.10
Absorbance at 655 nm	0.09 ± 0.01	0.002 ± 0.00
Conductivity (mS cm^{-1})	2.66 ± 0.04	2.48 ± 0.04
TSS (mg L^{-1})	24.91 ± 7.37	2.70 ± 0.46
VSS (mg L^{-1})	24.11 ± 6.03	2.63 ± 0.47
TOC (mg L^{-1})	31.74 ± 0.91	9.67 ± 0.48
HPC [lg (CFU mL^{-1})]	5.08 ± 4.25	4.70 ± 3.64
Ammonia	ND	ND
COD (mg L^{-1})	144.33 ± 5.86	27.33 ± 1.27
Chloride (mg Cl$^-$ L^{-1})	13.65 ± 0.14	708.23 ± 45.38
Sulfate (mg SO$_4^{2-}$ L^{-1})	79.78 ± 1.06	59.90 ± 3.19
Nitrite (mg NO$_2^-$ L^{-1})	0.25 ± 0.06	5.87 ± 0.36
Nitrate (mg NO$_3^-$ L^{-1})	ND	0.01 ± 0.01

Note: Mean value and standard deviation of triplicate measurements are shown. ND, not detected.

5.2.3 Characterization of the fixed bed and secondary treatment for the lignocellulosic supports

Biofilm matrices were withdrawn from top, middle and bottom of experimental reactor respectively after 57-day operation, followed by analysis of pesticide residues and ergosterol. Analogous measurements were carried out to the packing materials from control reactor except ergosterol analysis. Each analysis experiment was performed in triplicate.

Simultaneously, a secondary bioelimination test was implemented towards the lignocellulosic carrier. 90 g of the packing material mixture were withdrawn from both reactors. They were subsequently transferred into 500 mL Erlenmeyer flasks and re-inoculated with *T. versicolor* mycelium as described in Chapter 3 (Section 3.1.3). After 4 weeks incubation, samples were subjected to quantifications of pesticide residues and ergosterol. Erlenmeyer containing same amount of experimental wood chips without re-inoculation was set as control, and triplicate replications were set for each experiment.

5.2.4 Application of the trickle bed reactor in removing pesticides from real wastewater

The lab-scale TBR was subsequently applied to treat real water collected from Ebro

River Delta (southernmost of Catalonia, Spain), one of the largest wetlands (320 km^2) in the western Mediterranean areas where agricultural activities intensively occupy. According to analysis results from previous sampling campaign, numerous pesticides were detected in the water of irrigation and drainage channels of this delta during rice-growing season (Barbieri et al., 2021). The water used in this experiment was also collected during the same period and its physicochemical characteristics are listed in Table 5.3.

Table 5.3 Physicochemical characterization of the real water used for the trickle bed reactor.

Parameter	AW II
pH	7.85 ± 0.04
Absorbance at 655 nm	0.02 ± 0.00
Conductivity (mS cm^{-1})	1.73 ± 0.03
TSS (mg L^{-1})	8.43 ± 0.76
VSS (mg L^{-1})	3.00 ± 0.17
TOC (mg L^{-1})	15.60 ± 2.71
HPC [lg (CFU mL^{-1})]	5.09 ± 4.21
Ammonia (mg L^{-1})	1.79 ± 0.21
COD (mg L^{-1})	39.74 ± 1.77
Chloride (mg Cl$^-$ L^{-1})	268.08 ± 1.39
Sulfate (mg SO$_4^{2-}$ L^{-1})	115.92 ± 1.56
Nitrite (mg NO$_2^-$ L^{-1})	2.41 ± 0.14
Nitrate (mg NO$_3^-$ L^{-1})	ND

Note: Mean value and standard deviation of triplicate measurements are shown. ND, not detected.

The configuration of the TBR was essentially analogous to it in the spiked scenario and the discrepancy came from the operation conditions. The reactor was running in sequencing batch mode with a 5-day cycle and it treated 1.2 L real water in each cycle. To increase the contact time in order to meet high removal, F_r was raised to 200 mL min^{-1}. Liquid samples were taken from the tank periodically to measure laccase, pesticide concentration, microbial community structure. Solid samples were withdrawn from the upper, middle and bottom part of the reactor at the end of treatment to analyze microbial community structure and ergosterol. The wastewater was totally replenished at the end of each batch.

5.2.5 Pesticide analysis for the real water

The analysis was conducted by the group of Dr. Miren López de Alda, affiliated to Water, Environmental and Food Chemistry Unit (IDAEA-CSIC). The corresponding methodology

is given in Annex C.

5.3 Results and discussions

5.3.1 TBR contact time

To determine the contact time of the TBR, three different strategies were adopted in this study, and the responses and calculated results are presented in Figure 5.1 and Table 5.4. For the volumetric quantification technique shown in Figure 5.1a, the flow rate of the outlet became constant and equalled that of the inlet after 102 s, which can be assumed to be the average time required for the liquid to pass through the reactor, namely, the contact time. However, this characteristic changed to significantly higher values when pulse input and step input were used (Table 5.4) since the conductivity proportional responses were not symmetric and the curves contained long tails (Figure 5.1b and 5.1c). Similar profiles were obtained by Sá and Boaventura (2001) using siliceous granular material to support the biomass in the TBR. A reasonable explanation could be that part of the packing bed was relatively stagnant due to the irregular shape of the wood chips, for which even a rotary distributor had been provided at the top of the reactor. The main water flow went downwards through preferred routes, while a small amount of tracer was retained in the reactor and left very slowly.
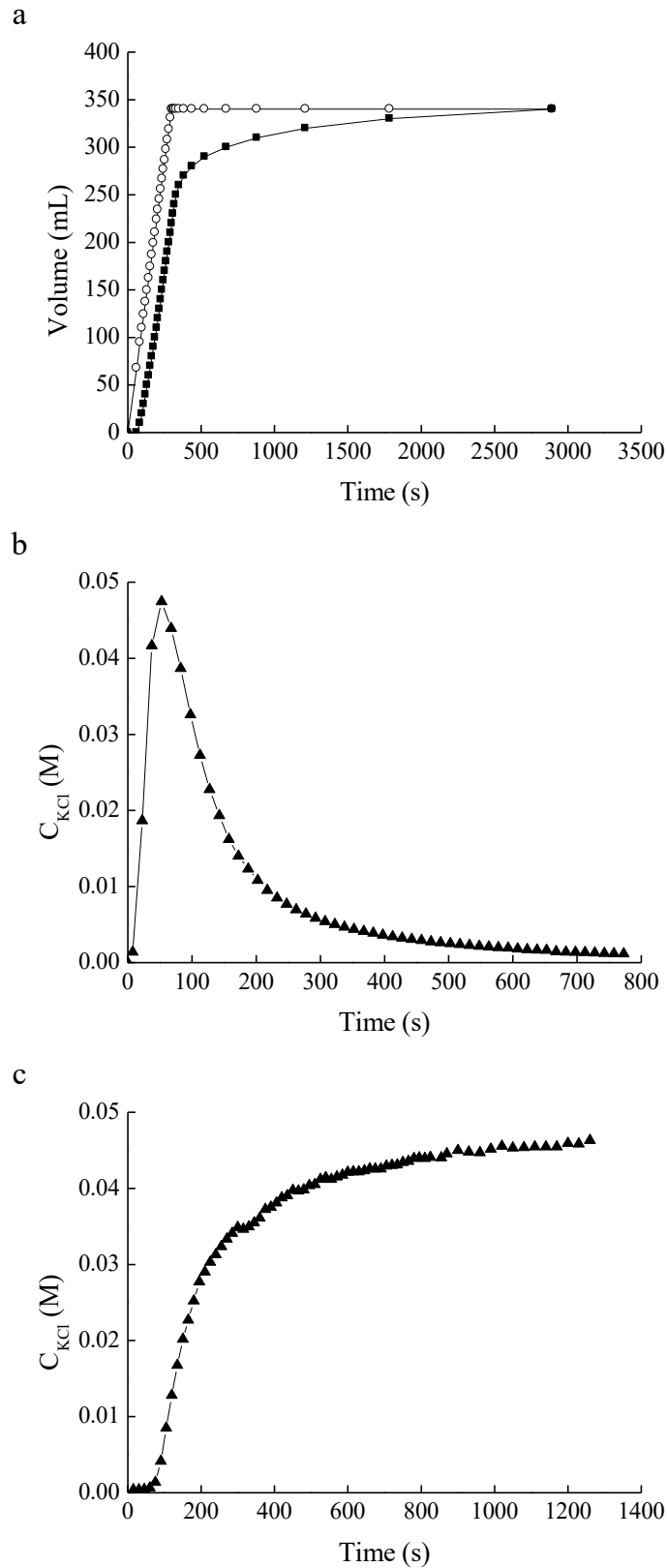
Figure 5.1 Responses to TBR contact time determination using different techniques. a. volumetric quantification. b. pulse tracer injection. c. step tracer input. *Empty circle*s, input volume; *filled squares*, output volume; *filled triangles*, tracer concentration at outlet.

Table 5.4 Average contact time of TBR determined through different techniques.

Technique	Residence time (s)
Volumetric quantification	102 ± 2
Pulse tracer injection	173 ± 1
Step tracer input	259 ± 6

Note: Means and standard deviation of duplicates are shown.

Therefore, it can be concluded that the TBR employed in this work did not perform as an ideal plug flow reactor. However, if the relatively stagnant volume (tails) was ignored, as mentioned by Levenspiel (2013), 102 s corresponds to the time at which half mass of 80% tracer injection (active volume) was collected in the scenario of pulse input and to the moment when half volume of flow in the rector was substituted by tracer solution in the scenario a step input. Hence, we consider that among the contact times, 102 s was the most representative one at the flow rate of 70 mL min^{-1}. The volumetric quantification technique was also adopted for the contact time determination in Chapter 6.

5.3.2 Comparison between the trickle bed reactor and air-pulsed fluidized bed reactor

An equivalent initial biomass was a prerequisite for this comparative study. Several pieces of colonized wood chips were used before operation to measure the initial biomass in the TBR, and the ergosterol concentration was approximately 0.044 ± 0.002 mg per g of dry wood. Considering that 367 g of dry chips was introduced and the ergosterol content of the selected strain corresponded to 6.61 mg g^{-1} DW^{-1} of *Trametes versicolor* biomass (Rodríguez-Rodríguez et al., 2010a), we determined that the total biomass of the TBR was approximately 2.45 g DW. Hence, an equivalent pelleted inoculum was transferred into the FBR for operation. These two reactors were compared in following different aspects based on one-month operation performance.

5.3.2.1 Pesticide removal

As shown in Figure 5.2, considerable removals of diuron and bentazon occurred in the TBR, yielding 69% and 47% removal on average, respectively; in contrast, the FBR was less effective, at 28% and 37% removal, respectively. However, the elimination

performance was similar between the two reactors at the beginning of operation, and this performance was even better for bentazon in the FBR than in the TBR.
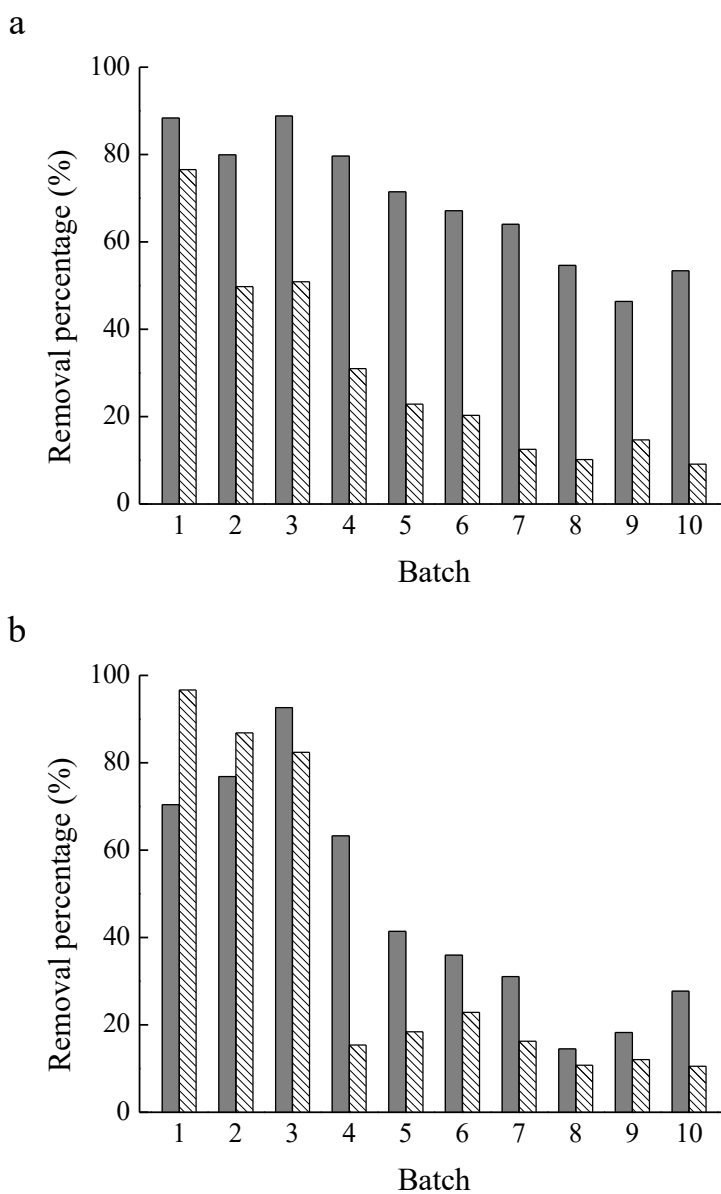
Figure 5.2 Profiles of pesticides removal during one-month sequencing batch treatment by the two different fungal reactors under non-sterile conditions. a. diuron; b. bentazon. *Gray columns*, trickle bed reactor; *medium columns*, fluidized bed reactor.

This result could be explained by the fact that although both sets employed a 3-day cycle, the contact time between the fungi and pollutant was quite low in the case of the TBR according to the above empirical calculations (8.5 h per cycle with the F_r at 70 mL min^{-1}). Therefore, the contribution of the cytochrome P450 system of *T. versicolor* to the selected pesticide degradation was restricted due to the configuration of the TBR, and this

particular intracellular enzyme is largely involved in diuron (Torán, 2018) and bentazon degradation (Chapter 4, Section 4.3.3).

On the other hand, bearing in mind that the lignocellulosic-supporting material in the TBR, namely, pine wood chips, played an indispensable role in the treatment owing to its adsorption since the results from the control reactor showed that 83% of diuron was removed and 28% of bentazon was removed; these values were 26% and 8%, respectively, in regard to pellets in an Erlenmeyer test (Chapter 4, Section 4.3.1.1 and 4.3.2). Such apparent differences between the two pesticides could be ascribed to their different hydrophobicity (PPDB, 2016). However, regardless, the presence of lignocellulosic carrier enhances and maintains the capability of reactors to eliminate target pesticides from water bodies, which is consistent with the results of a more recently published study where pharmaceuticals were adsorbed at a great extent (73%) by the bed that was mainly composed of rice husks (Tormo-Budowski et al., 2021). This evidence further indicates that these organic packing materials play a vital role in wastewater treatment using a TBR. Additionally, it is worth noting that a decreasing trend in the removal yield was observed in both reactors, probably ascribed to the fungal ageing behavior and biomass washing out.

5.3.2.2 bioactivity persistence

Clearly, the TBR demonstrated better results than the FBR based on the contaminant removal yield, as mentioned above, but this evidence is not strong enough to determine which fungal reactor is an ideal option. Therefore, attention was also paid to bioactivity persistence in the two systems. Laccase activity was monitored during operation because it partly reflects fungal activity (Mir-Tutusaus et al., 2017), and the results are shown in Figure 5.3. An enzymatic activity peak of 47 AU L^{-1} was achieved in the TBR at the end of first batch, probably resulting from accumulation within the static incubation, whereas this peak occurred in second running period of the FBR, at 31 AU L^{-1}. Then, although laccase activity displayed a decreasing pattern in both setups and eventually remained at a low constant level, its variation was obviously slower in the FBR than in the TBR. The primary reasons behind this observation could be the different nutrient conditions in the reactors and the possibility that extracellular laccase was adsorbed onto the wood (Arora

and Gill, 2001; Li et al., 2018). Furthermore, adequate oxygen transfer can be guaranteed by employing air-pulse conditions, while air supply should be included in future work using TBRs.
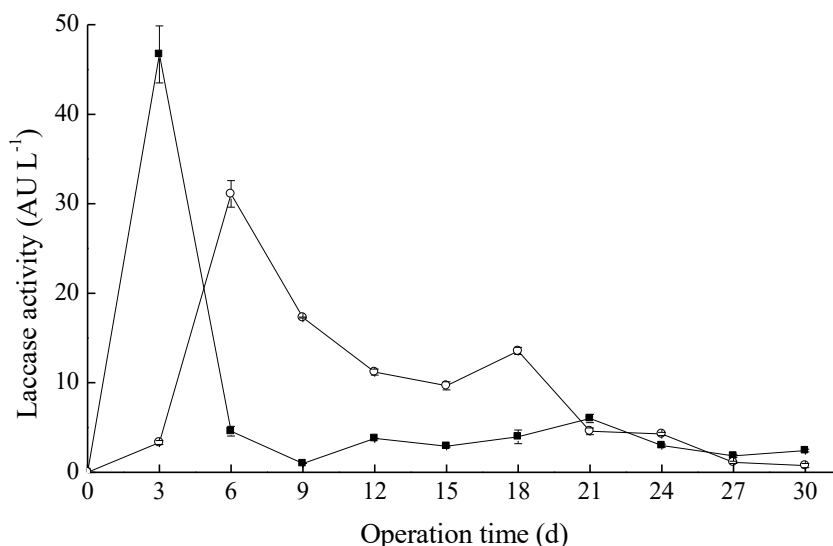
Figure 5.3 Profile of laccase activity during one-month operation. *Filled squares*, trickle bed reactor; *empty circles*, fluidized bed reactor.

5.3.2.3 HPC and COD

The HPC and COD of the wastewater after treatment by the trickle bed reactor and fluidized bed reactor are presented in Table 5.5. A dramatic increase in the bacterial amount was observed in the FBR compared that in the raw water. This result could be explained by the continuous feeding of glucose [1, 200 mg glucose (g DW d)$^{-1}$] for maintenance (Mir-Tutusaus et al., 2017), and the supplemented glucose was almost fully consumed in each batch (final concentration < 0.1 g L^{-1}). With respect to the TBR, although the microbial growth also accelerated after 4 batches, it was largely hindered initially, especially during the 3rd batch, appearing as having no microbial count. In addition, bacterial contamination remained at a lower level in the TBR than in the FBR, indicating that utilization of pine wood as a supporting material is a successful strategy to limit bacterial growth, and this represents a bottleneck in fungal reactor application regimes (Mir-Tutusaus et al., 2018). At the same time, the total COD increased in the two treatments compared with that in the initial wastewater. A common reason may be that the spiked pesticides were not completely

addressed. This result could also be explained by the elution of wood particles from the packed bed and/or wood rotting by *T. versicolor* in the TBR, whereas the contribution was from the addition of antifoam (Tween 80) in the FBR. Fortunately, foam formation was not a concern for the trickle bed reactor treatment since it is somewhat an open-scale system.

Table 5.5 HPC and COD of the agricultural wastewater throughout the one-month sequencing batch treatment by the two different fungal reactors.

Batch	Microbial counts [Log (CFU) mL^{-1}]		COD (mg L^{-1})	
	TBR	FBR	TBR	FBR
1	4.44	8.23	671	1, 172
2	2.90	8.90	590	1, 188
3	0	8.76	521	1, 706
4	3.90	8.52	438	2, 107
5	6.00	8.24	382	1, 695
6	6.10	7.85	318	1, 815
7	6.13	7.20	280	1, 696
8	5.99	7.29	288	2, 097
9	5.92	7.79	208	2, 565
10	5.87	7.95	248	2, 611

5.3.2.4 Economic cost

Regardless, future efforts need to focus economic costs while moving to a scaling-up process. Apart from preparing mycelial suspensions, there is an extra process before starting fluidized bed reactor treatments compared to starting trickle bed reactors, that is, pellet formation. Although a low-cost procedure using a defined medium instead of a malt extract to culture fungi was developed to obtain pellets and can satisfy a large demand (Borràs et al., 2008), other raw materials still bring cost concerns, such as the addition of maintenance nutrients and antifoam, which subsequently escalate bacterial contamination and increase COD. Another point of concern is that a partial biomass renovation strategy should be implemented in the case of long-term treatment, and the cost of heating energy resulting from sterilization during biomass preparation is reasonably higher than the mechanical energy that was necessary for recirculation with a pump. In addition, other problems related to pellet break-up appeared during operation, resulting in biomass loss because of adherence to the bioreactor wall and difficulties in separating biomass from the liquid phase during emptying. In contrast, the TBR is a relatively more robust configuration.

Pine wood performs two functions as a carrier and a source of nutrients, not only taking advantage this reusable waste but also building a natural aerial habitat in which *T. versicolor* demonstrates effectiveness. Based on the above information, the advantages and limitations of these two reactors are summarized in Table 5.6.

Table 5.6 Advantages and limitations of the two reactor configurations for pesticides contaminated wastewater treatment in sequencing batch mode under non-sterile conditions.

Reactor type	Advantages	Limitations
Trickle-bed	• Simple construction and great operational flexibility • Retain biomass in the reactor • Hinder bacterial growth • Low-cost and high sustainability • No nutrients required • Nature conditions emulated	• Short contact time • Low mass transfer • Poor oxygen supply • Risk of clogging in long term operation • Lack of homogeneity • High pumping energy
Fluidized-bed	• High homogeneity • Adequate cellular retention time • Efficient mass transfer	• Required pellet preparation process • Continuous nutrient supply • Higher bacterial competition • Foam formation • Pellet break-up or aggregation • Complicated separation of biomass • Biomass renovation for long term operation

Comprehensively, TBR is a preferred configuration for pesticide-contaminated wastewater fungal treatment in a long-term mode and it is easier to be scaled up, compared with FBR.

5.3.3 Performance of the trickle bed reactor after one-month operation

The TBR was kept running 9 batches more after one month operation, at a higher F_r of mL min^{-1}. The results are presented in Figure 5.4. In comparison with 10th batch, despite the RR was doubled (from 300 to 600) during the second running period, the removal efficacy did not rise significantly, possibly ascribed to that the mean contact time of TBR and the F_r may not fit into a linear regression (Eckenfelder, 2000).

a

b
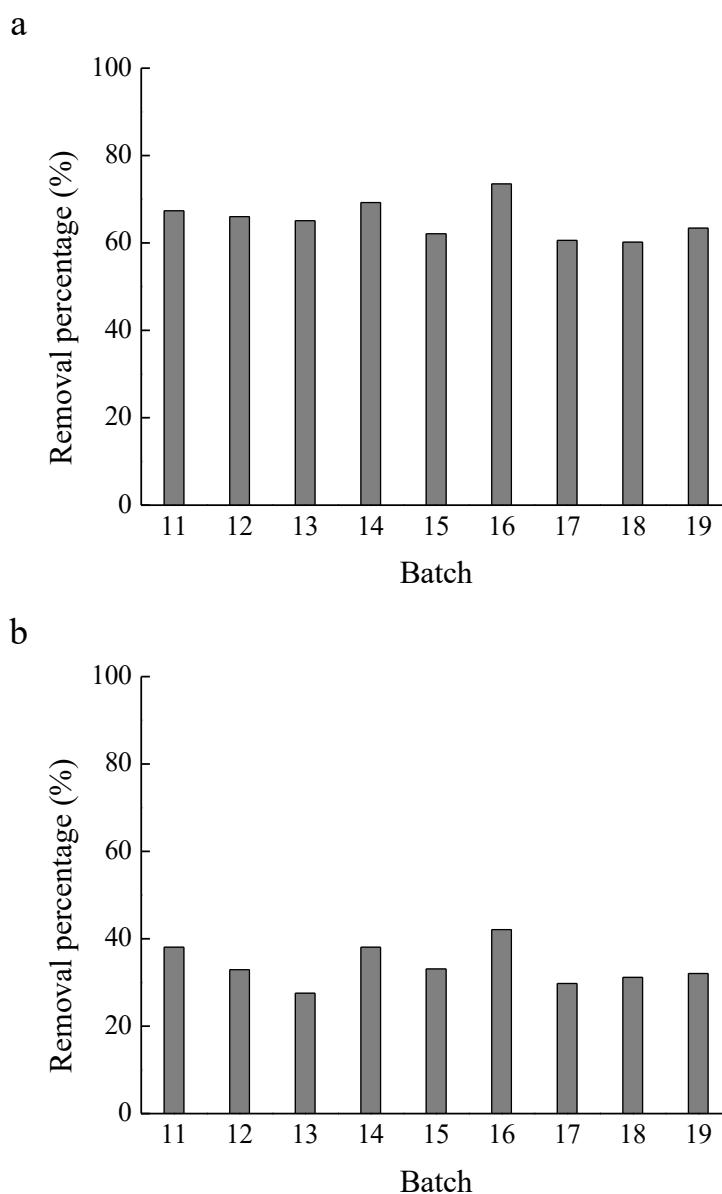
Figure 5.4 Profiles of pesticides removal by the trickle bed reactor during 11th–19th batches treatment. a. diuron; b. bentazon.

Lower mean removal yields were obtained towards diuron and bentazon along those 27 days than first month, showing 65% and 33%, respectively. It is probably due to a drop of bioactivity resulted either from fungal ageing behavior or biomass washing out, since the adsorption contributed more to removal than previously according to the results from the control reactor.

As for laccase, an apparent climb in enzymatic activity (up to 12 AU L^{-1}) was captured after the acceleration of recirculating (Figure 5.5), because of the enhanced dragging force from the water flow. Then, it decreased gradually to almost zero again since 13th batch.
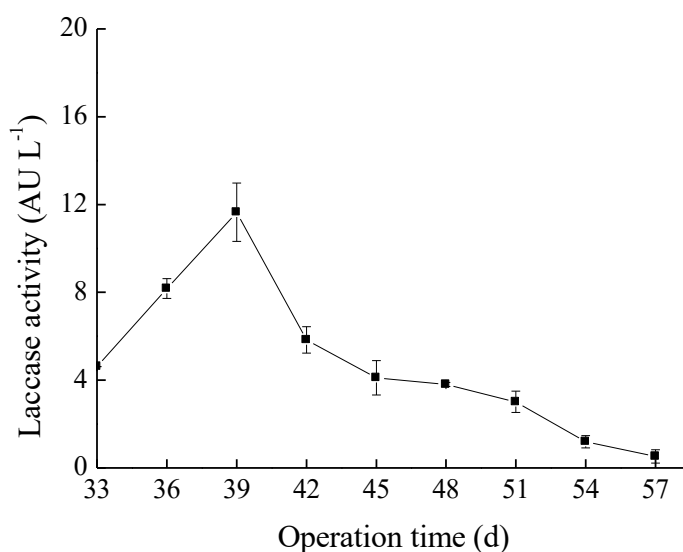
Figure 5.5 Profile of laccase activity in the trickle bed reactor during 11th–19th batches treatment.

The bacterial amount maintained at roughly same level as 8th–10th batch, ranging from 5.37 to 5.92 Log (CFU) mL^{-1} and it declined slightly at the end of running time (Table 5.7). With regard to COD, it increased significantly at the beginning of the second stage. A reasonable explanation could be that the accumulated matrices, such as wood decomposition products, were washed out from the fixed bed by the high-speed water flow.

Table 5.7 HPC and COD of the agricultural wastewater along 11th–19th treatment by the trickle bed reactor.

Batch	Microbial counts [Log (CFU) mL^{-1}]	COD (mg L^{-1})
11	5.65	473
12	5.92	418
13	5.63	358
14	5.37	359
15	5.49	303
16	5.58	290
17	5.37	281
18	4.81	244
19	4.99	328

It's supposed to emphasize that the wood was not visibly degraded during the whole process, indicating that a reinoculation strategy can be taken into consideration to enhance and maintain removal effectiveness.

5.3.4 Profiles of diuron, bentazon and ergosterol in the fixed bed after treatment

The distributions of diuron, bentazon and ergosterol along the fixed bed were assayed in order to further evaluate the operative removal process using trickle bed reactor, and the results are given in Table 5.8. Much more diuron remained in lignocellulosic support than bentazon, which could be attributed to their hydrophobicity and is in agreement with elimination performance obtained above. Both pollutants demonstrated reduction trends from the top part to the bottom part in experimental set up and control, but more dramatically variation occurred in the former. Specifically, diuron residues at the top in fungal reactor was 2.98 times the amount at bottom, while there was only a 9.1% decline in control reactor. On the contrary, ergosterol displayed in an opposite distribution profile and all samples contained less biomass than initially (0.044 mg g^{-1} DW^{-1}), probably due to a high stress promoting the drag effect and aging occurrence of immobilized fungus. This result actually evidences the fact that pesticide amount in packing material decreased along the fixed bed because of biodegradation.

Table 5.8 Distributions of diuron, bentazon and ergosterol along the trickle bed reactor after 19 sequencing batches.

Set up	Analyte	Fate of analytes (mg g^{-1} DW^{-1})		
		Upper	Middle	Bottom
Experimental	Diuron	0.25 ± 0.014	0.17 ± 0.018	0.084 ± 0.003
	Bentazon	0.022 ± 0.002	0.020 ± 0.001	0.014 ± 0.011
	Ergosterol	0.028 ± 0.002	0.030 ± 0.001	0.033 ± 0.003
Control	Diuron	0.22 ± 0.011	0.21 ± 0.005	0.20 ± 0.005
	Bentazon	0.020 ± 0.001	0.011 ± 0.000	0.015 ± 0.003

Note: Means and standard deviation of triplicate are shown; average introduced amount of diuron and betazon are 0.019 mg g^{-1} DW^{-1}, 0.020 mg g^{-1} DW^{-1} respectively in each batch.

Considering a large extent of contaminant remained in the packing material, another degradation experiment was carried out by secondly inoculating *T. versicolor*. As summarized in Table 5.9, promising elimination performance (22.3%) was demonstrated towards bentazon using wood chips from the control reactor, where the average pesticide residues before re-inoculation were: diuron 0.21 mg g^{-1} DW^{-1}, bentazon 0.015 mg g^{-1}

DW^{-1}, respectively. However, diuron remained nearly same in the absence and presence of re-inoculated fungus. With the wood chips from the fungal reactor, biomass enhanced by 61.6% after re-inoculating. But it's infeasible to figure whether biodegradation occurred because the introduced pesticides distributed unevenly in the experimental reactor. In any case, these findings open up new possibilities in avoiding secondary contamination through re-inoculation strategy, especially considering that the residual concentration of selected pollutants in real environment was much lower than 10 mg L^{-1}, and processing period could be extended accordingly.

Table 5.9 Contents of diuron, bentazon and ergosterol remaining in the lignocellulosic carrier after different treatments followed by 4-week incubation.

Wood source	Treatment	Amounts of analytes (mg g^{-1} DW^{-1})		
		Diuron	Bentazon	Ergosterol
Experimental	Re-inoculation	0.21 ± 0.0069	0.0002 ± 0.0002	0.066 ± 0.0060
reactor	Non re-inoculation	0.19 ± 0.0015	0.0050 ± 0.0006	0.041 ± 0.0085
Control reactor	Inoculation	0.20 ± 0.0022	0.012 ± 0.0004	0.046 ± 0.0003

Note: Means and standard deviation of triplicate are shown.

As we can see, biomass experienced washing out along operation and a re-inoculation approach is available to compensate the loss of biomass. Also, seeking for another lignocellulosic that can retain the biomass is worth trying.

5.3.5 Removal of pesticides from real wastewater by the TBR

Prior to scaling-up, lab-scale TBR was further applied for removing pesticide from real water, where the lignocellulosic carrier was substituted with oak wood, since from which the obtained biomass was more than 300 times higher than that from pine wood after two weeks incubation (Table 5.10). Consequently, the preparation time for solid culture was shortened from 4 weeks to 6 days, which is a great credit.

Table 5.10 Colonization of *T. versicolor* on two different lignocellulosic carriers after two weeks incubation.

Lignocellulosic material	Ergosterol (mg g^{-1} DW^{-1})
Pine wood	0.0008 ± 0.0010
Oak wood	0.30 ± 0.046

Note: Means and standard deviation of triplicate are shown.

5.3.5.1 Pesticides removal

Unfortunately, there were only 4 pesticides detected from the real water, namely quinoxyfen, bromoxynil, oxadiazon and triallate, ranging from 190.2–961.5 ng L^{-1}. Quinoxyfen [5,7-dichloro-4-(4-fluorophenoxy)quinoline] is a fungicide that belongs to the family of the quinolines (Cabras et al., 2000). Bromoxynil [3,5-dibromo-4-hydroxybenzonitrile] is a systemic post-emergency herbicide widely used for controlling broadleaved weeds (Baxter and Cummings, 2008). Oxadiazon [5-terbutyl-3-(2,4-dichloro-5-isopropoxyphenyl)-1,3,4-oxadiazol-2-one] is a pre-emergence herbicide (Clark and Kenna, 2010). Triallate [S-(2,3,3-trichloroprop-2-en-1-yl) di(propan-2-yl)carbamothioate] is a derivative of thiocarbamic acid and it possesses herbicide properties (Gupta, 2018). During previous sampling campaign, in total 35 pesticides had been detected, some of which reached the μg L^{-1} level, such as bentazon, propanil, acetamiprid, triallate, etc. (Barbieri et al., 2021). However, the occurrence of the pesticides in the water body is closely related to the local agricultural management practices and climate.

Anyway, their removals in the trickle bed reactor throughout one-month sequencing batch operation are presented in Figure 5.6. Except bromoxynil, all the detected pesticides could be completely removed by both fungal and control reactors. The average removal towards bromoxynil was 65%. There is a high possibility that adsorption onto the lignocellulosic carrier oak wood played a dominant role during treatment, considering no significant higher removal was observed in the presence of *T. versicolor*, and most of those pollutants possess higher hydrophobicity than diuron (Log K_{ow} 2.87), i.e., quinoxyfen (5.1), oxadiazon (5.33) and triallate (5.33). By contrast, low hydrophobicity (0.27) could account for the less efficient elimination of bromoxynil (PPDB, 2016) and the biofilm may negatively affect adsorption. Moreover, the concentrations of those pesticides were much lower than the spiking case.
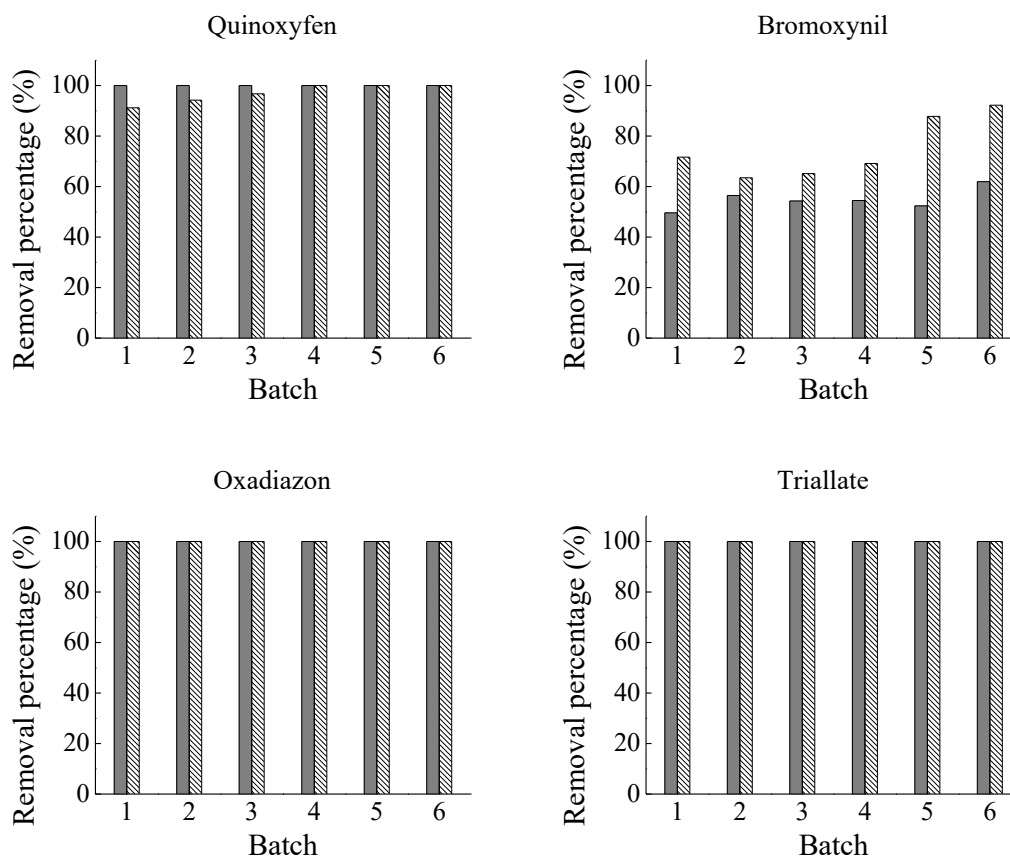
Figure 5.6 Profiles of pesticides removal from the real water during one-month sequencing batch treatment by the trickle bed reactor under non-sterile conditions. *Gray columns*, experimental reactor *medium columns*, control reactor.

5.3.5.2 Laccase activity

Similar to previous demonstration, a peak of laccase activity (54 AU L^{-1}) appeared at the end of the first batch (Figure 5.7). Then it started to decline since the second batch and disappeared after 25 days, which was slightly faster than previous case, probably owing to higher RR (1, 200) was picked.

Despite the performance was not as satisfying as we expected in the first place since no biological contribution was demonstrated, all the pesticides were considerably removed from the real water, presenting as a forward step to real application.

Figure 5.7 Profile of laccase activity in the trickle bed reactor during real water treatment.

5.3.5.3 Evolution of microbial population

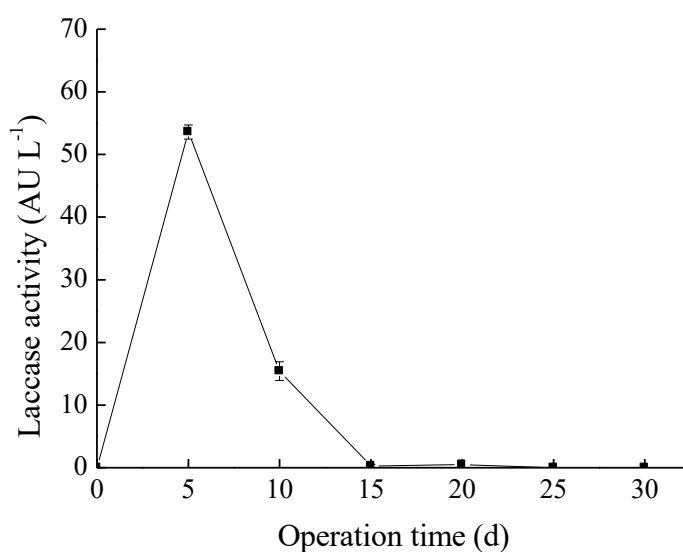Denaturing gradient gel electrophoresis (DGGE) fingerprint analysis indicates that there were more taxonomic groups in the liquid matrix than in the solid matrix along the operation. Besides *Trametes*, bacterial sequences belonging to *Acidisoma*, *Chitinophaga*, *Novosphingobium* and *Kosakonia* genus, fungal sequences belonging to *Cystobasidium*, *Rhodotorula*, *Coniochaeta*, *Penicillium* genus, were identified in both matrices (Table 5.11 and 5.12). *Acidisoma*, *Legionella* and *Novosphingobium* were introduced from the AW because they were not present in the lignocellulosic sample initially but existed in the liquid. *Kosakonia*, *Penicilium*, *Cystobasidium* were not found at the beginning, but they were abundant in the later period. During the long-term hospital wastewater fungal treatment using, *Fusarium* were abundant in the liquid fraction of the bioreactor and competing with *T. versicolor* (Mir-Tutusaus et al., 2019). In this work, our candidate kept the dominance throughout the operation without partial biomass renovation, revealing the positive effect of using wood waste.

Table 5.11 Relative abundance of different bacterial and fungal genera from the liquid matrix of the reactor.

Microflora	Genus	Operation time (d)						
		0	Experimental reactor			Control reactor		
			5	15	30	5	15	30
Bacteria	*Acidisoma*	++	++	+	−	++	+++	+
	Chitinophaga	−	−	+	+++	−	++	++
	Legionella	+	−	+	+	−	−	−
	Methylophylus	−	−	+	−	−	−	−
	Novosphingobium	+	+	++	−	+	+	++
	Kosakonia	−	+++	++	+	+++	−	−
Fungi	*Nakazawea*	−	−	+++	−	−	−	−
	Cystobasidium	−	−	−	−	−	−	−
	Rhodotorula	−	−	−	−	++	−	+
	Curvibasidium	−	−	−	−	−	++	−
	Coniochaeta	−	−	−	−	−	−	−
	Chaetomium	−	−	−	−	−	−	−
	Trametes	−	+++	−	−	++	+	++
	Capronia	−	−	−	−	−	−	++
	Peltigera	−	−	−	−	+	++	+
	UB1	+	−	−	−	−	−	−
	UB2	+	−	−	−	−	−	−
	UB3	++	−	−	−	−	−	−
	UB4	+	−	−	−	−	−	−
	UB5	++	−	−	−	−	−	−
	Lecitophora	−	−	−	−	+	−	+
	Penicilium	−	−	−	+++	−	−	−

Note: −, absent; +, ≥ 0.01%; ++, ≥ 25%; +++, ≥ 50%. UB, unidentified band.

Table 5.12 Relative abundance of different bacterial and fungal genera from the solid matrix of the reactor before and after the operation.

Microflora	Genus	Experimental reactor				Control reactor			
		Initial	Upper	Middle	Bottom	Initial	Upper	Middle	Bottom
Bacteria	*Acidisoma*	–	+++	+++	+++	–	–	–	–
	Chitinophaga	–	+	–	++	–	–	+	+
	Novosphingobium	–	+	–	–	–	+++	+++	+++
	Burkholderia	–	+	++	–	–	–	+	+
	Kosakonia	–	+	+	–	–	–	+	+
Fungi	*Cystobasidium*	–	++	+++	–	–	+	+	+
	Rhodotorula	–	–	–	–	–	–	–	–
	Fusarium	+	–	–	–	++	+	+	+
	Trametes	+++	+	–	+	++	+	+	+
	Coniochaeta	+	+	–	+++	–	++	+	++
	Aspergillus	–	+	–	+	+	+	–	–
	Penicillium	–	+	++	+	+	+	++	+

Note: –, absent; +, ≥ 0.01%; ++, ≥ 25%; +++, ≥ 50%.

From the view of *T. versicolor*, it was captured in both experimental and control reactor, which is fair because these reactors were installed closely. Immobilization on oak wood could successfully retained the fungus in the reactor, since *Trametes* was only found in the liquid at Day 5. However, in comparison with initial abundance, it was only detected at relative low concentration in the top and bottom fractions after running 30 days, which somewhat coincides with the results from ergosterol measurement (Table 5.13). But it is supposed to keep in mind that ergosterol reflects general fungal biomass (Gessner, 2020).

Table 5.13 Ergosterol distribution along trickle bed reactor after 30 days operation.

Section	Biomass (mg g^{-1} DW^{-1})
Upper	0.47 ± 0.09
Middle	0.32 ± 0.06
Bottom	0.38 ± 0.04

Note: Means and standard deviation of triplicate are shown.

Further work needs to be carried out in the future, to investigate the interactions between *Trametes* and other microorganisms amid operation using TBR, because they may produce synergistic effect on pollutant removal.

5.4 Conclusions

➢ For the employed trickle bed reactor configuration setup, volumetric quantification is a simple methodology to determine the representative mean contact time.

➢ Good pesticides removals were obtained by fungal TBR in both spiking and actual scenarios, during which the lignocellulosic supporting material played a vital role.

➢ It is feasible to address the adsorbed pesticides through a re-inoculation strategy.

➢ In comparison with FBR, TBR is a preferred option for the purpose of long-term treatment and scaling up.

➢ Immobilizing the fungus on wood chips could successfully retain biomass and tackle competitions from other microorganisms, especially bacteria.

➢ Working efficacy of fungal TBR can be enhanced by increasing contact time and biomass.

Chapter 6

Agricultural wastewater treatment by pilot-scale fungal reactor

6.1 Introduction

Several WRF-based trickle bed reactors have been reported to be applied for the abatement of different pollutants, both emerging and persistent contaminants, including dyes (Hambali et al.; Pocedič et al., 2009; Tavčar et al., 2006), pharmaceuticals (Tormo-Budowski et al., 2021), phenolic compounds (Ehlers and Rose, 2005), etc. In this regard, the work of Chapter 5 sheds light into pesticides elimination from real wastewater. On the other hand, to our best knowledge, so far there is no information about using scaled-up fungal TBR to treat pesticides contaminated wastewater under non-sterile conditions in a long-term mode, except that limited reports talking about the removals of endocrine disruptors and polychlorinated biphenyls by *Pleurous ostreatus* (Křesinová et al., 2018; Šrédlová et al., 2020).

In this chapter, a pilot-scale TBR with immobilized *T. versicolor* on oak wood was constructed, and it was operating continuously for 186 days under non-sterile conditions to treat real water from the irrigation canal of the Llobregat river, in which diuron and bentazon were spiked, meeting the analytical purpose. Prior to run the reactor, the contact time in the scaled-up system was determined using the technique proposed in Chapter 5. During the long-term operation, the wood waste acted as the only carbon source, without addition of any other nutrient. The influence of the main parameters was explored, accompanied with the verification of the configuration robustness against contingencies and the analysis of the microbial community evolution. After stopping the reactor, the effect of using agricultural wastewater on laccase generation by *T. versicolor* was explored, together with characterizing the lignocellulosic carrier, such as fiber analysis, pesticide residues quantification and biopile test.

6.2 Specific methods in this chapter

6.2.1 Contact time determination

Several trials were carried out using the control reactor in the absence of aeration to determine the average contact time, before starting up the operation. In this case, volumetric quantification technique was served, as described in Chapter 5 (Section 5.2.1).

6.2.2 Removing selected pesticides by the scaled-up trickle bed reactor in continuous mode

Due to the quarantine driven by covid-19 pandemic, after 14 days static incubation, the solid culture was conserved at 4 °C for 72 days. Then, in order to confirm if the fungus was still active, the solid culture was supplemented with fresh oak wood chips accounting for approximately 37% of its total weight, followed by mixing and further incubating at room temperature for 41 days before transferring to reactor. Actually, 41-day incubation was far beyond the necessity, but we were waiting for the scaffold materials.

Two reactors (fungal reactor and blank control) were running simultaneously in a continuous mode with an HRT of 3 days. HRT is defined as Eq (6-1):

$$\mathrm{HRT} = \frac{V_r}{F_{in}} \tag{6-1}$$

where V_r represents liquid volume in the reservoir tank (3.6 L) and F_{in} corresponds to influent flow rate ($mL\ min^{-1}$).

Three different RRs, defined as Eq (6-2), have been adopted along 186 days operation.

$$\mathrm{RR} = \frac{F_r}{F_{in}} \tag{6-2}$$

Accordingly, the operation was divided into different periods (Table 6.1). Liquid samples were withdrawn from the reservoir tank periodically for analyses, including laccase activity, pesticide residues, HPCs, COD, turbidity and microbial community structure. Solid samples were taken from the top part of each section at designated time for ergosterol measurement, scanning electron microscope (SEM), microbial community structure and fiber content analysis.

Table 6.1 Conditions tested in the TBR during long-term operation.

Period	Days	Recirculation ratio
I	0–90	284
II	90–153	142
III	153–174	71
IV	174–186	142

Agricultural wastewater (AW) III–VI were utilized for the long-term treatment, among which the physicochemical characteristics of AW III and IV have been listed before (Table 5.2). For AW V and VI, they are as follows:

Table 6.2 Physicochemical characterization of the agricultural wastewater used for the long-term treatment.

Parameter	AW V & VI
pH	8.06 ± 0.02
Absorbance at 655 nm	0.10 ± 0.01
Conductivity (mS cm^{-1})	3.17 ± 0.01
TSS (mg L^{-1})	15.87 ± 1.62
VSS (mg L^{-1})	11.07 ± 2.01
TOC (mg L^{-1})	16.31 ± 0.81
HPC [lg (CFU mL^{-1})]	4.54 ± 4.18
Ammonia	ND
COD (mg O$_2$ L^{-1})	43.60 ± 4.23
Chloride (mg Cl$^-$ L^{-1})	653.69 ± 6.14
Sulfate (mg SO$_4^{2-}$ L^{-1})	86.26 ± 1.58
Nitrite (mg NO$_2^-$ L^{-1})	0.41 ± 0.02
Nitrate (mg NO$_3^-$ L^{-1})	0.02 ± 0.02

Mean value and standard deviation are shown. ND, not detected.

6.2.3 Quantification of ergosterol and pesticide residues for the packing material after long-term treatment and biopile test

After stopping the reactor, all the packing beds were withdrawn from the cylinders and mixed. Several samples were taken and subjected to ergosterol and pesticide extraction. In parallel, 120 g of packing material were transferred into 250 mL Schott bottle and inoculated with *T. versicolor* mycelia suspension as described in in Chapter 3 (Section 3.1.3), followed by one-month static incubation at 25 °C. Then, the cultures were totally scarified for ergosterol and pesticide extraction.

6.2.4 Batch laccase tests

Six batch tests were conducted to evaluate the effect of utilizing AW on laccase production by immobilized *T. versicolor*. The detailed conditions are given in Table 6.3. 5 g of mixed wood chips were withdrawn from experimental reactor after the long-term operation and transferred into 500 mL Erlenmeyer flask containing 100 mL of either wastewater or define medium. Then the cultures were incubated at 25 °C in the dark under continuous orbital-shaking (135 rpm) for 4 days. Specifically, in Group B both diuron and bentazon were spiked at final concentration as 10 mg L^{-1}, and in Group C Cu^{2+} was supplemented up to the same amount as it in the defined medium. As for Group F, a certain amount of pellets were aseptically inoculated into 100 mL of modified defined medium (without adding glucose and ammonium tartrate), achieving the equal biomass to 5 g wood chips, based on the correlation between ergosterol and pelletized biomass (Rodríguez-Rodríguez et al., 2010a). Each condition was tested in triplicate. Aliquots were taken daily to measure laccase activity.

Table 6.3 Conditions tested in batch experiment.

Groups	Conditions
A	Wood chips + wastewater
B	Wood chips + wastewater + selected pesticides
C	Wood chips + wastewater + Cu^{2+}
D	Wood chips + defined medium
E	Wood chips + defined medium (no glucose and ammonium tartrate)
F	Pellets + defined medium (no glucose and ammonium tartrate)

6.2.5 Analytical methods

6.2.5.1 SEM

Field emission scanning electron microscopy (FESEM) images were collected on a Zeiss EVO MA 10 scanning electron microscope. The sample pretreatment was conducted by Microscopy Service of the Universitat Autónoma de Barcelona (Bellaterra, Spain), and the methodology is depicted in Annex D.

6.2.5.2 Fiber content analysis

Cellulose, hemicellulose and lignin were determined by the method of Van Soest et al.

(1991). These analyses were performed by the Laboratory of Agriculture and Animal Production, Department of Animal and Food Science, Faculty of Veterinary Medicine, Universitat Autónoma de Barcelona (Bellaterra, Spain). The detailed protocol is given in Annex D.

6.2.5.3 Copper concentration of the agricultural wastewater

The copper in the agricultural wastewater was quantified by Chemical Analysis Service of the Universitat Autónoma de Barcelona (Bellaterra, Spain), and the method is clarified in Annex D.

6.3 Results and discussions

6.3.1 The contact time in the pilot-scale TBR

It has been proposed that the mean contact time between the fluid and the bedding material in TBR configuration is positively related to the fixed-bed length (Eckenfelder, 2000), as described in Equation (6-3):

$$t_c = \frac{cH}{L^n} \tag{6-3}$$

where t_c is the mean contact time (s), H represents the height of packing bed (cm), and L corresponds to the hydraulic loading rate (mL cm^{-2} min^{-1}). c and n are constants that depend on characteristics of biomass carrier.

Based on obtained responses and the control reactor configuration, Eq (6-3) could be verified as:

$$t_c = \frac{1.024\,H}{L^{0.573}} \tag{6-4}$$

Given that H = 176 cm and in each HRT the total contact time $\sum t_c$ (h) can be calculated by expression

$$\sum t_c = t_c N_c \tag{6-5}$$

where the number of recirculation cycles N_c is a function of F_r and V_r, as Eq. (6-6)

$$N_c = \frac{F_r \times HRT}{V_r} \tag{6-6}$$

So, the $\sum t_c$ can be determined by Eq. (6-7):

$$\sum t_c = 0.878 \, F_r^{0.427} \qquad\qquad (6\text{-}7)$$

Clearly, the total contact time is positively related to the recirculation flow rate, but practical concerns such as energy cost, pump workload, biomass washing out, etc. should be taken into consideration. Hence, a suitable F_r as 236 mL min^{-1} (RR 284) was fixed for the first period of running, together with twice continuously reducing by half during Periods II and III, to evaluate the efficacy and robustness of the established system. Table 6.4 exhibits the comprehensive information of parameters chosen in this chapter. Specifically, the liquid phase hold-up rate ε_L (%) was calculated by expression

$$\varepsilon_L = \frac{V_L}{V_T} \qquad\qquad (6\text{-}8)$$

where the total volume of reactor V_T (cm^3) is a constant while the volume of liquid residing in the reactor V_L (cm^3) can be substituted with

$$V_L = F_r t_c \qquad\qquad (6\text{-}9)$$

As can be observed, appropriate liquid holding-up rates between 1% and 2.5% (v/v) were granted, at which both mycelium growth and enzyme production would proceed properly (Pocedič et al., 2009), besides flooding accident could be avoided. However, it is assured that those values will be higher in experimental reactor because they were measured in the absence of mycelium that actually will enhance the compactness of packing bed.

Table 6.4 RRs selected within operation and their corresponding characteristics.

RR	F_r (mL min^{-1})	$\sum t_c$ (h)	ε_L (%)
284	236	9.04	2.39
142	118	6.72	1.78
71	59	5.00	1.32

6.3.2 Response of pesticide residues during the long-term operation

Time-course profile of the residual diuron concentration in effluent is depicted in Figure 6.1. As can be seen, a great extent of fortified pollutant was removed on the first operational day, which would be attributed to the adsorption effect from oak wood since a more dramatically diuron concentration plunge occurred in control reactor, down to 0.58 mg L^{-1}. This keeps in line with previous behaviors (Chapter 5), indicating again that the adsorption contributed by lignocellulosic carriers play vital role in wastewater treatment

using this type of bioreactor. From the second running day onwards, the residual diuron concentration in the control reactor continuously increased during Period I and surpassed the experimental group level at Day 21, then it maintained at a constant concentration of 3.42 ± 0.16 mg L^{-1} until the end of Period IV in spite of different RRs. This remarkable sorption capacity towards diuron by oak wood is in agreement with the study of Beltrán-Flores et al. (2020) using pine wood. Such findings reveal new potential in valorizing those natural reusable wastes.
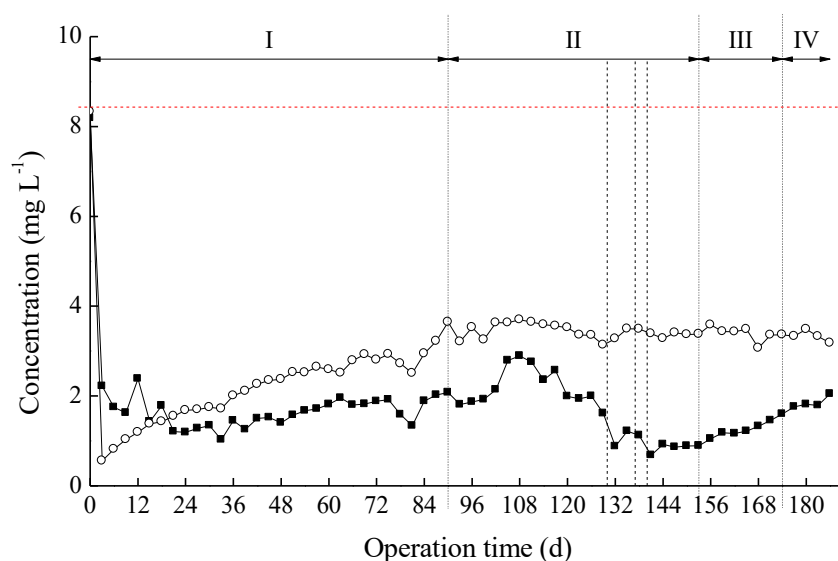

Figure 6.1 Time-course of diuron residues during the long-term continuous treatment with an HRT of 3 d. *Filled squares*, experimental; *empty circles*, control; *red horizontal dashed line*, average concentration of diuron in the influent; *black vertical dotted line*, four different periods; *black vertical dashed line*, the reconstitution of packing material.

In the scenario of experimental reactor, the system entered a stationary state since Day 21, given that 7 times the HRT had passed, after which a progressive increase in diuron residues can be observed, ranging from 1.03 mg L^{-1} to 2.08 mg L^{-1}. During Period II, despite the RR was reduced by half, the total contact time per hydraulic cycle just shortened 2.32 h (Table 6.4). Thence the residual diuron concentration didn't rise significantly, and it even started to decrease at Day 108. This is possibly owing to the clogging accident that frequently occurs in bio-tricking filtration regime (Zhang et al., 2020), which also reflects in pressure measurement through a U-tube manometer (Figure 6.2).
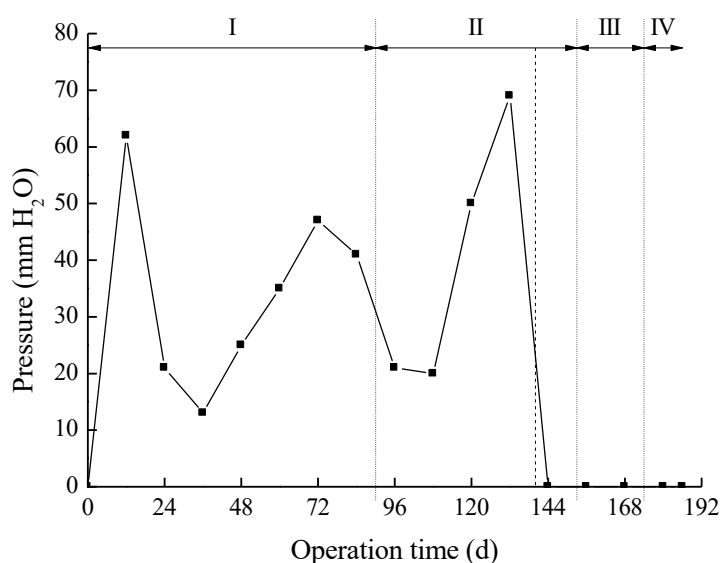
Figure 6.2 Pressure variation during the long-term continuous treatment. *Vertical dotted line*, four different periods; *vertical dashed line*, the time when all the packing beds have been reconstituted.

However, such issue perhaps in turn caused to prolong the $\sum t_c$, by which the contribution from the cytochrome P450 system of *T. versicolor* to diuron degradation was enhanced (Torán, 2018), displaying as the concentration at Day 129 dropped by 44% compared to Day 108. Nevertheless, the packing beds were necessarily reconstituted as shown in Figure 6.3 since Day 130, which triggered further decline in the diuron concentration thanks to the adsorption took place on virgin wood chips.
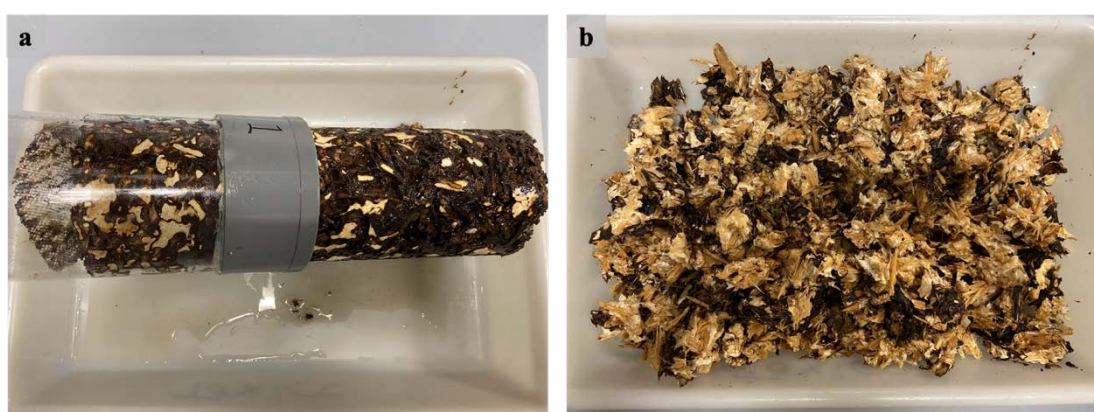

Figure 6.3 The packing bed of TBR after 130 days operation. a. before reconstitution; b. after reconstitution.

Then the experimental reactor entered next steady state after 144 days. Considering that t_c is a critical point in TBR treatment and it was limiting in Period III (5 h), the RR was

adjusted back to 142, to evaluate the resilience of the system. Although a progressive decrease in diuron removal was shown within Period III and Period IV, its concentration still in the range of Period I, varying from 0.89 mg L^{-1} to 2.05 mg L^{-1}. In spite of that, it seems more likely that the system required longer time than 3 times the HRT to achieve equilibrium. The residual concentration difference between the control and the experimental reactor represents the effect of biodegradation, contributing an average reduction of 1.38 ± 0.65 mg L^{-1} in diuron from Day 21 to Day 186. Furthermore, it demonstrated a gradually enhancing tendency before Day 156.

By contrast, bentazon showed some discrepancies in its profile. On one hand, a sharp increase in bentazon residues of the control reactor was observed after the first step of adsorption, exceeding the influent concentration at Day 45 (Figure 6.4). This behavior suggested that a saturation point of bentazon adsorption by oak wood chips had been reached, after which desorption and adsorption emerged alternately, coinciding well with using pine wood. Similar buffering effect has also been reported by Bourneuf et al. (2016) using a granular activated carbon as adsorbent. On the other hand, even if the residues variation patterns of both contaminants in experimental reactor were essentially analogous, comprehensively bentazon exhibited lager fluctuations than diuron throughout the long-term operation. For instance, residual bentazon concentration was almost triple towards the end of Period IV as high as that at the beginning of Period III, whereas it was nearly double when it comes to diuron. Those differences between the two selected pesticides could be ascribed not only to their different hydrophobicity (PPDB, 2016), but also possibly to the fact that laccase involves in bentazon degradation (Chapter 4, Section 4.3.3) instead of diuron (Torán, 2018). This involvement also embodied in the fungal contribution, since an average reduction of 6.26 ± 0.97 mg L^{-1} in bentazon was obtained in the experimental system compared with the control setup from Day 21 onwards. It was a large proportion (66%) of spiked amount and significantly higher than diuron case (16%). Alternatively, if the proportion was calculated by comparing the pesticide concentration in the effluent and the influent of the experimental reactor, an opposite superiority can be caught, exhibiting as 81% reduce for diuron and 68% for bentazon, from Day 21 onwards. In any word, the fungal activity demonstrated persistent.
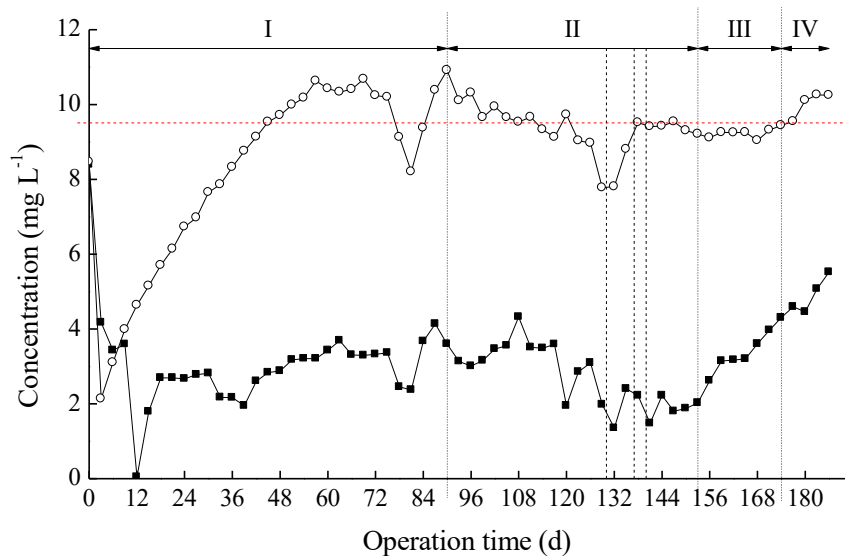
Figure 6.4 Time-course of bentazon residues during the long-term continuous treatment with an HRT of 3 d. *Filled squares*, experimental; *empty circles*, control; *red horizontal dashed line*, average concentration of bentazon in the influent; *black vertical dotted line*, four different periods; *black vertical dashed line*, the reconstitution of packing material.

The sorption process of diuron and bentazon on oak wood was deeply investigated in another work, where the adsorption capacity values were estimated to be 0.29 and 0.012 mg per g dry weight (DW) wood, respectively (Beltrán-Flores et al., 2021). In this chapter, the initial amount of wood chips loaded into the control reactor was 3096.14 g in term of DW. Based to those numbers, it is feasible to propose an approximate mass balance in the control reactor because the remained pesticide mass (M_R) throughout 186 days operation can be quantified by Eq (6-10):

$$M_R = F_{in} \int_0^{186} C_t d_t \qquad (6\text{-}10)$$

where C_t equals to the pesticide concentration in the effluent of the control reactor at each time.

And the introduced mass (M_I) was:

$$M_I = 186 \times C_{in} F_{in} \qquad (6\text{-}11)$$

where C_{in} equals to the average pesticide concentration in the influent of the control reactor.

Accordingly, mass balances for each pesticide in the control reactor are presented in Table 6.5. It can be obtained that adsorption contributed around 72% and 24% to diuron

and bentazon removal, respectively, suggesting there were other mechanisms participating the cleaning process, such as biodegradation by indigenous microorganisms or photodegradation (Carena et al., 2020; Giacomazzi and Cochet, 2004).

Table 6.5 Mass balance profile of pesticides in the control reactor throughout 186 days operation.

Mass (mg)	Diuron	Bentazon
Introduced	1, 882.63	2, 122.82
Remained	637.20	1, 967.47
Removed	1, 245.43	155.34
Adsorbed	879.88	37.15

From the operational perspective, the packing bed needs to be rearranged after 120 days, to address the clogging accident resulted from continuously fungal growth.

6.3.3 Reactor performance

The TBR performance was evaluated during 186-day continuous operation based on pesticides removal, HPC and COD data acquired from steady state in different periods. As summarized in Table 6.6, majority of fortified diuron (> 75%) were removed by experimental reactor during stationary period, of which 63% yield was from the adsorption by lignocellulosic carrier. Interestingly, diuron removal efficiency did not decrease significantly in experimental setup during Period II together with the reduction of RR, instead it even increased during Period III. It can be assumed that the occurrence of clogging led to strengthening the involvement of cytochrome P450 in degradation and substantial virgin adsorption sites emerged after reconstitution as aforementioned. Moreover, it's reasonable that the rise of diuron removal efficiency during Period III is mainly governed by the adsorption on virgin sites since the total contact time was shortened by 45% whereas it was just 26% during Period II (Table 6.4). But the effect of flow routes rearrangement on mean contact time should be also considered. Although the RR was adjusted back to the same level as Period II, a considerable decline in bentazon removal by experimental reactor was observed during Period IV, yielding as 44%. This is possibly because some extent of adsorbed bentazon was released due to its low affinity to the oak wood.

Table 6.6 Evaluation of reactor performance during steady state for each operational period.

Set	Period	Days	Diuron removal (%)	Bentazon removal (%)	lg CFU mL^{-1}	COD$_{effluent}$ (mg O$_2$ L^{-1})
Experimental	I	0–90	81 ± 4	69 ± 6	5.08 ± 0.21	1, 143 ± 376
	II	90–153	76 ± 8	69 ± 8	5.53 ± 0.42	873 ± 489
	III	153–174	84 ± 2	62 ± 5	5.73 ± 0.32	723 ± 219
	IV	174–186	77 ± 2	44 ± 3	5.14 ± 0.22	296 ± 63
Control	I	0–90	71 ± 6	7 ± 11	6.51 ± 0.75	594 ± 100
	II	90–153	59 ± 2	3 ± 5	6.87 ± 0.28	276 ± 55
	III	153–174	60 ± 2	3 ± 2	6.80 ± 0.18	438 ± 112
	IV	174–186	61 ± 1	0 ± 0	6.04 ± 0.36	481 ± 7

Note: Means and standard deviation are shown. COD$_{influent}$ was 2, 978 ± 686 mg O$_2$ L^{-1}.

In fact, present scale-up system obviously improved pesticides removal and demonstrated much stronger persistence in comparison with lab-scale TBR (Chapter 5), highlighting the feasibility of fungal treatment in a long-term operation without nutrients maintenance.

As one bottleneck of fungal treatment, bacterial contamination severely hinders its way to real application (Mir-Tutusaus et al., 2018). The work of Torán (2018) and Chapter 5 have proved that the immobilization of fungus on lignocellulosic material reacted as a successful therapy to address this concern. The consequence of the strategy in long-term running mode was explored in this Chapter, turned out there was apparently less bacterial contamination in experimental reactor than in control set, displaying a decline of 0.90–1.43 lg CFU mL^{-1} in HPC during each stationary period (Table 6.6). Actually, this benefit offered by the predominance of *T. versicolor* in the reactor gradually rose until Day 140, then it was weakened after reconstitution, followed by improving again from Day 156 onwards (Figure 6.5). A plausible explanation could be the rearrangement of packing material broke existing balance and fungus required time to restore it, during which the bioreactor was relatively fragile. Nevertheless, the system was robust enough to allow stable performance. On the other hand, the presence of bacterial community may involve in pesticide biodegradation.
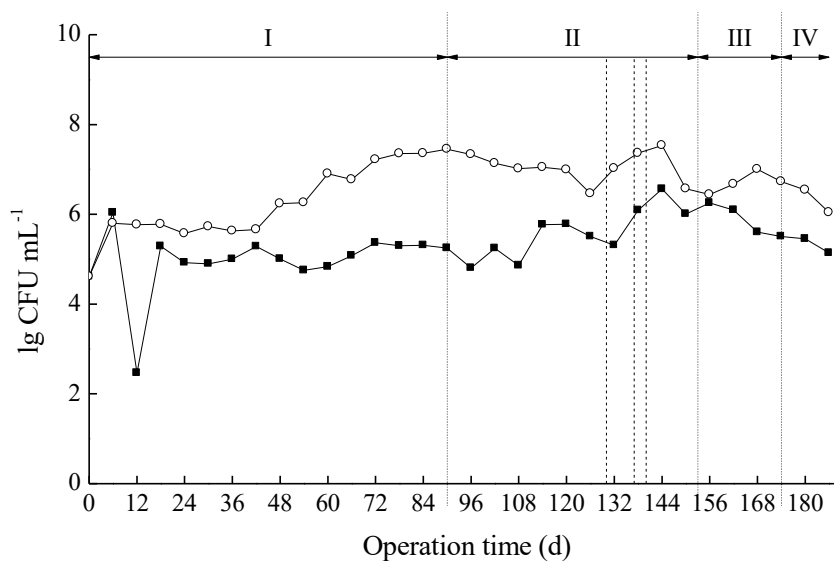
Figure 6.5 Profiles of heterotrophic plate count during the long-term continuous treatment. *Filled squares*, experimental; *empty circles*, control; *vertical dotted line*, four different periods; *vertical dashed line*, the reconstitution of packing material.

With regard to COD, although its elimination stepwise increased in experimental reactor no matter what RR was applied, it showed higher residues than control group in the effluent at the beginning of Period I towards to the end of Period III (Table 6.6). This demonstration is similar to previous chapter and it's due to the wood rotting mediated by fungus, which somewhat could address why the deviations of data acquired from experimental setup are larger than control. As a matter of fact, fungal treatment is always accompanied with increase of COD, ascribed either to the release of organic matter from biomass (Prigione et al., 2008) or to the addition of nutrients (Mir-Tutusaus et al., 2018). The decay process further affected the water holding capacity of fungal fixed bed, rising the ratio between the wet weight and the dry weight from 2.18 before start-up to 6.76 after running, whilst it varied from 2.41 to 2.69 in the control scenario. Meanwhile, it can be supposed that there was a sustained accumulation of wood decomposition matrices in the fungal reactor owing to the fact that the main water flow went downwards through preferred routes while some parts of packing bed were rarely rinsed before reconstitution. Consequently, as presented in Figure 6.6, a sharp COD rise appeared in the effluent after Day 130 and reached a certain point at Day 144, by almost tripling that of Day 126 and concomitantly bringing the data deviation up. Despite it subsequently declined and the elimination capacity eventually

surpassed the control reactor during Period IV (Table 6.6), this is still a concern in the regime of fungal TBR utilizing lignocellulosic material as carrier.
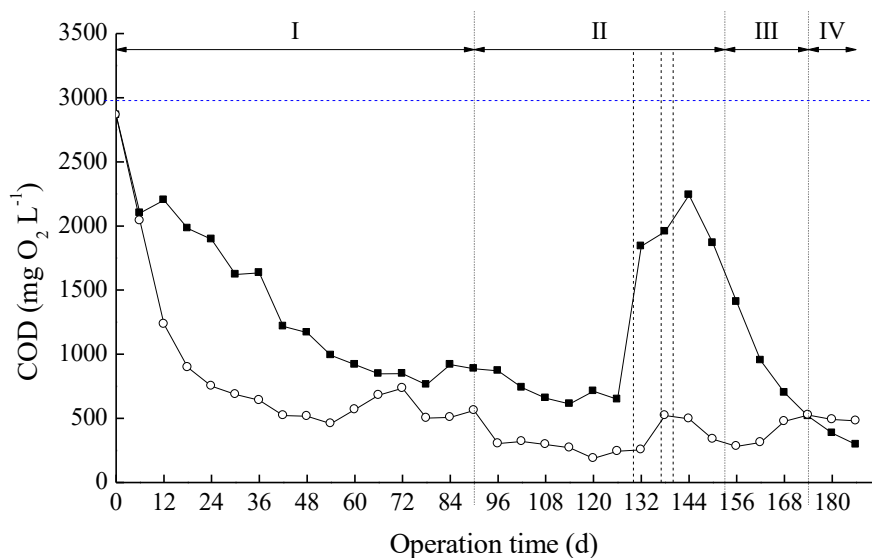

Figure 6.6 Profiles of effluent COD variation during the long-term continuous treatment. *Filled squares*, experimental; *empty circles*, control; *blue horizontal dashed line*, average COD concentration in the influent; *vertical dotted line*, four different periods; *vertical dashed line*, the reconstitution of packing material.

Nonetheless, the dedication from *T. versicolor* to reduce water turbidity, especially from Day 132 to the end of Period IV (Figure 6.7), could be hypothesized as being a silver lining in this aspect.
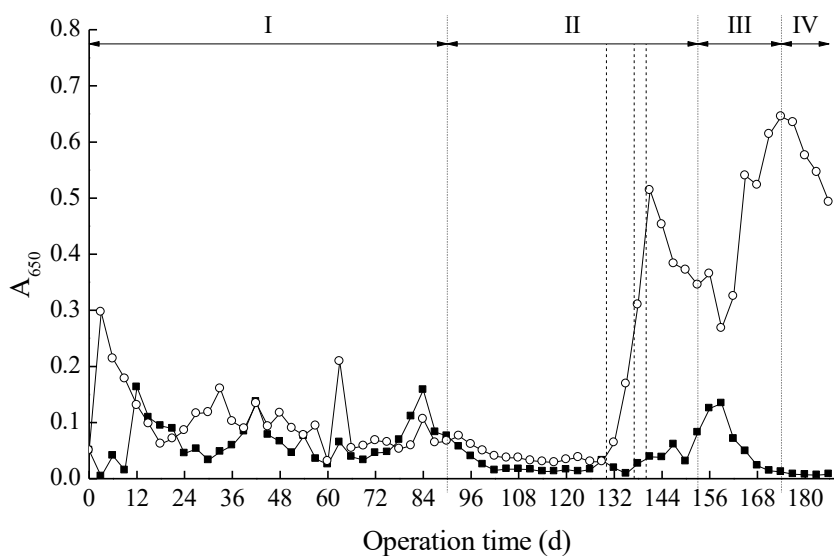
Figure 6.7 Evaluation of turbidity during the long-term continuous treatment. *Filled squares*, experimental; *empty circles*, control; *vertical dotted line*, four different periods; *vertical dashed line*, the reconstitution of packing material.

Apart from those results mentioned above, laccase activity was also routinely monitored along the treatment, and its profile during the long-term operation is presented in Figure 6.8. Expectedly, a maximum enzymatic activity as 42 AU L^{-1} was captured at Day 18, after a relatively small range rise, probably resulted from accumulation within the static incubation. Then, it dropped slowly to almost zero. More fluctuations were observed during Period I than Period II. Notably, a couple of sudden climbs of laccase activity with peaks of over 15 AU L^{-1} were observed between Day 130 and Day 140, owing to that some laccase stranded in the reactor previously but they were eluted out together with wood decomposition matrices after the reconstitution. Then, laccase activity plunged again and eventually disappeared even a higher F_r was run. This profile could be linked to those relatively large fluctuations of bentazon residual concentration in fungal reactor. However, the low or non-detectable laccase activity in liquid phase could not be regarded as an indication of the fungus inactivity, especially considering that laccase can also exist intracellularly (Blánquez et al., 2004) or be adsorbed onto wood (Cristóvão et al., 2011; Li et al., 2018). Furthermore, promising biodegradation yield was demonstrated throughout the runtime (Table 6.6), and similar findings have been reported elsewhere (Mir-Tutusaus et al., 2016).
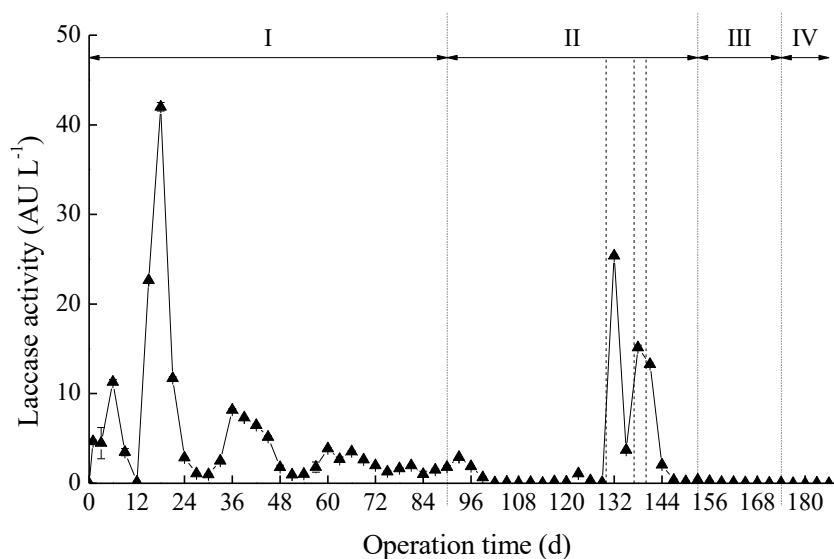
Figure 6.8 Evaluation of laccase activity during the long-term continuous treatment. *Vertical dotted line*, four different periods; *vertical dashed line*, the reconstitution of packing material.

Nonetheless, in contrast with the work of textile dye and pharmaceutical compounds removal in long-term continuous process (Blánquez et al., 2006; Mir-Tutusaus et al., 2019), *T. versicolor* yielded significantly lower laccase activity along the operation in present study. Therefore, several batch experiments were carried out, seeking to understand this behavior. The results are summarized in Table 6.7. Obviously, in comparison with Group D and E, using fresh pellets provoked laccase generation (Group F), suggesting that the immobilized biomass was so aged that its laccase producing capacity disabled even if nutrients were rendered. It matches well with previously mentioned research works where a partial biomass renovation strategy was implemented (Blánquez et al., 2006; Mir-Tutusaus et al., 2019). Beyond that, it's also likely attributable to the binding of extracellular laccase by wood fiber (Cristóvão et al., 2011; Li et al., 2018) that made it undetectable in liquid phase. The addition of Cu^{2+} was somewhat beneficial for laccase activity since it was captured on the first day in Group C. However, this activity was negligible and it disappeared very soon. Unlike textile industry and hospital wastewaters, the copper concentration of the agricultural wastewater used in this study was quite low (< 0.02 mg L^{-1}) that was not favorable for laccase formation (Galhaup and Haltrich, 2001). On the other side, Coelho et al., (2010a) found that both diuron and bentazon could act as inducers of laccase from *Ganoderma lucidum*. However, it did not ring any bell in our work because

laccase activity was detected in neither Group A nor B.

Table 6.7 Evaluation of laccase activity under different conditions.

Groups	Laccase activity (AU L^{-1})			
	Incubation time (d)			
	1	2	3	4
A	−	−	−	−
B	−	−	−	−
C	+	−	−	−
D	−	−	−	−
E	−	−	−	−
F	++	+++	+++	+++

Note: −, laccase activity = 0; +, 0 < laccase activity ≤ 1; ++, 1 < laccase activity ≤ 20; +++, laccase activity > 20.

6.3.4 Evaluation of fungal biomass persistence

A significant declining tendency in biodegradation ability was observed after running 30 days in Chapter 5 with a lab-scale TBR possibly ascribed to biomass washing out, so the fungal immobilization was periodically evaluated through ergosterol measurement, to see if it's necessary to implement partial biomass renovation as described elsewhere (Blánquez et al., 2006). Surprisingly, compared with initial value, a stepwise increase was observed in all sections during first four months operation, and an averagely threefold increase at Day 186 over the biomass at Day 30 (Table 6.8). It reveals that there was continuous fungal growth in the reactor which essentially led to enhancing the compactness of packing bed, and it easily caused clogging issue (Zhang et al., 2020).

Table 6.8 Evaluation of ergosterol during the long-term continuous treatment.

Section	Amounts (mg g^{-1} DW^{-1})					
	Operation time (d)					
	30	60	90	120	150	186
1	0.35 ± 0.01	0.56 ± 0.08	0.48 ± 0.04	0.57 ± 0.06	1.71 ± 0.11	1.86 ± 0.12
2	0.46 ± 0.02	0.54 ± 0.02	0.87 ± 0.05	0.46 ± 0.05	1.38 ± 0.01	1.54 ± 0.11
3	0.48 ± 0.02	0.56 ± 0.01	0.71 ± 0.06	0.58 ± 0.02	1.46 ± 0.06	1.68 ± 0.06
4	0.43 ± 0.03	0.53 ± 0.10	0.52 ± 0.02	0.57 ± 0.06	1.65 ± 0.05	1.62 ± 0.49

Note: Means and standard deviation are shown; initial amount was 0.41 ± 0.03 mg g^{-1} DW^{-1}.

In spite of the decline of porosity, the fungal growth was not negatively affected because the dissolved oxygen of recirculation flow maintained at an average level of over 87%

along 186 days operation. On the contrary, it perhaps enhanced the removal due to that longer contact time were assigned as aforementioned and the fact that the more biomass there was, the more degraders there would be, which can be considered as bright side. But it cannot be denied that the excess pressure drop had to be alleviated by reconstitution of packing material because the experimental reactor was blocked after Day 130 and liquid started to accumulate. It was shown that the implemented physical approach seemed not to be harmful to the biofilm, representing as effective pesticides removal (Table 6.6) and increase in biomass (Table 6.8). Additionally, biomass redistribution could give profit to ergosterol amount (Table 6.8) as a result of the rearrangement of packed bed. In any word, not only does this re-indicate our system possesses a good resistance against the impact load when addressing the problems of clogging, but also confirm above discussion in Section 6.3.3 that laccase may be undetectable even if the fungus is still active and notable degradation can be accomplished. Similar phenomenon was also found in solid-state bioremediation processes using *T. versicolor* (Rodríguez-Rodríguez et al., 2010b).

In addition to ergosterol quantification, the surficial colonization by *T. versicolor* on single wood was examined by SEM. As we can see in Figure 6.9, in contrast to the initial effective attachment of fungal mycelia, clearly observable wood surface was found at low magnification after the long-term continuous operation, together with filamentous structures. However, it is hard to tell the difference in term of hyphal density at high magnification.
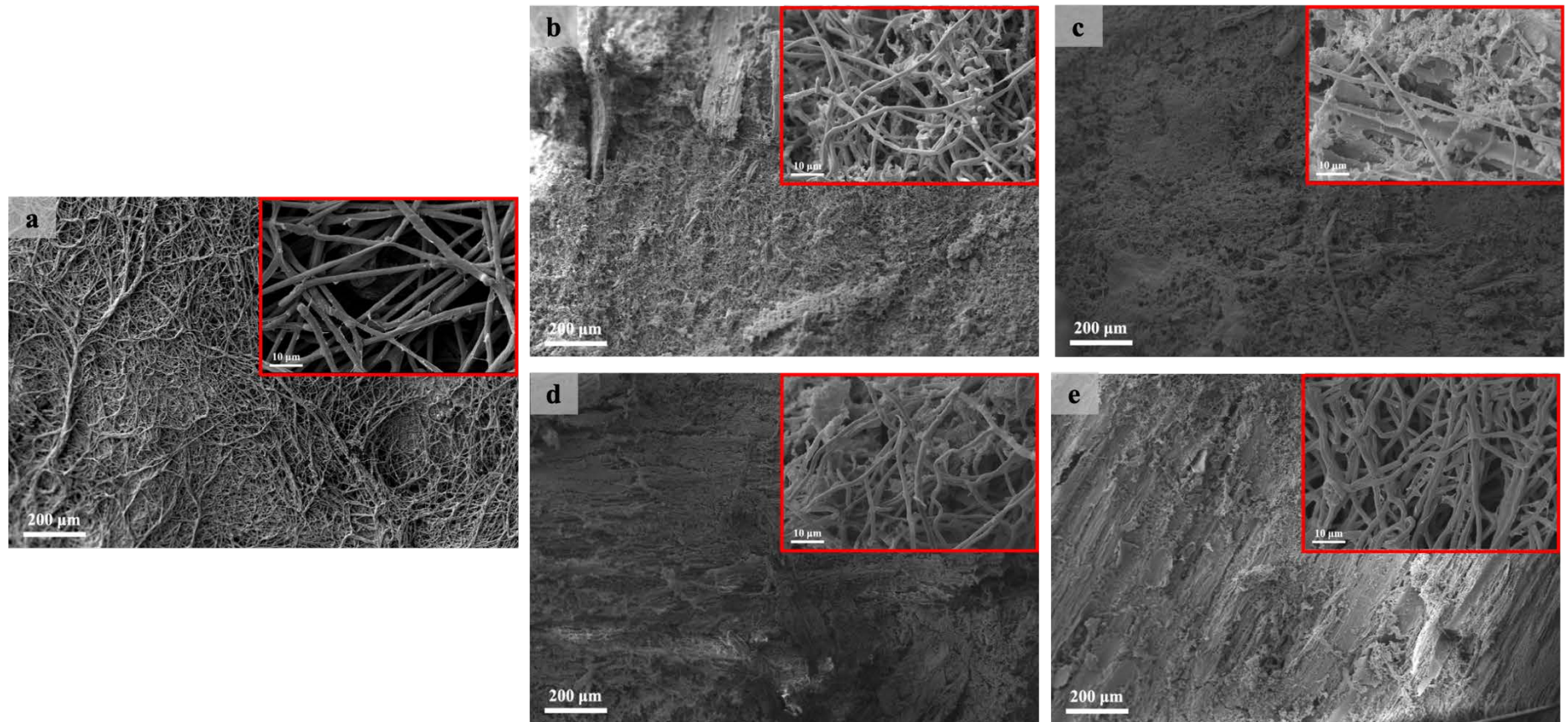
Figure 6.9 SEM images of single wood chip colonized by *T. versicolor* from initial solid culture and different sections after the long-term continuous treatment. a. initial; b. Section 1; c. Section 2; d. Section 3; e. Section 4.

Likewise, it was also observed in other sections, and those images somewhat correlate to ergosterol amount, especially the wood chip from Section 2, exhibiting noticeable less hyphae in comparison with others. High biomass stability was also gained by Ehlers and Rose (2005) using pine wood as carrier in biodegradation of phenol and 2,4,6-trichlorophenol by fungal TBR. But it is worthy to point out that the fungus employed in the mentioned study was *Phanerochaete chrysosporium*, besides the running time was 24–30 h that was even much shorter than our previous work with lab-scale TBR. Last but not least, a firm conclusion cannot be drawn until a microbial community investigation is accomplished, bearing in mind that ergosterol is not only a biomarker for living fungal biomass, but also persistent in the environment after fungal death (Mille-Lindblom et al., 2004). So, its quantification is not specific for *Trametes*.

In order to monitor the dominance of *T. versicolor* in the reactor, the denaturing gradient gel electrophoresis (DGGE) fingerprint analysis in this chapter only focused on fungal diversity. Results indicate that *Trametes* was detected in the lignocellulosic matrix throughout 186 days operation. Despite a marked reduce in its relative abundance was observed after four months, it increased again up to the level similar to initial, at Day 186, which was very abundant. Besides, there were no difference with respect to *Trametes* relative abundance between each section. Zhang et al. (2019) set up a fungi-based bio-trickling filter for degrading toluene. During a period of 117-day runtime, the initial dominant fungus *Fusarium oxysporum* immobilized on ceramic particles was replaced by other microorganism after 10 days, and the dominant strains in the tower changed alternately with the operating conditions. In our case, the inoculated biomass demonstrated high persistence. Similar to lab-scale application (Chapter 5, Section 5.3.6.3), *Penicilium* and *Rhodorula* were also found in the effluent of the fungal reactor. Specifically, the former was dominant in the first place, mainly originated from the influent, and the latter was the most abundant fungus at Day 120, which was replaced by *Dipodascus* at the end of running period. In the text of control reactor, *Penicilium* was the dominant in the solid sample during the whole treatment and it has been also mostly detected in the effluent at Day 186. *Trametes* was also captured in the control setup as a consequence of spatial shift, which coincidences with the behavior in lab-scale reactor. Apart from those mentioned fungal

genera, *Vanrija*, *Exophiala* and *Geotrichum* were also detected in the fungal reactor, at relative low concentrations.

Future work should focus on the connection between immobilized fungus and microflora evolution along the long-term operation, seeking for appropriate microbial indicator of reactor status.

6.3.5 Biopile test

Results showed that fungal growth appeared after re-inoculation using wood chips from the fungal reactor (Table 6.9). However, it was less than the value before treatment, possibly ascribed to the low biomass homogeneity. Compared to non-treatment, removals were obtained at different levels towards both pollutants, ranging from 10% to 38%, of which the highest yield was bentazon elimination from the control reactor carrier. There was around 10% contaminant attenuation in the absence of re-inoculated fungi, which means the remained biomass were still available to dismiss diuron and bentazon.

Table 6.9 Contents of ergosterol, diuron and bentazon remaining in the lignocellulosic carrier after different treatments followed by one-month incubation.

Wood source	Treatment	Ergosterol (mg g^{-1} DW^{-1})	Diuron (mg g^{-1} DW^{-1})	Bentazon (mg g^{-1} DW^{-1})
Experimental reactor	Before treatment	1.85 ± 0.23	0.15 ± 0.01	0.005 ± 0.002
	Re-inoculation	1.35 ± 0.08	0.13 ± 0.004	0.004 ± 0.001
	Non re-inoculation	1.30 ± 0.11	0.14 ± 0.01	0.004 ± 0.001
Control reactor	Before treatment	ND	0.16 ± 0.01	0.020 ± 0.010
	Inoculation	0.33 ± 0.01	0.14 ± 0.01	0.012 ± 0.007

Note: Means and standard deviation of triplicate are shown; ND, not data.

In a big picture, the performance of this biopile trial was better than that of Chapter 5 (Section 5.3.4), especially considering the adsorption period was much longer than the previous one. The wood fiber could be substantially consumed by *T. versicolor* after long-period colonization, suggesting that either extra nutrients or fresh wood chips should be supplemented in the further secondary treatment to guarantee fungal growth. In addition, the treatment period can be prolonged and combined with mixing action, to enhance fungal accessibility to the pollutants.

6.3.6 Variation of fiber content in lignocellulosic carrier during the long-term operation

Solid sample also underwent fiber content analysis taking into account that no additional nutrient source had been supplemented during 186-day running period. The sample withdrawn at the end of the operation was a mixture of packing beds from all sections and the original wood chips were set as control. Their chemical compositions are summarized in Table 6.10. Although variations in cellulose and lignin proportion can be observed for the wood chips from the experimental reactor compared to the original wood, it is hard to tell the exact mass balance in term of each fiber. To better understand those results, a further calculation was carried out assuming the ash as an inert fraction and internal standard. Accordingly, the relative content of each fiber was quantified by referring the initial value that of the original wood, and the results are organized in Table 6.11. As can be seen, *T. versicolor* demonstrated different preferences towards each fiber. Almost 60% of lignin had been degraded when the operation reached 90 days. By contrast, a great extent of hemicellulose and cellulose still remained, however, all of which were substantially depleted after 186 days. These findings confirm the aforementioned hypothesis that new wood chips are supposed to be added for the secondary treatment. From the point of remained wood mass view, the consumption rate seemed to be a constant (0.35 g DW d^{-1}), suggesting that the packing bed would need to be renovated in one or two months later the stopping because the lignocellulosic carrier wood be exhausted by then.

Table 6.10 Comparison of wood ingredients between the wood chips from the reactors along the long-term operation and the original wood.

Sample source	Operation time (d)	Analytes (% DW^{-1})				
		Dry matter	Hemicellulose	Cellulose	Lignin	Ash
Original	0	97.07 ± 0.11	26.09 ± 0.40	47.41 ± 0.72	5.15 ± 0.79	2.15 ± 0.00
Experimental reactor	90	96.20 ± 0.20	29.44 ± 0.56	42.65 ± 0.51	3.16 ± 0.73	3.18 ± 0.07
	186	97.80 ± 0.18	30.26 ± 0.93	26.89 ± 1.47	3.93 ± 1.10	6.25 ± 0.07
Control reactor	90	97.51 ± 0.06	25.40 ± 0.34	49.10 ± 0.33	8.64 ± 0.30	1.88 ± 0.03
	186	97.87 ± 0.36	28.42 ± 0.23	43.56 ± 1.38	9.41 ± 0.63	2.55 ± 0.04

Note: Mean value and standard deviation are shown.

Table 6.11 Variations of wood mass and fiber content along the long-term operation.

Item	Value (%)	
	90 d	186 d
Remained wood mass	67.13 ± 1.13	34.73 ± 0.34
Hemicellulose reduction	24.24 ± 2.60	59.72 ± 1.46
Cellulose reduction	39.61 ± 0.58	80.30 ± 1.17
Lignin reduction	58.93 ± 7.60	70.53 ± 4.82

Note: Mean value and standard deviation are shown; 15.61% of wood mass was lost due to elution after 186 days.

A diagram (Figure 6.10) is given below to illustrate the wood evolution, in which the reduction in the external diameter of the ring reflects the lost wood mass. Furthermore, the wood decomposition process and the elution effect may give an explanation to the aforementioned rises in water holding capacity and effluent COD, respectively.
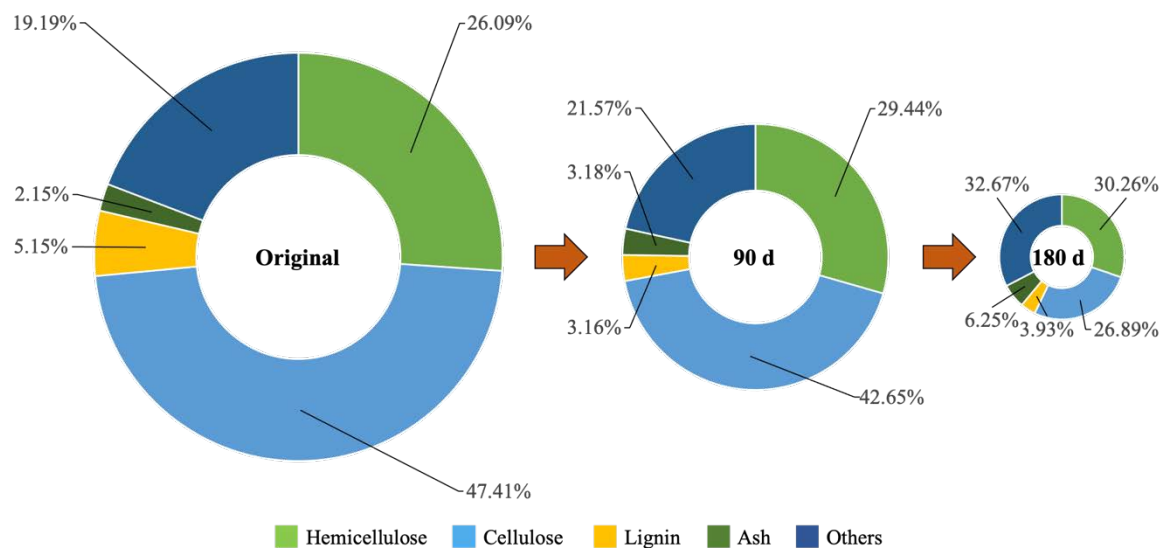

Figure 6.10 Evolution of lignocellulosic carrier in the experimental reactor along the long-term operation. Values present the content of each fiber, ring external diameters correspond to the relative remained wood mass compared to the original wood.

To sum up, the results from fiber analysis evidence that fresh wood chips are necessarily complemented and mixed with the previous lignocellulosic materials when processing the reconstitution. Anther feasible strategy could be replacing the packing bed directly after 6 or 8 months running. Otherwise, it is not available for the reactor to maintain operation for another long period.

6.4 Conclusions

➢ A long-term of fungal treatment without adding any nutrients for removing pesticides from agricultural wastewater was successfully established for the first time.

➢ The scaling-up trickle bed reactor demonstrated persistent fungal activity and high robustness throughout 186 days continuous operation, during which stable and promising performance were attained under different recirculation rates.

➢ A pressure-reducing technique is supposed to be implemented after 120 days operation, to avoid clogging issue.

➢ A stimulation strategy should be taken into consideration during the secondary treatment, nourishing the fungus.

➢ New lignocellulosic supporting material should be complemented after running 200 days.

➢ This study paves the way to full-scale practice of fungal TBR.

Chapter 7

Conclusions

Based on the results obtained within the framework of this dissertation, the main conclusions that can be drawn are given below:

- *T. versicolor* possesses versatility in degrading various pesticides mainly through oxidative reactions, especially hydroxylation, which are catalyzed by cytochrome P450 and laccase. Both enzymes are also involved in the degradation process of other emerging pollutants according to previous research works by our group.

- In comparison with fluidized bed reactor, trickle bed reactor configuration is a preferred alternative for fungal long-term treatment and scaling-up, since the lignocellulosic material not only behaves as an immobilization carrier but also acts as nutrients, through which economic cost is brought down and bacterial contamination is successfully dismissed.

- A pilot-scale fungal TBR was successfully constructed and operated for a long period. Good pesticide removals were obtained in continuous mode, and the scaled-up fungal reactor exhibited persistent bioactivity and enough robustness against contingencies.

- A clogging issue was observed during the long-term treatment, which was properly addressed by reconstituting the packing bed and good results were obtained. Other strategy, such as lignocellulosic material replenishment, can be also taken into consideration, since it is available to relieve wood exhausting as well.

- Although different lignocellulosic materials, for example pine wood chips, can be utilized as carrier in the TBR, the oak wood renders a natural habitat for *T. versicolor*, enhancing biomass growth and working effectiveness.

- Adsorption by the lignocellulosic carrier played a vital role during pesticides removal process.

- The established system could serve in other applications, bearing in mind that *T. versicolor* harbor the capacity to deal with a broad spectrum of xenobiotics, both emerging and persistent contaminants.

In general, this thesis has accomplished the development of a pilot plant treating agricultural wastewater. Several difficulties encountered with the fungal treatment process have been tackled. The elimination mechanisms have been revealed.

For the future work that could be undertaken in the regime of fungal TBR, the following recommendations and suggestions are proposed:

- Focusing on the full-scale implementations, and seeking for appropriate managements to deal with the wood waste adsorbing high amount of pesticides after treatment, together with the life cycle assessment study and economic evaluation.

- Given the important contribution by adsorption, some parameters such as HRT could be adjusted in order to improve biodegradation.

- A co-culture of different WRF possessing special degradation capacity can be considered in the future treatment using TBR.

Bibliography

Abdel-Halim, K.Y., Salama, A.K., El-khateeb, E.N., Bakry, N.M. 2006. Organophosphorus pollutants (OPP) in aquatic environment at Damietta Governorate, Egypt: Implications for monitoring and biomarker responses. Chemosphere 63(9), 1491-1498.

Adjei, M.D., Heinze, T.M., Deck, J., Freeman, J.P., Williams, A.J., Sutherland, J.B. 2006. Transformation of the antibacterial agent norfloxacin by environmental mycobacteria. Applied and Environmental Microbiology 72(9), 5790-5793.

Aiyesanmi, A.F., Idowu, G.A. 2012. Organochlorine pesticides residues in soil of cocoa farms in Ondo State Central District, Nigeria. Environment and Natural Resources Research 2(2), 65-73.

Al-Shawabkah, R., Al-Qodah, Z., Al-Bsoul, A. 2015. Bio-adsorption of triadimenol pesticide from aqueous solutions using activated sludge of dairy plants. Desalination and Water Treatment 53(9), 2555-2564.

Alalm, M.G., Tawfik, A., Ookawara, S. 2015. Comparison of solar TiO_2 photocatalysis and solar photo-Fenton for treatment of pesticides industry wastewater: Operational conditions, kinetics, and costs. Journal of Water Process Engineering 8, 55-63.

Alawi, M.A., Al-Antary, T.M., Estityah, H., Haddad, N. 2017. Evaluation of chlorinated pesticides residues in foodstuff of animal origin from middle districts of Jordan in 2013-2014. Toxin Reviews 36(2), 94-100.

Anderson, J., Dubetz, C., Palace, V. 2015. Neonicotinoids in the Canadian aquatic environment: A literature review on current use products with a focus on fate, exposure, and biological effects. Science of the Total Environment 505, 409-422.

Arias-Estévez, M., López-Periago, E., Martínez-Carballo, E., Simal-Gándara, J., Mejuto, J.C., García-Río, L. 2008. The mobility and degradation of pesticides in soils and the pollution of groundwater resources. Agriculture, Ecosystems & Environment 123(4), 247-260.

Arora, D.S., Gill, P.K. 2001. Effects of various media and supplements on laccase production by some white rot fungi. Bioresource Technology 77(1), 89-91.

Aswathi, A., Pandey, A., Sukumaran, R.K. 2019. Rapid degradation of the organophosphate pesticide-Chlorpyrifos by a novel strain of *Pseudomonas nitroreducens* AR-3. Bioresource Technology 292, 122025.

Bibliography

Atwood, D., Paisley-Jones, C. 2017. Pesticides industry sales and usage: 2008-2012 market estimates. Washington, DC: US Environmental Protection Agency, 20460.

Aznar-Alemany, Ò., Eljarrat, E. 2020. Bioavailability and bioaccumulation of pyrethroid insecticides in wildlife and humans. In: Eljarrat, E. Pyrethroid insecticides. Cham: Springer Nature. pp. 205-225.

Badawi, N., Rønhede, S., Olsson, S., Kragelund, B.B., Johnsen, A.H., Jacobsen, O.S., Aamand, J. 2009. Metabolites of the phenylurea herbicides chlorotoluron, diuron, isoproturon and linuron produced by the soil fungus *Mortierella* sp. Environmental Pollution 157(10), 2806-2812.

Baird, R.B., Rice, C.E.W., Eaton, A.D. 2017. Standard methods for the examination of water and wastewater (23rd), Water Environment Federation, American Public Health Association, American Water Works Association.

Barbieri, M.V., Monllor-Alcaraz, L.S., Postigo, C., de Alda, M.L. 2020. Improved fully automated method for the determination of medium to highly polar pesticides in surface and groundwater and application in two distinct agriculture-impacted areas. Science of the Total Environment 745, 140650.

Barbieri, M.V., Peris, A., Postigo, C., Moya-Garcés, A., Monllor-Alcaraz, L.S., Rambla-Alegre, M., Eljarrat, E., de Alda, M.L. 2021. Evaluation of the occurrence and fate of pesticides in a typical Mediterranean delta ecosystem (Ebro River Delta) and risk assessment for aquatic organisms. Environmental Pollution 274, 115813.

Bardi, A., Yuan, Q., Siracusa, G., Becarelli, S., Di Gregorio, S., Tigini, V., Levin, D.B., Petroni, G., Munz, G. 2019. Stability of fungal biomass continuously fed with tannic acid in a non-sterile moving-packed bed reactor. Journal of Environmental Management 247, 67-77.

Baxter, J., Cummings, S.P. 2008. The degradation of the herbicide bromoxynil and its impact on bacterial diversity in a top soil. Journal of Applied Microbiology 104(6), 1605-1616.

Belal, E.B., Elkhateeb, N.M. 2014. Biodegradation of pendimethalin residues by *P. chrysosporium* in aquatic system and soils. Journal of Biological Chemistry and Environmental Sciences 9(3), 383-400.

Beltrán-Flores, E., Torán, J., Caminal, G., Blánquez, P., Sarrà, M. 2020. The removal of diuron from agricultural wastewaters by *Trametes versicolor* immobilized on pinewood in simple channel reactors. Science of the Total Environment 728, 138414.

Beltrán-Flores, E., Sarrà, M., Blánquez, P. 2021. Pesticide bioremediation by *Trametes versicolor*: Application in a fixed-bed reactor, sorption contribution and bioregeneration. Science of the Total Environment, 148386.

Bempah, C.K., Asomaning, J., Boateng, J. 2021. Market basket survey for some pesticides residues in fruits and vegetables from Ghana. Journal of Microbiology, Biotechnology and Food Sciences 2(3), 850-871.

Bending, G.D., Friloux, M., Walker, A. 2002. Degradation of contrasting pesticides by white rot fungi and its relationship with ligninolytic potential. FEMS Microbiology Letters 212(1), 59-63.

Bhattacharya, S., Das, A., Prashanthi, K., Palaniswamy, M., Angayarkanni, J. 2014. Mycoremediation of Benzo[*a*]pyrene by *Pleurotus ostreatus* in the presence of heavy metals and mediators. 3 Biotech 4, 205-211.

Bilal, M., Asgher, M., Parra-Saldivar, R., Hu, H., Wang, W., Zhang, X., Iqbal, H.M.N. 2017. Immobilized ligninolytic enzymes: An innovative and environmental responsive technology to tackle dye-based industrial pollutants-A review. Science of the Total Environment 576, 646-659.

Bilal, M., Iqbal, H.M.N., Barceló, D. 2019. Persistence of pesticides-based contaminants in the environment and their effective degradation using laccase-assisted biocatalytic systems. Science of the Total Environment 695, 133896.

Blánquez, P., Casas, N., Font, X., Gabarrell, X., Sarrà, M., Caminal, G., Vicent, T. 2004. Mechanism of textile metal dye biotransformation by *Trametes versicolor*. Water Research 38(8), 2166-2172.

Blánquez, P., Sarrà, M., Vicent, T. 2006. Study of the cellular retention time and the partial biomass renovation in a fungal decolourisation continuous process. Water Research 40(8), 1650-1656.

Bonmatin, J.M., Giorio, C., Girolami, V., Goulson, D., Kreutzweiser, D.P., Krupke, C., Liess, M., Long, E., Marzaro, M., Mitchell, E.A.D, Noome, D.A., Simon-Delso, N.

Tapparo, A. 2015. Environmental fate and exposure; neonicotinoids and fipronil. Environmental Science and Pollution Research 22, 35-67.

Borràs, E., Blánquez, P., Sarrà, M., Caminal, G., Vicent, T. 2008. *Trametes versicolor* pellets production: low-cost medium and scale-up. Biochemical Engineering Journal 42(1), 61-66.

Bouki, C., Venieri, D., Diamadopoulos, E. 2013. Detection and fate of antibiotic resistant bacteria in wastewater treatment plants: A review. Ecotoxicology and Environmental Safety 91, 1-9.

Bourneuf, S., Jacob, M., Albasi, C., Sochard, S., Richard, R., Manero, M.H. 2016. Desorption experiments and modeling of micropollutants on activated carbon in water phase: application to transient concentrations mitigation. International Journal of Environmental Science and Technology 13, 1-10.

Brausch, J.M., Rand, G.M. 2011. A review of personal care products in the aquatic environment: environmental concentrations and toxicity. Chemosphere 82(11), 1518-1532.

Bu, Q., Wang, B., Huang, J., Deng, S., Yu, G. 2013. Pharmaceuticals and personal care products in the aquatic environment in China: A review. Journal of Hazardous Materials 262, 189-211.

Bumpus, J.A., Aust, S.D. 1987. Biodegradation of DDT [1,1,1-trichloro-2,2-bis(4-chlorophenyl)ethane] by the white rot fungus *Phanerochaete chrysosporium*. Applied Environmental Microbiology. 53(9), 2001-2008.

Bumpus, J.A., Powers, R.H., Sun, T. 1993. Biodegradation of DDE (1,1-dichloro-2,2-bis(4-chlorophenyl)ethene) by *Phanerochaete chrysosporium*. Mycological Research 97(1), 95-98.

Cabras, P., Angioni, A., Garau, V.L., Pirisi, F.M., Cabitza, F., Pala, M., Farris, G.A. 2000. Fate of quinoxyfen residues in grapes, wine, and their processing products. Journal of Agricultural and Food Chemistry 48(12), 6128-6131.

Caldas, S.S., Arias, J.L.O., Rombaldi, C., Mello, L.L., Cerqueira, M.B.R., Martins, A.F., Primel, E.G. 2019. Occurrence of pesticides and PPCPs in surface and drinking water in southern Brazil: Data on 4-year monitoring. Journal of the Brazilian Chemical

Society 30(1), 71-80.

Calvo, S., Romo, S., Soria, J., Picó, Y. 2021. Pesticide contamination in water and sediment of the aquatic systems of the Natural Park of the Albufera of Valencia (Spain) during the rice cultivation period. Science of the Total Environment 774, 145009.

Carena, L., Fabbri, D., Passananti, M., Minella, M., Pazzi, M., Vione, D. 2020. The role of direct photolysis in the photodegradation of the herbicide bentazone in natural surface waters. Chemosphere 246, 125705.

Carra, I., Sánchez Pérez, J.A., Malato, S., Autin, O., Jefferson, B., Jarvis, P. 2016. Performance of different advanced oxidation processes for tertiary wastewater treatment to remove the pesticide acetamiprid. Journal of Chemical Technology & Biotechnology 91(1), 72-81.

Carratalá, A., Moreno-González, R., León, V.M. 2017. Occurrence and seasonal distribution of polycyclic aromatic hydrocarbons and legacy and current-use pesticides in air from a Mediterranean coastal lagoon (Mar Menor, SE Spain). Chemosphere 167, 382-395.

Casals-Casas, C., Desvergne, B. 2011. Endocrine disruptors: From endocrine to metabolic disruption. Annual Review of Physiology 73, 135-162.

Casida, J.E. 2011. Neonicotinoid metabolism: Compounds, substituents, pathways, enzymes, organisms, and relevance. Journal of Agricultural and Food Chemistry 59(7), 2923-2931.

Ccanccapa, A., Masiá, A., Navarro-Ortega, A., Picó, Y., Barceló, D. 2016. Pesticides in the Ebro River basin: occurrence and risk assessment. Environmental Pollution 211, 414-424.

Chakraborty, P., Zhang, G., Li, J., Sivakumar, A., Jones, K.C. 2015. Occurrence and sources of selected organochlorine pesticides in the soil of seven major Indian cities: Assessment of air-soil exchange. Environmental Pollution 204, 74-80.

Chen, S., Liu, C., Peng, C., Liu, H., Hu, M., Zhong, G. 2012. Biodegradation of chlorpyrifos and its hydrolysis product 3,5,6-trichloro-2-pyridinol by a new fungal strain *Cladosporium cladosporioides* Hu-01. PloS One 7(10), e47205.

Chen, X., Zhou, Q., Liu, F., Peng, Q., Bian, Y. 2021. Performance and kinetic of pesticide

residues removal by microporous starch immobilized laccase in a combined adsorption and biotransformation process. Environmental Technology & Innovation 21, 101235.

Chen, X., Zhou, Q., Liu, F., Peng, Q., Teng, P. 2019. Removal of nine pesticide residues from water and soil by biosorption coupled with degradation on biosorbent immobilized laccase. Chemosphere 233, 49-56.

Chopra, A.K., Sharma, M.K., Chamoli, S. 2011. Bioaccumulation of organochlorine pesticides in aquatic system-an overview. Environmental Monitoring and Assessment 173, 905-916.

Clark, D.R. 1990. Dicofol (Kelthane) as an environmental contaminant: A review. Fish and Wildlife Technical Report 29

Clark, J.M., Kenna, M.P. 2010. In: Krieger, R. Hayes' Handbook of Pesticide Toxicology (3rd), Amsterdam: Elsevier pp. 1047-1076.

Climent, M.J., Herrero-Hernández, E., Sánchez-Martín, M.J., Rodríguez-Cruz, M.S., Pedreros, P., Urrutia, R. 2019. Residues of pesticides and some metabolites in dissolved and particulate phase in surface stream water of Cachapoal River basin, central Chile. Environmental Pollution 251, 90-101.

Coelho, J.S., de Oliveira, A.L., de Souza, C.G.M., Bracht, A., Peralta, R.M. 2010a. Effect of the herbicides bentazon and diuron on the production of ligninolytic enzymes by *Ganoderma lucidum*. International Biodeterioration & Biodegradation 64(2), 156-161.

Coelho, J.S., de Souza, C.G.M., de Oliveira, A.L., Bracht, A., Costa, M.A.F., Peralta, R.M. 2010b. Comparative removal of bentazon by *Ganoderma lucidum* in liquid and solid state cultures. Current Microbiology 60(5), 350-355.

Coelho-Moreira, J.S., Bracht, A., Souza, A.C.S., Oliveira, R.F., Sá-Nakanishi, A.B., de Souza, C.G.M., Peralta, R.M. 2013. Degradation of diuron by *Phanerochaete chrysosporium*: role of ligninolytic enzymes and cytochrome P450. BioMed Research International 2013, 251354.

Coelho-Moreira, J.S., Brugnari, T., Sá-Nakanishi, A.B., Castoldi, R., de Souza, C.G.M., Bracht, A., Peralta, R.M. 2018. Evaluation of diuron tolerance and biotransformation by the white-rot fungus *Ganoderma lucidum*. Fungal Biology 122(6), 471-478.

Cohen, Y. 2001. Biofiltration-the treatment of fluids by microorganisms immobilized into the filter bedding material: a review. Bioresource Technology 77(3), 257-274.

Coscollà, C., Colin, P., Yahyaoui, A., Petrique, O., Yusà, V., Mellouki, A., Pastor, A. 2010. Occurrence of currently used pesticides in ambient air of Centre Region (France). Atmospheric Environment 44(32), 3915-3925.

Costa, L.G. 2015. The neurotoxicity of organochlorine and pyrethroid pesticides. In: Lotti, M., Bleecker, M.L. Handbook of clinical neurology volume 131. Amsterdam: Elsevier. pp. 135-148.

Črešnar, B., Petrič, Š. 2011. Cytochrome P450 enzymes in the fungal kingdom. Biochimica et Biophysica Acta (BBA)-Proteins and Proteomics 1814(1), 29-35.

Cristóvão, R.O., Tavares, A.P.M., Brígida, A.I., Loureiro, J.M., Boaventura, R.A.R, Macedo, E.A., Coelho, M.A.Z. 2011. Immobilization of commercial laccase onto green coconut fiber by adsorption and its application for reactive textile dyes degradation. Journal of Molecular Catalysis B: Enzymatic 72(1-2), 6-12.

Cruz-Morató, C., Ferrando-Climent, L., Rodriguez-Mozaz, S., Barceló, D., Marco-Urrea, E., Vicent, T., Sarrà, M. 2013. Degradation of pharmaceuticals in non-sterile urban wastewater by *Trametes versicolor* in a fluidized bed bioreactor. Water Research 47(14), 5200-5210.

Cruz del Álamo, A., Pariente, M., Martínez, F., Molina, R. 2020. *Trametes versicolor* immobilized on rotating biological contactors as alternative biological treatment for the removal of emerging concern micropollutants. Water Research 170, 115313.

Curran, W.S. 2016. Persistence of herbicides in soil. Crops & Soils 49(5), 16-21.

da Luz, J.M.R., Paes, S.A., Nunes, M.D., da Silva, M.C.S, Kasuya, M.C.M. 2013. Degradation of oxo-biodegradable plastic by *Pleurotus ostreatus*. PLoS One 8(8), e69386.

Damalas, C.A., Eleftherohorinos, I.G. 2011. Pesticide exposure, safety issues, and risk assessment indicators. International Journal of Environmental Research and Public Health 8(5), 1402-1419.

de García, S.A.O., Pinto, G.P., García-Encina, P.A., Irusta-Mata, R. 2014. Ecotoxicity and environmental risk assessment of pharmaceuticals and personal care products in

aquatic environments and wastewater treatment plants. Ecotoxicology 23, 1517-1533.

Gaffney, V.J., Almeida, C.M.M., Rodrigues, A., Ferreira, E., Benoliel, M.J., Cardoso, V.V. 2015. Occurrence of pharmaceuticals in a water supply system and related human health risk assessment. Water Research 72, 199-208.

de Souza, R.M., Seibert, D., Quesada, H.B., Bassetti, F.J., Fagundes-Klen, M.R., Bergamasco, R. 2020. Occurrence, impacts and general aspects of pesticides in surface water: A review. Process Safety and Environmental Protection 135, 22-37.

Castillo, M.P., Ander, P., Stenström, J., Torstensson, L. 2000. Degradation of the herbicide bentazon as related to enzyme production by *Phanerochaete chrysosporium* in two solid substrate fermentation systems. World Journal of Microbiology and Biotechnology 16, 289-295.

DeLorenzo, M.E., Scott, G.I., Ross, P.E. 2001. Toxicity of pesticides to aquatic microorganisms: A review. Environmental Toxicology and Chemistry 20(1), 84-98.

Diari Oficial de la Generalitat de Catalunya (DOGC). DECRET 130/2003. https://portaljuridic.gencat.cat/ca/document-del-pjur/?documentId=322238.

Doulia, D.S., Anagnos, E.K., Liapis, K.S., Klimentzos, D.A. 2016. Removal of pesticides from white and red wines by microfiltration. Journal of Hazardous Materials 317, 135-146.

Ebele, A.J., Abdallah, M.A.E., Harrad, S. 2017. Pharmaceuticals and personal care products (PPCPs) in the freshwater aquatic environment. Emerging Contaminants 3(1), 1-16.

Eckenfelder, W. 2000. Industrial water pollution control. New York: McGraw-Hill.

Ehlers, G.A., Rose, P.D. 2005. Immobilized white-rot fungal biodegradation of phenol and chlorinated phenol in trickling packed-bed reactors by employing sequencing batch operation. Bioresource Technology 96(11), 1264-1275.

Ellegaard-Jensen, L., Knudsen, B.E., Johansen, A., Albers, C.N., Aamand, J., Rosendahl, S. 2014. Fungal-bacterial consortia increase diuron degradation in water-unsaturated systems. Science of the Total Environment 466, 699-705.

Ensminger, M.P., Budd, R., Kelley, K.C., Goh, K.S. 2013. Pesticide occurrence and aquatic benchmark exceedances in urban surface waters and sediments in three urban areas of California, USA, 2008-2011. Environmental Monitoring and Assessment 185, 3697-

3710.

Espinosa-Ortiz, E.J., Rene, E.R., Pakshirajan, K., van Hullebusch, E.D., Lens, P.N.L. 2016. Fungal pelleted reactors in wastewater treatment: Applications and perspectives. Chemical Engineering Journal 283, 553-571.

Estellano, V.H., Pozo, K., Efstathiou, C., Pozo, K., Corsolini, S., Focardi, S. 2015. Assessing levels and seasonal variations of current-use pesticides (CUPs) in the Tuscan atmosphere, Italy, using polyurethane foam disks (PUF) passive air samplers. Environmental Pollution 205, 52-59.

European Commission (EC). 1998. Coucil Directive 98/83/EC of November 1998 on the quality of water intended for human consumption. Official Journal of the European Communities 330, 32-54. https://eur-lex.europa.eu/legal-content/EN/TXT/PDF/?uri=CELEX:31998L0083&from=EN.

EC. 2008. Directive 2008/105/EC of 16 December 2008 on environmental quality standards in the field of water policy, amending and subsequently repealing Council Directives 82/176/EEC, 83/513/EEC, 84/156/EEC, 84/491/EEC, 86/280/EEC and amending Directive 2000/60/EC of the European Parliament and of the Council. Official Journal of the European Union 348, 84-97. https://eur-lex.europa.eu/legal-content/EN/TXT/PDF/?uri=CELEX:32008L0105&from=EN.

EC. 2013. Coucil Directive 2013/39/EU of 12 August 2013 amending Directives 2000/60/EC and 2008/105/EC as regards priority substances in the field of water policy. Official Journal of the European Union 226, 1-17. https://eur-lex.europa.eu/legal-content/EN/TXT/PDF/?uri=CELEX:32013L0039&from=EN.

EC. 2018. Implementing Decision (EU) 2018/840 of 5 June 2018 establishing a watch list of substances for Union-wide monitoring in the field of water policy pursuant to Directive 2008/105/EC of the European Parliament and of the Council and repealing Commission Implementing Decision (EU) 2015/495. Official Journal of the European Union 141, 9-12. https://eur-lex.europa.eu/legal-content/EN/TXT/PDF/?uri=CELEX:32018D0840&from=EN.

European Food Safty Authority (EFSA). 2015. Conclusion on the peer review of the pesticide risk assessment of the active substance bentazone. EFSA Journal 13(4), 4077.

Falconer, I.R., Chapman, H.F., Moore, M.R., Ranmuthugala, G. 2006. Endocrine-disrupting compounds: A review of their challenge to sustainable and safe water supply and water reuse. Environmental Toxicology 21(2), 181-191.

Fenner, K., Canonica, S., Wackett, L.P., Elsner, M. 2013. Evaluating pesticide degradation in the environment: blind spots and emerging opportunities. Science 341(6147), 752-758.

Firouzsalari, N.Z., Shakerkhatibi, M., Pourakbar, M., Yadeghari, A., Safari, G.H., Sarbakhsh, P. 2019. Pyrethroid pesticide residues in a municipal wastewater treatment plant: occurrence, removal efficiency, and risk assessment using a modified index. Journal of Water Process Engineering 29, 100793.

Font, X., Caminal, G., Gabarrell, X., Romero, S., Vicent, T. 2003. Black liquor detoxification by laccase of *Trametes versicolor* pellets. Journal of Chemical Technology & Biotechnology 78(5), 548-554.

Food and Agriculture Organization of the United Nations (FAO). 2020. World Food and Agriculture-Statistical Pocketbook 2020. Rome: FAO.

FAO Statistics (FAOSTAT). 2019. Pesticides Use. http://www.fao.org/faostat/en/#data/RP/visualize.

Fosu-Mensah, B.Y., Okoffo, E.D., Darko, G., Gordon, C. 2016. Assessment of organochlorine pesticide residues in soils and drinking water sources from cocoa farms in Ghana. SpringerPlus 5, 869.

Frédéric, O., Yves, P. 2014. Pharmaceuticals in hospital wastewater: Their ecotoxicity and contribution to the environmental hazard of the effluent. Chemosphere 115, 31-39.

Galhaup, C., Haltrich, D. 2001. Enhanced formation of laccase activity by the white-rot fungus *Trametes pubescens* in the presence of copper. Applied Microbiology and Biotechnology 56, 225-232.

Gao, Y., Truong, Y.B., Cacioli, P., Butler, P., Kyratzis, I.L. 2014. Bioremediation of pesticide contaminated water using an organophosphate degrading enzyme immobilized on nonwoven polyester textiles. Enzyme and Microbial Technology 54, 38-44.

Gardes, M., Bruns, T.D. 1993. ITS primers with enhanced specificity for basidiomycetes-

application to the identification of mycorrhizae and rusts. Molecular Ecology 2(2), 113-118.

Gavrilescu, M. 2005. Fate of pesticides in the environment and its bioremediation. Engineering in Life Sciences 5(6), 497-526.

Gessner, M.O. 2020. Ergosterol as a Measure of Fungal Biomass. In: Bärlocher, F., Gessner, M.O., Graça, M.A.S. Methods to study litter decomposition (2nd). Cham: Springer. pp. 247-255.

Giacomazzi, S., Cochet, N. 2004. Environmental impact of diuron transformation: a review. Chemosphere 56(11), 1021-1032.

Gil, Y., Sinfort, C. 2005. Emission of pesticides to the air during sprayer application: A bibliographic review. Atmospheric Environment 39(28), 5183-5193.

Gillespie, W., Czapar, G., Hager, A. 2011. Pesticide fate in the environment: a guide for field inspectors. Illinois State Water Survey (ISWS), Contract Report CR-2011-07.

Glinski, D.A., Purucker, S.T., Van Meter, R.J., Black, M.C., Henderson, W.M. 2018. Analysis of pesticides in surface water, stemflow, and throughfall in an agricultural area in South Georgia, USA. Chemosphere 209, 496-507.

Gonzalez-Rey, M., Tapie, N., Le Menach, K., Dévier, M.H., Budzinski, H., Bebianno, M.J. 2015. Occurrence of pharmaceutical compounds and pesticides in aquatic systems. Marine Pollution Bulletin 96(1-2), 384-400.

Goswami, L., Kumar, R.V., Borah, S.N., Manikandan, N.A., Pakshirajan, K., Pugazhenthi, G. 2018. Membrane bioreactor and integrated membrane bioreactor systems for micropollutant removal from wastewater: A review. Journal of Water Process Engineering 26, 314-328.

Graillot, V., Takakura, N., Le Hegarat, L., Fessard, V., Audebert, M., Cravedi, J.P. 2012. Genotoxicity of pesticide mixtures present in the diet of the French population. Environmental and Molecular Mutagenesis 53(3), 173-184.

Grandclément, C., Seyssiecq, I., Piram, A., Wong-Wah-Chung, P., Vanot, G., Tiliacos, N., Roche, N., Doumenq, P. 2017. From the conventional biological wastewater treatment to hybrid processes, the evaluation of organic micropollutant removal: A review. Water Research 111, 297-317.

Guengerich, F.P. 2001. Common and uncommon cytochrome P450 reactions related to metabolism and chemical toxicity. Chemical Research in Toxicology 14(6), 611-650.

Guler, G.O., Cakmak, Y.S., Dagli, Z., Aktumsek, A., Ozparlak, H. 2010. Organochlorine pesticide residues in wheat from Konya region, Turkey. Food and Chemical Toxicology 48(5), 1218-1221.

Guyton, K.Z., Loomis, D., Grosse, Y., El Ghissassi, F., Benbrahim-Tallaa, L., Guha, N., Scoccianti, C., Mattock, H., Straif, K. 2015. Carcinogenicity of tetrachlorvinphos, parathion, malathion, diazinon, and glyphosate. The Lancet Oncology 16(5), 490-491.

Guo, W., Ngo, H.H., Li, J. 2012. A mini-review on membrane fouling. Bioresource Technology 122, 27-34.

Gupta, P.K. 2018. Toxicity of herbicides. In: Gupta, R.C. Veterinary toxicology- basic and clinical principles (3rd). Cambridge: Academic Press. pp. 553-567.

Gupta, S., Gupta, K. 2020. Bioaccumulation of pesticides and its impact on biological systems. In: Srivastava, P.K., Singh, V.P., Singh, A., Tripathi, D.K., Singh, S., Prasad, S.M., Chauhan, D.K. Pesticides in Crop Production: Physiological and Biochemical Action. Hoboken: Wiley. pp. 55-67.

Haddaoui, I., Mahjoub, O., Mahjoub, B., Boujelben, A., Di Bella, G. 2016. Occurrence and distribution of PAHs, PCBs, and chlorinated pesticides in Tunisian soil irrigated with treated wastewater. Chemosphere 146, 195-205.

Hall, L.M., Moss, S.R., Powles, S.B. 1995. Mechanism of resistance to chlorotoluron in two biotypes of the grass weed *Alopecurus myosuroides*. Pesticide Biochemistry and Physiology 53(3), 180-192.

Hambali, H.C., Suwito, E., Suhardi, S.H., Setiadi, T. 2009. Textile wastewater decolorization performance using *Marasmius* sp. in immersion and trickling systems. The 3rd IWA Aspire Conference & Exhibition, 151. Taiwan.

Hedegaard, M.J., Deliniere, H., Prasse, C., Dechesne, A., Smets, B.F., Albrechtsen, H.J. 2018. Evidence of co-metabolic bentazone transformation by methanotrophic enrichment from a groundwater-fed rapid sand filter. Water Research 129, 105-114.

Hedegaard, M.J., Prasse, C., Albrechtsen, H.J. 2019. Microbial degradation pathways of the herbicide bentazone in filter sand used for drinking water treatment.

Environmental Science: Water Research & Technology 5(3), 521-532.

Hedegaard, M.J., Schliemann-Haug, M.A., Milanovic, N., Lee, C.O., Boe-Hansen, R., Albrechtsen, H.J. 2020. Importance of methane oxidation for microbial degradation of the herbicide bentazone in drinking water production. Frontiers in Environmental Science 8, 79.

Heitz, T., Widemann, E., Lugan, R., Miesch, L., Ullmann, P., Désaubry, L., Holder, E., Grausem, B., Kandel, S., Miesch, M., Werck-Reichhart, D., Pinot, F. 2012. Cytochromes P450 CYP94C1 and CYP94B3 catalyze two successive oxidation steps of plant hormone jasmonoyl-isoleucine for catabolic turnover. Journal of Biological Chemistry 287(9), 6296-6306.

Herrero-Hernández, E., Andrades, M.S., Álvarez-Martín, A., Pose-Juan, E., Rodríguez-Cruz, M.S., Sánchez-Martín, M.J. 2013. Occurrence of pesticides and some of their degradation products in waters in a Spanish wine region. Journal of Hydrology 486, 234-245.

Hirai, H., Nakanishi, S., Nishida, T. 2004. Oxidative dechlorination of methoxychlor by ligninolytic enzymes from white-rot fungi. Chemosphere 55(4), 641-645.

Hladik, M.L., Kolpin, D.W., Kuivila, K.M. 2014. Widespread occurrence of neonicotinoid insecticides in streams in a high corn and soybean producing region, USA. Environmental Pollution 193, 189-196.

Hladik, M.L., Vandever, M., Smalling, K.L. 2016. Exposure of native bees foraging in an agricultural landscape to current-use pesticides. Science of the Total Environment 542, 469-477.

Huang, Y., Zhang, W., Pang, S., Chen, J., Bhatt, P., Mishra, S., Chen, S. 2020. Insights into the microbial degradation and catalytic mechanisms of chlorpyrifos. Environmental Research 194, 110660.

Huber, R., Otto, S. 1994. Environmental behavior of bentazon herbicide. In: Ware, G.W. Reviews of environmental contamination and toxicology volume 137. New York: Springer. pp. 111-134.

Hultberg, M., Ahrens, L., Golovko, O. 2020. Use of lignocellulosic substrate colonized by oyster mushroom (*Pleurotus ostreatus*) for removal of organic micropollutants from

water. Journal of Environmental Management 272, 111087.

Hvězdová, M., Kosubová, P., Košíková, M., Scherr, K.E., Šimek, Z., Brodský, L., Šudoma, M., Škulcová, L., Sáňka, M., Svobodová, M., Krkošková, L., Vašíčková, J., Neuwirthová, N., Bielská, L., Hofman, J. 2018. Currently and recently used pesticides in Central European arable soils. Science of the Total Environment 613-614, 361-370.

Iakovides, M., Apostolaki, M., Stephanou, E.G. 2021. PAHs, PCBs and organochlorine pesticides in the atmosphere of Eastern Mediterranean: Investigation of their occurrence, sources and gas-particle partitioning in relation to air mass transport pathways. Atmospheric Environment 244, 117931.

Imfeld, G.,Vuilleumier, S. 2012. Measuring the effects of pesticides on bacterial communities in soil: A critical review. European Journal of Soil Biology 49, 22-30.

Jacobsen-Pereira, C.H., dos Santos, C.R., Maraslis, F.T., Pimentel, L., Feijó, A.J.L., Silva, C.I., de Medeiros, G.S., Zeferino, R.C., Pedrosa, R.C., Maluf, S.W. 2018. Markers of genotoxicity and oxidative stress in farmers exposed to pesticides. Ecotoxicology and Environmental Safety 148, 177-183.

Jauregui, J., Valderrama, B., Albores, A., Vazquez-Duhalt, R. 2003. Microsomal transformation of organophosphorus pesticides by white rot fungi. Biodegradation 14, 397-406.

Jayaraj, R., Megha, P., Sreedev, P. 2016. Organochlorine pesticides, their toxic effects on living organisms and their fate in the environment. Interdisciplinary Toxicology 9(3-4), 90-100.

Juwarkar, A.A., Misra, R.R., Sharma, J.K. 2014. Recent trends in bioremediation In: Parmar, N., Singh, A. Geomicrobiology and biogeochemistry. Berlin: Springer. pp. 81-100.

Köck, M., Farré, M., Martínez, E., Gajda-Schrantz, K., Ginebreda, A., Navarro, A., de Alda, M.L., Barceló, D. 2010. Integrated ecotoxicological and chemical approach for the assessment of pesticide pollution in the Ebro River delta (Spain). Journal of Hydrology 383(1-2), 73-82.

Köck-Schulmeyer, M., Ginebreda, A., González, S., Cortina, J.L., de Alda, M.L., Barceló, D. 2012. Analysis of the occurrence and risk assessment of polar pesticides in the

Llobregat River Basin (NE Spain). Chemosphere 86(1), 8-16.

Köck-Schulmeyer, M., Olmos, M., de Alda, M.L., Barceló, D. 2013a. Development of a multiresidue method for analysis of pesticides in sediments based on isotope dilution and liquid chromatography-electrospray-tandem mass spectrometry. Journal of Chromatography A 1305, 176-187.

Köck-Schulmeyer, M., Villagrasa, M., de Alda, M.L., Céspedes-Sánchez, R., Ventura, F., Barceló, D. 2013b. Occurrence and behavior of pesticides in wastewater treatment plants and their environmental impact. Science of the Total Environment 458-460, 466-476.

Köck-Schulmeyer, M., Postigo, C., Farré, M., Barceló, D., de Alda, M.L. 2019. Medium to highly polar pesticides in seawater: analysis and fate in coastal areas of Catalonia (NE Spain). Chemosphere 215, 515-523.

Kabir, E.R., Rahman, M.S., Rahman, I. 2015. A review on endocrine disruptors and their possible impacts on human health. Environmental Toxicology and Pharmacology 40(1), 241-258.

Kamei, I., Takagi, K., Kondo, R. 2011. Degradation of endosulfan and endosulfan sulfate by white-rot fungus *Trametes hirsuta*. Journal of Wood Science 57, 317-322.

Kanaujiya, D.K., Paul, T., Sinharoy, A., Pakshirajan, K. 2019. Biological treatment processes for the removal of organic micropollutants from wastewater: a review. Current Pollution Reports 5, 112-128.

Kandil, M.M., Trigo, C., Koskinen, W.C., Sadowsky, M.J. 2015. Isolation and characterization of a novel imidacloprid-degrading *Mycobacterium* sp. strain MK6 from an Egyptian soil. Journal of Agricultural and Food Chemistry 63(19), 4721-4727.

Karas, P.A., Perruchon, C., Exarhou, K., Ehaliotis, C., Karpouzas, D.G. 2011. Potential for bioremediation of agro-industrial effluents with high loads of pesticides by selected fungi. Biodegradation 22, 215-228.

Karimi, A., Vahabzadeh, F., Mohseni, M., Mehranian, M. 2009. Decolorization of Maxilon-Red by Kissiris immobilized *Phanerochaete Chrysosporium* in a trickle-bed bioreactor-involvement of ligninolytic enzymes. Iranian Journal of Chemistry and Chemical Engineering 28(2), 50.

Kermani, M., Bina, B., Movahedian, H., Amin, M.M., Nikaein, M. 2008. Application of moving bed biofilm process for biological organics and nutrients removal from municipal wastewater. American Journal of Environmental Sciences 4(6), 682-689.

Kirk, T.K., Schultz, E., Connors, W.J., Lorenz, L.F., Zeikus, J.G. 1978. Influence of culture parameters on lignin metabolism by *Phanerochaete chrysosporium*. Archives of Microbiology 117, 277-285.

Klarich, K.L., Pflug, N.C., DeWald, E.M., Hladik, M.L., Kolpin, D.W., Cwiertny, D.M., LeFevre, G.H. 2017. Occurrence of neonicotinoid insecticides in finished drinking water and fate during drinking water treatment. Environmental Science & Technology Letters 4(5), 168-173.

Knauber, W.R., Krotzky, A.J., Schink, B. 2000. Microbial metabolism and further fate of bentazon in soil. Environmental Science & Technology 34(4), 598-603.

Koshlukova, S.E., Reed, N.R. 2014. Chlorpyrifos. In: Richardson R.J. Encyclopedia of toxicology (3rd). Amsterdam: Elsevier. pp. 930-934.

Křesinová, Z., Linhartová, L., Filipová, A., Ezechiáš, M., Mašín, P., Cajthaml, T. 2018. Biodegradation of endocrine disruptors in urban wastewater using *Pleurotus ostreatus* bioreactor. New Biotechnology 43, 53-61.

Kudanga, T., Nemadziva, B., Le Roes-Hill, M. 2017. Laccase catalysis for the synthesis of bioactive compounds. Applied Microbiology and Biotechnology 101, 13-33.

Kupski, L., Salcedo, G.M., Caldas, S.S., de Souza, T.D., Furlong, E.B., Primel, E.G. 2019. Optimization of a laccase-mediator system with natural redox-mediating compounds for pesticide removal. Environmental Science and Pollution Research 26, 5131-5139.

Lehmann, E., Turrero, N., Kolia, M., Konaté, Y., de Alencastro, L.F. 2017. Dietary risk assessment of pesticides from vegetables and drinking water in gardening areas in Burkina Faso. Science of the Total Environment 601-602, 1208-1216.

Levenspiel, O. 2013. Chemical Reactor Omnibook. Morrisville: Lulu Press, Inc.

Li, H., Ma, H., Lydy, M.J., You, J. 2014. Occurrence, seasonal variation and inhalation exposure of atmospheric organophosphate and pyrethroid pesticides in an urban community in South China. Chemosphere 95, 363-369.

Li, N., Xia, Q., Niu, M., Ping, Q., Xiao, H. 2018. Immobilizing laccase on different species

wood biochar to remove the chlorinated biphenyl in wastewater. Scientific Reports 8, 13947.

Li, X., Xu, J., de Toledo, R.A., Shim, H. 2015. Enhanced removal of naproxen and carbamazepine from wastewater using a novel countercurrent seepage bioreactor immobilized with *Phanerochaete chrysosporium* under non-sterile conditions. Bioresource Technology 197, 465-474.

Li, X., Xu, J., de Toledo, R.A., Shim, H. 2016. Enhanced carbamazepine removal by immobilized *Phanerochaete chrysosporium* in a novel rotating suspension cartridge reactor under non-sterile condition. International Biodeterioration & Biodegradation 115, 102-109.

Liu, J. 2014. Diuron. In: Richardson R.J. Encyclopedia of toxicology (3rd). Amsterdam: Elsevier. pp. 215-216.

Liu, Y., Li, S., Ni, Z., Qu, M., Zhong, D., Ye, C., Tang, F. 2016. Pesticides in persimmons, jujubes and soil from China: Residue levels, risk assessment and relationship between fruits and soils. Science of the Total Environment 542 Part A, 620-628.

Liu, Z., Kanjo, Y., Mizutani, S. 2009. Removal mechanisms for endocrine disrupting compounds (EDCs) in wastewater treatment-physical means, biodegradation, and chemical advanced oxidation: A review. Science of the Total Environment 407(2), 731-748.

Liu, Z., Dai, Y., Huan, Y., Liu, Z., Sun, L., Zhou, Q., Zhang, W., Sang, Q., Wei, H., Yuan, S. 2013. Different utilizable substrates have different effects on cometabolic fate of imidacloprid in *Stenotrophomonas maltophilia*. Applied Microbiology and Biotechnology 97, 6537-6547.

Llorca, M., Castellet-Rovira, F., Farré, M.J., Jaén-Gil, A., Martínez-Alonso, M., Rodríguez-Mozaz, S., Sarrà, M., Barceló, D. 2019. Fungal biodegradation of the N-nitrosodimethylamine precursors venlafaxine and O-desmethylvenlafaxine in water. Environmental Pollution 246, 346-356.

Lozowicka, B., Kaczynski, P., Paritova, A.E., Kuzembekova, G.B., Abzhalieva, A.B., Sarsembayeva, N.B., Alihan, K. 2014. Pesticide residues in grain from Kazakhstan and potential health risks associated with exposure to detected pesticides. Food and

Chemical Toxicology 64, 238-248.

Lucas, D., Castellet-Rovira, F., Villagrasa, M., Badia-Fabregat, M., Barceló, D., Vicent, T., Caminal, G., Sarrà, M., Rodríguez-Mozaz, S. 2018. The role of sorption processes in the removal of pharmaceuticals by fungal treatment of wastewater. Science of the Total Environment 610-611, 1147-1153.

Luo, Y., Guo, W., Ngo, H.H., Nghiem, L.D., Hai, F.I., Zhang, J., Liang, S., Wang, X.C. 2014. A review on the occurrence of micropollutants in the aquatic environment and their fate and removal during wastewater treatment. Science of the Total Environment 473, 619-641.

Ma, Y., Zhai, S., Mao, S., Sun, S., Wang, Y., Liu, Z., Dai, Y., Yuan, S. 2014. Co-metabolic transformation of the neonicotinoid insecticide imidacloprid by the new soil isolate *Pseudoxanthomonas indica* CGMCC 6648. Journal of Environmental Science and Health, Part B 49, 661-670.

Macedo, R.S., Lombardi, A.T., Omachi, C.Y., Rörig, L.R. 2008. Effects of the herbicide bentazon on growth and photosystem II maximum quantum yield of the marine diatom *Skeletonema costatum*. Toxicology in Vitro 22(3), 716-722.

Mahai, G., Wan, Y., Xia, W., Wang, A., Shi, L., Qian, X., He, Z., Xu, S. 2021. A nationwide study of occurrence and exposure assessment of neonicotinoid insecticides and their metabolites in drinking water of China. Water Research 189, 116630.

Majewski, M.S., Coupe, R.H., Foreman, W.T., Capel, P.D. 2014. Pesticides in Mississippi air and rain: A comparison between 1995 and 2007. Environmental Toxicology and Chemistry 33(6), 1283-1293.

Malhautier, L., Khammar, N., Bayle, S., Fanlo, J.L. 2005. Biofiltration of volatile organic compounds. Applied Microbiology and Biotechnology 68, 16-22.

Manavalan, T., Manavalan, A., Heese, K. 2015. Characterization of lignocellulolytic enzymes from white-rot fungi. Current Microbiology 70, 485-498.

Maqbool, Z., Hussain, S., Imran, M., Mahmood, F., Shahzad, T., Ahmed, Z., Azeem, F., Muzammil, S. 2016. Perspectives of using fungi as bioresource for bioremediation of pesticides in the environment: a critical review. Environmental Science and Pollution Research 23, 16904-16925.

Marco-Urrea, E., Pérez-Trujillo, M., Vicent, T., Caminal, G. 2009. Ability of white-rot fungi to remove selected pharmaceuticals and identification of degradation products of ibuprofen by *Trametes versicolor.* Chemosphere 74(6), 765-772.

Margot, J., Rossi, L., Barry, D.A., Holliger, C. 2015. A review of the fate of micropollutants in wastewater treatment plants. WIREs Water 2(5), 457-487.

Marican, A., Durán-Lara, E.F. 2018. A review on pesticide removal through different processes. Environmental Science and Pollution Research 25, 2051-2064.

Masiá, A., Campo, J., Navarro-Ortega, A., Barceló, D., Picó, Y. 2015. Pesticide monitoring in the basin of Llobregat River (Catalonia, Spain) and comparison with historical data. Science of the Total Environment 503-504, 58-68.

Massarsky, A., Trudeau, V.L., Moon, T.W. 2011. β-blockers as endocrine disruptors: the potential effects of human β-blockers on aquatic organisms. Journal of Experimental Zoology Part A: Ecological Genetics and Physiology 315A(5), 251-265.

McDonnell, A.M., Dang, C.H. 2013. Basic review of the cytochrome P450 system. Journal of the Advanced Practitioner in Oncology 4(4), 263-268.

McNevin, D., Barford, J. 2000. Biofiltration as an odour abatement strategy. Biochemical Engineering Journal 5(3), 231-242.

Minnesota Department of Agriculture (MDA), Pesticides and Bee toxicity. 2020. https://www.mda.state.mn.us/protecting/bmps/pollinators/beetoxicity.

Meftaul, I.M., Venkateswarlu, K., Dharmarajan, R., Annamalai, P., Megharaj, M. 2020. Pesticides in the urban environment: A potential threat that knocks at the door. Science of the Total Environment 711, 134612.

Mekonnen, M.M., Hoekstra, A.Y. 2016. Four billion people facing severe water scarcity. Science Advances 2(2), e1500323.

Michael, I., Rizzo, L., McArdell, C.S., Manaia, C.M., Merlin, C., Schwartz, T., Dagot, C., Fatta-Kassinos, D. 2013. Urban wastewater treatment plants as hotspots for the release of antibiotics in the environment: A review. Water Research 47(3), 957-995.

Mille-Lindblom, C., von Wachenfeldt, E., Tranvik, L.J. 2004. Ergosterol as a measure of living fungal biomass: persistence in environmental samples after fungal death. Journal of Microbiological Methods 59(2), 253-262.

Mir-Tutusaus, J.A., Baccar, R., Caminal, G., Sarrà, M. 2018. Can white-rot fungi be a real wastewater treatment alternative for organic micropollutants removal? A review. Water Research 138, 137-151.

Mir-Tutusaus, J.A., Masís-Mora, M., Corcellas, C., Eljarrat, E., Barceló, D., Sarrà, M., Caminal, G., Vicent, T., Rodríguez-Rodríguez, C.E. 2014. Degradation of selected agrochemicals by the white rot fungus *Trametes versicolor*. Science of the Total Environment 500, 235-242.

Mir-Tutusaus, J.A., Parladé, E., Llorca, M., Villagrasa, M., Barceló, D., Rodriguez-Mozaz, S., Martinez-Alonso, M., Gaju, N., Caminal, G., Sarrà, M. 2017. Pharmaceuticals removal and microbial community assessment in a continuous fungal treatment of non-sterile real hospital wastewater after a coagulation-flocculation pretreatment. Water Research 116, 65-75.

Mir-Tutusaus, J.A., Parladé, E., Villagrasa, M., Barceló, D., Rodríguez-Mozaz, S., Martínez-Alonso, M., Gaju, N., Sarrà, M., Caminal, G. 2019. Long-term continuous treatment of non-sterile real hospital wastewater by *Trametes versicolor*. Journal of Biological Engineering 13, 47.

Mir-Tutusaus, J.A., Sarrà, M. 2020. Fungal reactors: A solution for the removal of pharmaceuticals in urban and hospital wastewater. In: The handbook of environmental chemistry. Berlin: Springer. pp. 1-20.

Mir-Tutusaus, J.A., Sarrà, M., Caminal, G. 2016. Continuous treatment of non-sterile hospital wastewater by *Trametes versicolor*: How to increase fungal viability by means of operational strategies and pretreatments. Journal of Hazardous Materials 318, 561-570.

Mojiri, A., Zhou, J.L., Robinson, B., Ohashi, A., Ozaki, N., Kindaichi, T., Farraji, H., Vakili, M. 2020. Pesticides in aquatic environments and their removal by adsorption methods. Chemosphere 253, 126646.

Mori, T., Ohno, H., Ichinose, H., Kawagishi, H., Hirai, H. 2021. White-rot fungus *Phanerochaete chrysosporium* metabolizes chloropyridinyl-type neonicotinoid insecticides by an N-dealkylation reaction catalyzed by two cytochrome P450s. Journal of Hazardous Materials 402, 123831.

Mori, T., Wang, J., Tanaka, Y., Nagai, K., Kawagishi, H., Hirai, H. 2017. Bioremediation of the neonicotinoid insecticide clothianidin by the white-rot fungus *Phanerochaete sordida*. Journal of Hazardous Materials 321, 586-590.

Mostafa, I.Y., Bahig, M.R.E., Fakhr, I.M.I., Adam, Y. 1972. Metabolism of organophosphorus insecticides, XIV malathion breakdown by soil fungi. Zeitschrift für Naturforschung B 27(9), 1115-1116.

Mostafalou, S., Abdollahi, M. 2017. Pesticides: an update of human exposure and toxicity. Archives of Toxicology 91, 549-599.

Muenze, R., Hannemann, C., Orlinskiy, P., Gunold, R., Paschke, A., Foit, K., Becker, J., Kaske, O., Paulsson, E., Peterson, M., Jernstedt, H., Kreuger, J., Schüürmann G., Liess, M. 2017. Pesticides from wastewater treatment plant effluents affect invertebrate communities. Science of the Total Environment 599-600, 387-399.

Murillo-Zamora, S., Castro-Gutiérrez, V., Masís-Mora, M., Lizano-Fallas, V., Rodríguez-Rodríguez, C.E. 2017. Elimination of fungicides in biopurification systems: effect of fungal bioaugmentation on removal performance and microbial community structure. Chemosphere 186, 625-634.

Muyzer, G., de Waal, E.C., Uitterlinden, A.G. 1993. Profiling of complex microbial populations by denaturing gradient gel electrophoresis analysis of polymerase chain reaction-amplified genes coding for 16S rRNA. Applied and Environmental Microbiology 59(3), 695-700.

National Pesticide Information Center (NPIC). http://npic.orst.edu/.

Newhart, K. 2006. Environmental fate of malathion. California Environmental Protection Agency.

Nicolopoulou-Stamati, P., Maipas, S., Kotampasi, C., Stamatis, P., Hens, L. 2016. Chemical pesticides and human health: The urgent need for a new concept in agriculture. Frontiers in Public Health 4, 148.

Novotný, Č., Erbanová, P., Šašek, V., Kubátová, A., Cajthaml, T., Lang, E., Krahl, J., Zadražil, F. 1999. Extracellular oxidative enzyme production and PAH removal in soil by exploratory mycelium of white rot fungi. Biodegradation 10, 159-168.

Novotný, Č., Svobodová, K., Benada, O., Kofroňová, O., Heissenberger, A., Fuchs, W.

2011. Potential of combined fungal and bacterial treatment for color removal in textile wastewater. Bioresource Technology 102(2), 879-888.

Palli, L., Castellet-Rovira, F., Pérez-Trujillo, M., Caniani, D., Sarrà-Adroguer, M., Gori, R. 2017. Preliminary evaluation of *Pleurotus ostreatus* for the removal of selected pharmaceuticals from hospital wastewater. Biotechnology Progress 33(6), 1529-1537.

Palli, L., Gullotto, A., Tilli, S., Caniani, D., Gori, R., Scozzafava, A. 2016. Biodegradation of 2-naphthalensulfonic acid polymers by white-rot fungi: Scale-up into non-sterile packed bed bioreactors. Chemosphere 164, 120-127.

Palli, L., Gullotto, A., Tilli, S., Gori, R., Lubello, C., Scozzafava, A. 2014. Effect of carbon source on the degradation of 2-naphthalenesulfonic acid polymers mixture by *Pleurotus ostreatus* in petrochemical wastewater. Process Biochemistry 49(12), 2272-2278.

Pesticide Action Network (PAN), Pesticide Database. 2020. https://www.pesticideinfo.org.

Papadakis, E.N., Tsaboula, A., Vryzas, Z., Kotopoulou, A., Kintzikoglou, K., Papadopoulou-Mourkidou, E. 2018. Pesticides in the rivers and streams of two river basins in northern Greece. Science of the Total Environment 624, 732-743.

Pareja, L., Colazzo, M., Pérez-Parada, A., Besil, N., Heinzen, H., Böcking, B., Cesio, V., Fernández-Alba, A.R. 2012. Occurrence and distribution study of residues from pesticides applied under controlled conditions in the field during rice processing. Journal of Agricultural and Food Chemistry 60(18), 4440-4448.

Paris, D.F., Lewis, D.L., Wolfe, N.L. 1975. Rates of degradation of malathion by bacteria isolated from aquatic system. Environmental Science & Technology 9, 135-138.

Park, H.O., Oh, S., Bade, R., Shin, W.S. 2011. Application of fungal moving-bed biofilm reactors (MBBRs) and chemical coagulation for dyeing wastewater treatment. KSCE Journal of Civil Engineering 15, 453-461.

Patisaul, H.B., Adewale, H.B. 2009. Long-term effects of environmental endocrine disruptors on reproductive physiology and behavior. Frontiers in Behavioral Neuroscience 3, 10.

Peris, A., Eljarrat, E. 2021. Multi-residue methodologies for the analysis of non-polar pesticides in water and sediment matrices by GC-MS/MS. Chromatographia 84, 425-

439.

Pietrzak, D., Kania, J., Malina, G., Kmiecik, E., Wątor, K. 2019. Pesticides from the EU first and second Watch Lists in the water environment. Clean-Soil, Air, Water 47(7), 1800376.

Pimentel, D., Burgess, M. 2012 Small amounts of pesticides reaching target insects. Environment, Development and Sustainability 14, 1-2.

Pinto, A.P., Serrano, C., Pires, T., Mestrinho, E., Dias, L., Teixeira, D.M., Caldeira, A.T. 2012. Degradation of terbuthylazine, difenoconazole and pendimethalin pesticides by selected fungi cultures. Science of the Total Environment 435-436, 402-410.

Pinto, A.P., Caldeira, A.T., Martins Teixeira, D., Mestrinho, E., Dordio, A.V., Romeiras, M.D.C. 2011. Degradation of terbuthylazine, diflufenican and pendimethalin pesticides by *Lentinula edodes* cultures. Current Opinion in Biotechnology 22S, S70: G14.

Pizzul, L., Castillo, M.P., Stenström, J. 2009. Degradation of glyphosate and other pesticides by ligninolytic enzymes. Biodegradation 20, 751-759.

Pocedič, J., Hasal, P., Novotný, Č. 2009. Decolorization of organic dyes by *Irpex lacteus* in a laboratory trickle-bed biofilter using various mycelium supports. Journal of Chemical Technology & Biotechnology 84(7), 1031-1042.

Pesticide Properties Database (PPDB), University of Hertfordshire. 2016. https://sitem.herts.ac.uk/aeru/ppdb/en/index.htm.

Prigione, V., Tigini, V., Pezzella, C., Anastasi, A., Sannia, G., Varese, G.C. 2008. Decolourisation and detoxification of textile effluents by fungal biosorption. Water Research 42(12), 2911-2920.

Purnomo, A.S., Mori, T., Kamei, I., Nishii, T., Kondo, R. 2010. Application of mushroom waste medium from *Pleurotus ostreatus* for bioremediation of DDT-contaminated soil. International Biodeterioration & Biodegradation 64(5), 397-402.

Purnomo, A.S., Nawfa, R., Martak, F., Shimizu, K., Kamei, I. 2017. Biodegradation of aldrin and dieldrin by the white-rot fungus *Pleurotus ostreatus*. Current Microbiology 74, 320-324.

Ramakrishnan, B., Venkateswarlu, K., Sethunathan, N., Megharaj, M. 2019. Local

applications but global implications: Can pesticides drive microorganisms to develop antimicrobial resistance? Science of the Total Environment 654, 177-189.

Rani, L., Thapa, K., Kanojia, N., Sharma, N., Singh, S., Grewal, A.S., Srivastav, A.L., Kaushal, J. 2020. An extensive review on the consequences of chemical pesticides on human health and environment. Journal of Cleaner Production 283, 124657.

Reed, N.R., Rubin, A.L. 2014. Malathion. In: Richardson R.J. Encyclopedia of toxicology (3rd). Amsterdam: Elsevier. pp. 133-137.

Relyea, R.A. 2003. Predator cues and pesticides: A double dose of danger for amphibians. Ecological Applications 13(6), 1515-1521.

Ren, X., Zeng, G., Tang, L., Wang, J., Wan, J., Liu, Y., Yu, J., Yi, H., Ye, S., Deng, R. 2018. Sorption, transport and biodegradation-an insight into bioavailability of persistent organic pollutants in soil. Science of the Total Environment 610-611, 1154-1163.

Riah, W., Laval, K., Laroche-Ajzenberg, E., Mougin, C., Latour, X., Trinsoutrot-Gattin, I. 2014. Effects of pesticides on soil enzymes: a review. Environmental Chemistry Letters 12, 257-273.

Riascos-Flores, L., Bruneel, S., Van der Heyden, C., Deknock, A., Van Echelpoel, W., Forio, M.A.E., De Saeyer, N., Berghe, W.V., Spanoghe, P., Bermudez, R., Dominguez-Granda, L., Goethals, P. 2021. Polluted paradise: Occurrence of pesticide residues within the urban coastal zones of Santa Cruz and Isabela (Galapagos, Ecuador). Science of the Total Environment 763, 142956.

Richardson, J.R., Fitsanakis, V., Westerink, R.H.S., Kanthasamy, A.G. 2019. Neurotoxicity of pesticides. Acta Neuropathologica 138, 343-362.

Rippy, M.A., Deletic, A., Black, J., Aryal, R., Lampard, J.L., Tang, J.Y.M., McCarthy, D., Kolotelo, P., Sidhu, J., Gernjak, W. 2017. Pesticide occurrence and spatio-temporal variability in urban run-off across Australia. Water Research 115, 245-255.

Rizzo, L., Manaia, C., Merlin, C., Schwartz, T., Dagot, C., Ploy, M.C., Michael, I., Fatta-Kassinos, D. 2013. Urban wastewater treatment plants as hotspots for antibiotic resistant bacteria and genes spread into the environment: A review. Science of the Total Environment 447, 345-360.

Rodríguez-Rodríguez, C.E., Madrigal-León, K., Masís-Mora, M., Pérez-Villanueva, M.,

Chin-Pampillo, J.S. 2017. Removal of carbamates and detoxification potential in a biomixture: fungal bioaugmentation versus traditional use. Ecotoxicology and Environmental Safety 135, 252-258.

Rodríguez-Rodríguez, C.E., Marco-Urrea, E., Caminal, G. 2010a. Degradation of naproxen and carbamazepine in spiked sludge by slurry and solid-phase *Trametes versicolor* systems. Bioresource Technology 101(7), 2259-2266.

Rodríguez-Rodríguez, C.E., Marco-Urrea, E., Caminal, G. 2010b. Naproxen degradation test to monitor *Trametes versicolor* activity in solid-state bioremediation processes. Journal of Hazardous materials 179(1-3), 1152-1155.

Rosa, L., Chiarelli, D.D., Rulli, M.C., Dell'Angelo, J., D'Odorico, P. 2020. Global agricultural economic water scarcity. Science Advances 6, eaaz6031.

Ruggeri, B., Sassi, G. 2003. Experimental sensitivity analysis of a trickle bed bioreactor for lignin peroxidases production by *P. chrysosporium.* Process Biochemistry 38(12), 1669-1676.

Sánchez-Bayo, F. 2014. The trouble with neonicotinoids. Science 346(6211), 806-807.

Sørensen, S.R., Albers, C.N., Aamand, J. 2008. Rapid mineralization of the phenylurea herbicide diuron by *Variovorax* sp. strain SRS16 in pure culture and within a two-member consortium. Applied Environmental Microbiology 74(8), 2332-2340.

Sá, C.S.A., Boaventura, B.A.R. 2001. Biodegradation of phenol by *Pseudomonas putida* DSM 548 in a trickling bed reactor. Biochemical Engineering Journal 9(3), 211-219.

Sadiq, S., Haq, M.I., Ahmad, I., Ahad, K., Rashid, A., Rafiq, N. 2015. Bioremediation potential of white rot fungi, *Pleurotus* spp against organochlorines. Journal of Bioremediation and Biodegradation 6(5), 1000308.

Saini, R., Kumar, P. 2016. Simultaneous removal of methyl parathion and chlorpyrifos pesticides from model wastewater using coagulation/flocculation: Central composite design. Journal of Environmental Chemical Engineering 4(1), 673-680.

Saleh, I.A., Zouari, N., Al-Ghouti, M.A. 2020. Removal of pesticides from water and wastewater: Chemical, physical and biological treatment approaches. Environmental Technology & Innovation 19, 101026.

Sauvé, S., Desrosiers, M. 2014. A review of what is an emerging contaminant. Chemistry

Central Journal 8, 15.

Schymanski, E.L., Jeon, J., Gulde, R., Fenner, K., Ruff, M., Singer, H.P., Hollender, J. 2014. Identifying small molecules via high resolution mass spectrometry: Communicating confidence. Environmental Science & Technology 48(4), 2097-2098.

Sharma, S., Singh, B., Gupta, V.K. 2014. Assessment of imidacloprid degradation by soil-isolated *Bacillus alkalinitrilicus*. Environmental Monitoring and Assessment 186, 7183-7193.

Sheets, L.P. 2014. Imidacloprid. In: Richardson R.J. Encyclopedia of toxicology (3rd). Amsterdam: Elsevier. pp. 1000-1003.

Silva, V., Mol, H.G.J., Zomer, P., Tienstra, M., Ritsema, C.J., Geissen, V. 2019. Pesticide residues in European agricultural soils-A hidden reality unfolded. Science of the Total Environment 653, 1532-1545.

Singh, B., Kaur, J., Singh, K. 2012. Biodegradation of malathion by *Brevibacillus* sp. strain KB2 and *Bacillus cereus* strain PU. World Journal of Microbiology and Biotechnology 28, 1133-1141.

Singh, B., Kaur, J., Singh, K. 2014. Microbial degradation of an organophosphate pesticide, malathion. Critical Reviews in Microbiology 40(2), 146-154.

Singh, B.K., Walker, A. 2006. Microbial degradation of organophosphorus compounds. FEMS Microbiology Reviews 30(3), 428-471.

Singh, B.K., Walker, A., Morgan, J.A.W., Wright, D.J. 2004. Biodegradation of chlorpyrifos by *Enterobacter* strain B-14 and its use in bioremediation of contaminated soils. Applied Environmental Microbiology 70(8), 4855-4863.

Sjerps, R.M.A., Kooij, P.J.F., van Loon, A., Van Wezel, A.P. 2019. Occurrence of pesticides in Dutch drinking water sources. Chemosphere 235, 510-518.

Šrédlová, K., Škrob, Z., Filipová, A., Mašín, P., Holecová, J., Cajthaml, T. 2020. Biodegradation of PCBs in contaminated water using spent oyster mushroom substrate and a trickle-bed bioreactor. Water Research 170, 115274.

Syed, J.H., Malik, R.N. 2011. Occurrence and source identification of organochlorine pesticides in the surrounding surface soils of the Ittehad Chemical Industries Kalashah Kaku, Pakistan. Environmental Earth Sciences 62, 1311-1321.

Tang, Z., Huang, Q., Yang, Y., Zhu, X., Fu, H. 2013. Organochlorine pesticides in the lower reaches of Yangtze River: Occurrence, ecological risk and temporal trends. Ecotoxicology and Environmental Safety 87, 89-97.

Tasca, A.L., Fletcher, A. 2018. State of the art of the environmental behaviour and removal techniques of the endocrine disruptor 3,4-dichloroaniline. Journal of Environmental Science and Health, Part A 53(3), 260-270.

Tavčar, M., Svobodová, K., Kuplenk, J., Novotný, Č., Pavko, A. 2006. Biodegradation of azo dye RO16 in different reactors by immobilized *Irpex lacteus*. Acta Chimica Slovenica 53, 338-343.

Teló, G.M., Senseman, S.A., Marchesan, E., Camargo, E.R., Jones, T., McCauley, G. 2015. Residues of thiamethoxam and chlorantraniliprole in rice grain. Journal of Agricultural and Food Chemistry 63(8), 2119-2126.

Tiryaki, O., Temur, C. 2010. The fate of pesticide in the environment. Journal of Biological & Environmental Sciences 4(10), 29-38.

Tiwari, B., Sellamuthu, B., Ouarda, Y., Drogui, P., Tyagi, R.D., Buelna, G. 2017. Review on fate and mechanism of removal of pharmaceutical pollutants from wastewater using biological approach. Bioresource Technology 224, 1-12.

Torán, M.J. 2018. Continuous wastewater treatment by *Trametes versicolor* immobilized on lignocellulosic support. Universitat Autònoma de Barcelona.

Torán, J., Blánquez, P., Caminal, G. 2017. Comparison between several reactors with *Trametes versicolor* immobilized on lignocellulosic support for the continuous treatments of hospital wastewater. Bioresource Technology 243, 966-974.

Tormo-Budowski, R., Cambronero-Heinrichs, J.C., Durán, J.E., Masís-Mora, M., Ramírez-Morales, D., Quirós-Fournier, J.P., Rodríguez-Rodríguez, C.E. 2021. Removal of pharmaceuticals and ecotoxicological changes in wastewater using *Trametes versicolor*: A comparison of fungal stirred tank and trickle-bed bioreactors. Chemical Engineering Journal 410, 128210.

Tran, N.H., Reinhard, M., Gin, K.Y.H. 2018. Occurrence and fate of emerging contaminants in municipal wastewater treatment plants from different geographical regions-a review. Water Research 133, 182-207.

Turcant, A., Harry, P., Cailleux, A., Puech, M., Bruhat, C., Vicq, N., Le Bouil, A., Allain, P. 2003. Fatal acute poisoning by bentazon. Journal of Analytical Toxicology 27(2), 113-117.

Ullah, S., Zorriehzahra, M.J. 2015. Ecotoxicology: A review of pesticides induced toxicity in fish. Advances in Animal and Veterinary Sciences 3(1), 40-57.

United Nations Environment Programme (UNEP). 2016. Stockholm Convention on persistent organic pollutants. Report of the Persistent Organic Pollutants Review Committee on the work of its twelfth meeting, 12/11/Add.1. http://chm.pops.int/?tabid=5171.

Van den Berg, F., Kubiak, R., Benjey, W.G., Majewski, M.S., Yates, S.R., Reeves, G.L., Smelt, J.H., Van der Linden, A.M.A. 1999. Emission of pesticides into the air. In: Van Dijk, H.F.G., Van Pul, W.A.J., Voogt, P.D. Fate of pesticides in the atmosphere: implications for environmental risk assessment. Dordrecht: Springer. pp. 195-218,.

Van Soest, P.J., Robertson, J.B., Lewis, B.A. 1991. Methods for dietary fiber, neutral detergent fiber, and nonstarch polysaccharides in relation to animal nutrition. Journal of Dairy Science 74(10), 3583-3597.

Verlicchi, P., Al Aukidy, M., Zambello, E. 2012. Occurrence of pharmaceutical compounds in urban wastewater: removal, mass load and environmental risk after a secondary treatment-A review. Science of the Total Environment 429, 123-155.

Voběrková, S., Solčány, V., Vršanská, M., Adam, V. 2018. Immobilization of ligninolytic enzymes from white-rot fungi in cross-linked aggregates. Chemosphere 202, 694-707.

Vryzas, Z., Papadakis, E.N., Vassiliou, G., Papadopoulou-Mourkidou, E. 2012. Occurrence of pesticides in transboundary aquifers of North-eastern Greece. Science of the Total Environment 441, 41-48.

Wallace, D.R. 2014. Acetamiprid. In: Richardson R.J. Encyclopedia of toxicology (3rd). Amsterdam: Elsevier. pp. 30-32.

Wang, J., Hirai, H., Kawagishi, H. 2012. Biotransformation of acetamiprid by the white-rot fungus *Phanerochaete sordida* YK-624. Applied Microbiology and Biotechnology 93, 831-835.

Wang, J., Ohno, H., Ide, Y., Ichinose, H., Mori, T., Kawagishi, H., Hirai, H. 2019a.

Identification of the cytochrome P450 involved in the degradation of neonicotinoid insecticide acetamiprid in *Phanerochaete chrysosporium*. Journal of Hazardous Materials 371, 494-498.

Wang, J., Tanaka, Y., Ohno, H., Jia, J., Mori, T., Xiao, T., Yan, B., Kawagishi, H., Hirai, H. 2019b. Biotransformation and detoxification of the neonicotinoid insecticides nitenpyram and dinotefuran by *Phanerochaete sordida* YK-624. Environmental Pollution 252 Part A, 856-862.

Wang, S., Steiniche, T., Romanak, K.A., Johnson, E., Quirós, R., Mutegeki, R., Wasserman, M.D., Venier, M. 2019c. Atmospheric occurrence of legacy pesticides, current use pesticides, and flame retardants in and around protected areas in Costa Rica and Uganda. Environmental Science & Technology 53(11), 6171-6181.

Wang, T., Zhong, M., Lu, M., Xu, D., Xue, Y., Huang, J., Blaney, L., Yu, G. 2021. Occurrence, spatiotemporal distribution, and risk assessment of current-use pesticides in surface water: A case study near Taihu Lake, China. Science of the Total Environment 782, 146826.

Wang, X., Goulson, D., Chen, L., Zhang, J., Zhao, W., Jin, Y., Yang, S., Li, Y., Zhou, J. 2020. Occurrence of neonicotinoids in Chinese apiculture and a corresponding risk exposure assessment. Environmental Science & Technology 54(8), 5021-5030.

Wariishi, H., Valli, K., Gold, M.H. 1992. Manganese (II) oxidation by manganese peroxidase from the basidiomycete *Phanerochaete chrysosporium*. Kinetic mechanism and role of chelators. Journal of Biological Chemistry 267(33), 23688-23695.

White, T.J., Bruns, T., Lee, S., Taylor, J. 1990. Amplification and direct sequencing of fungal ribosomal RNA genes for phylogenetics. In: Innis, M.A., Gelfand, D.H., Sninsky, J.J., White, T.J. PCR protocols: a guide to methods and applications. New York: Academic Press, Inc. pp. 315-322.

Wołejko, E., Jabłońska-Trypuć, A., Wydro, U., Butarewicz, A., Łozowicka, B. 2020. Soil biological activity as an indicator of soil pollution with pesticides-A review. Applied Soil Ecology 147, 103356.

Wolfand, J.M., LeFevre, G.H., Luthy, R.G. 2016. Metabolization and degradation kinetics

of the urban-use pesticide fipronil by white rot fungus *Trametes versicolor*. Environmental Science: Processes & Impacts 18, 1256-1265.

World Health Organization (WHO). 2020. The WHO recommended classification of pesticides by hazard and guidelines to classification 2019. Geneva: WHO.

World Resources Institute (WRI). 2019. Aqueduct 3.0: Updated Decision-Relevant Global Water Risk Indicators. https://www.wri.org/applications/aqueduct/water-risk-atlas/#/?advanced=false&basemap=hydro&indicator=w_awr_def_tot_cat&lat=30&lng=-80&mapMode=view&month=1&opacity=0.5&ponderation=DEF&predefined=false&projection=absolute&scenario=optimistic&scope=baseline&timeScale=annual&year=baseline&zoom=3.

World Water Assessment Programme (WWAP). 2017. The United Nations World Water Development Report 2017. Wastewater: The Untapped Resource. Paris: The United Nations Educational, Scientific and Cultural Organization (UNESCO). https://unesdoc.unesco.org/ark:/48223/pf0000247153.

WWAP. 2020. The United Nations World Water Development Report 2020. Water and Climate Change. Paris: UNESCO. https://unesdoc.unesco.org/ark:/48223/pf0000372985.locale=en.

Wu, P., Zhang, X., Niu, T., Wang, Y., Liu, R., Zhang, Y. 2020. The imidacloprid remediation, soil fertility enhancement and microbial community change in soil by *Rhodopseudomonas capsulata* using effluent as carbon source. Environmental Pollution 267, 114254.

Xiao, P., Kondo, R. 2020. Potency of Phlebia species of white rot fungi for the aerobic degradation, transformation and mineralization of lindane. Journal of Microbiology 58, 395-404.

Xie, Q., Xue, C., Chen, A., Shang, C., Luo, S. 2020. *Phanerochaete chrysosporium*-driven quinone redox cycling promotes degradation of imidacloprid. International Biodeterioration & Biodegradation 151, 104965.

Yadav, I.C., Devi, N.L. 2017. Pesticides classification and its impact on human and environment. In: Chandra, R., Gurjar, B.R. Environmental science and engineering

volume 6 toxicology. Houston: Studium Press Llc. pp. 140-158.

Yadav, I.C., Devi, N.L., Li, J., Zhang, G., Shakya, P.R. 2016. Occurrence, profile and spatial distribution of organochlorines pesticides in soil of Nepal: Implication for source apportionment and health risk assessment. Science of the Total Environment 573, 1598-1606.

Yadav, J.S., Reddy, C.A. 1993. Mineralization of 2,4-dichlorophenoxyacetic acid (2,4-D) and mixtures of 2,4-D and 2,4,5-trichlorophenoxyacetic acid by *Phanerochaete chrysosporium*. Applied and Environmental Microbiology 59(9), 2904-2908.

Ying, G., Kookana, R.S., Ru, Y. 2002. Occurrence and fate of hormone steroids in the environment. Environment International 28(6), 545-551.

Zeinat K.M., Nashwa, A.H., Mohamed, A.I., Sherif, E.N. 2008. Biodegradation and detoxification of malathion by of *Bacillus thuringiensis* MOS-5. Australian Journal of Basic and Applied Sciences 2(3), 724-732.

Zhan, L., Lin, T., Wang, Z., Cheng, Z., Zhang, G., Lyu, X., Cheng, H. 2017. Occurrence and air-soil exchange of organochlorine pesticides and polychlorinated biphenyls at a CAWNET background site in central China: Implications for influencing factors and fate. Chemosphere 186, 475-487.

Zhang, Q., Chen, Z., Li, Y., Wang, P., Zhu, C., Gao, G., Xiao, K., Sun, H., Zheng, S., Liang, Y., Jiang G. 2015. Occurrence of organochlorine pesticides in the environmental matrices from King George Island, west Antarctica. Environmental Pollution 206, 142-149.

Zhang, W., Jiang, F., Ou, J. 2011. Global pesticide consumption and pollution: with China as a focus. Proceedings of the International Academy of Ecology and Environmental Sciences 1(2), 125-144.

Zhang, Y., Liu, J., Li, J. 2020. Comparison of four methods to solve clogging issues in a fungi-based bio-trickling filter. Biochemical Engineering Journal 153, 107401.

Zhang, Y., Liu, J., Qin, Y., Yang, Z., Cao, J., Xing, Y., Li, J. 2019. Performance and microbial community evolution of toluene degradation using a fungi-based bio-trickling filter. Journal of Hazardous Materials 365, 642-649.

Zhao, Y., Liu, D., Huang, W., Yang, Y., Ji, M., Nghiem, L.D., Trinh, Q.T., Tran, N.H. 2019.

Insights into biofilm carriers for biological wastewater treatment processes: current state-of-the-art, challenges, and opportunities. Bioresource Technology 288, 121619.

Zhuo, R., Fan, F. 2021. A comprehensive insight into the application of white rot fungi and their lignocellulolytic enzymes in the removal of organic pollutants. Science of the Total Environment 778, 146132.

List of publications

Paper published on Indexed journals

➢ Hu, K., Peris, A., Torán, J., Eljarrat, E., Sarrà, M., Blánquez, P., Caminal, G. 2020. Exploring the degradation capability of *Trametes versicolor* on selected hydrophobic pesticides through setting sights simultaneously on culture broth and biological matrix. Chemosphere 250, 126293.

➢ Hu, K., Torán, J., López-García, E., Barbieri, M.V., Postigo, C., de Alda, M.L., Caminal, G., Sarrà, M., Blánquez, P. 2020. Fungal bioremediation of diuron-contaminated waters: evaluation of its degradation and the effect of amendable factors on its removal in a trickle-bed reactor under non-sterile conditions. Science of the Total Environment 743, 140628.

➢ Hu, K., Barbieri, M.V., López-García, E., Postigo, C., de Alda, M.L., Caminal, G., Sarrà, M. 2021. Fungal degradation of selected medium to highly polar pesticides by *Trametes versicolor*: kinetics, biodegradation pathways, and ecotoxicity of treated waters. Analytical and Bioanalytical Chemistry.

➢ Hu, K., Sarrà, M., Caminal, G. 2021. Comparison between two reactors using *Trametes versicolor* for agricultural wastewater treatment under non-sterile condition in sequencing batch mode. Journal of Environmental Management 293, 112859.

➢ García-Vara, M., Hu, K., Postigo, C., Olmo, L., Caminal, G., Sarrà, M., de Alda, M.L. 2021. Remediation of bentazone contaminated water by *Trametes versicolor*: characterization, identification of transformation products, and implementation in a trickle-bed reactor under non-sterile conditions. Journal of Hazardous Materials 409, 124476.

Paper in preparation

➢ Hu, K., Caminal, G., Sarrà, M. Removal of pesticides from agricultural wastewater with immobilized *Trametes versicolor* in a pilot plant trickle bed reactor. Chemical Engineering Journal, under revision.

Annexes

Annex A

Microbial community analysis

Liquid samples were firstly filtered through a 0.22 μm polyvinylidene fluoride (PDVF) filter (Durapore®, Merck Millipore, USA) and the filter was subsequently stored in a 15 mL Falcon® tube at – 80 °C prior to DNA extraction. In the case of solid samples, the fungal mycelium was removed from wood surface using forceps and conserved at 4 °C. After that, wood chips together with phosphate buffer (0.1 M, pH at 7.0) underwent a process of agitation (200 rpm, 30 min) and sonication (7 min) inside a bag. The obtained liquid was then centrifuged (8, 500 rpm, 30 min), and the resultant precipitates were mixed with the previously extracted mycelium and stored at – 20 °C until DNA extraction. All the steps were conducted aseptically.

Total DNA extraction was performed using DNeasy® PowerWater DNA extraction kit (Qiagen, Germany) and DNeasy® PowerSoil DNA extraction kit (Qiagen, Germany) for liquid and solid samples, respectively. DNA samples were stored at – 20 °C.

For bacterial microflora analysis, 16S rRNA sequence was amplified through PCR (S1000 ThermalCycler, Bio-Rad, USA) using primer set 341f/907rM (Muyzer et al., 1993) with a GC clamp added at the 5' end of the primer 341f. Amplification protocol consisted of: 94 °C for 5 min; 20 cycles of 94 °C for 1 min, 65 °C for 1 min (– 0.5 °C per cycle), 72 °C for 3 min; 15 cycles of 94 °C for 1 min, 55 °C for 1 min, 72 °C for 3 min; and a single final extension of 72 °C for 7 min. As respect to fungal community, ITS sequence was amplified using primer sets: EF4/ITS4 and ITS1f/ITS2r (Gardes and Bruns, 1993; White et al., 1990). The GC clamp was added at the 5' side of ITS1f. The PCR program was as follows: 95 °C for 5 min; 35 cycles of 94 °C for 30 s, 55 °C for 30 s, 72 °C for 30 s; and a single final extension of 72 °C for 5 min.

Denaturing gradient gel electrophoresis (DGGE) was performed in a Dcode™ Universal Mutation Detection System (Bio-Rad, USA). Desired PCR products were loaded into 6% (w/v) polyacrylamide gels (acrylamide/bis-acrylamide solution, 37.5:1) containing linear chemical gradients 30–70% denaturant for bacteria and 15–55% denaturant for fungi. 80% denaturing solution contained 7 M urea and 32% (v/v) deionized formamide. Gels were run

in 1 × TAE (40 mM Tris acetate at pH 7.4, 20 mM sodium acetate, 1 mM EDTA) for 16 h at 75 V and 60 °C using Bio-Rad Power Pac 1000 power supply.

After electrophoresis, bands were visualized by ethidium bromide staining. Target bands were excised and conserved in a mixture solution of PCR buffer and $MgCl_2$ at − 20 ºC. Reamplified DNA fragments were sequenced by Macrogen (South Korea) and further analyzed using Finch TV software and nucleotide BLAST on the National Center for Biotechnology Information (NCBI), successively.
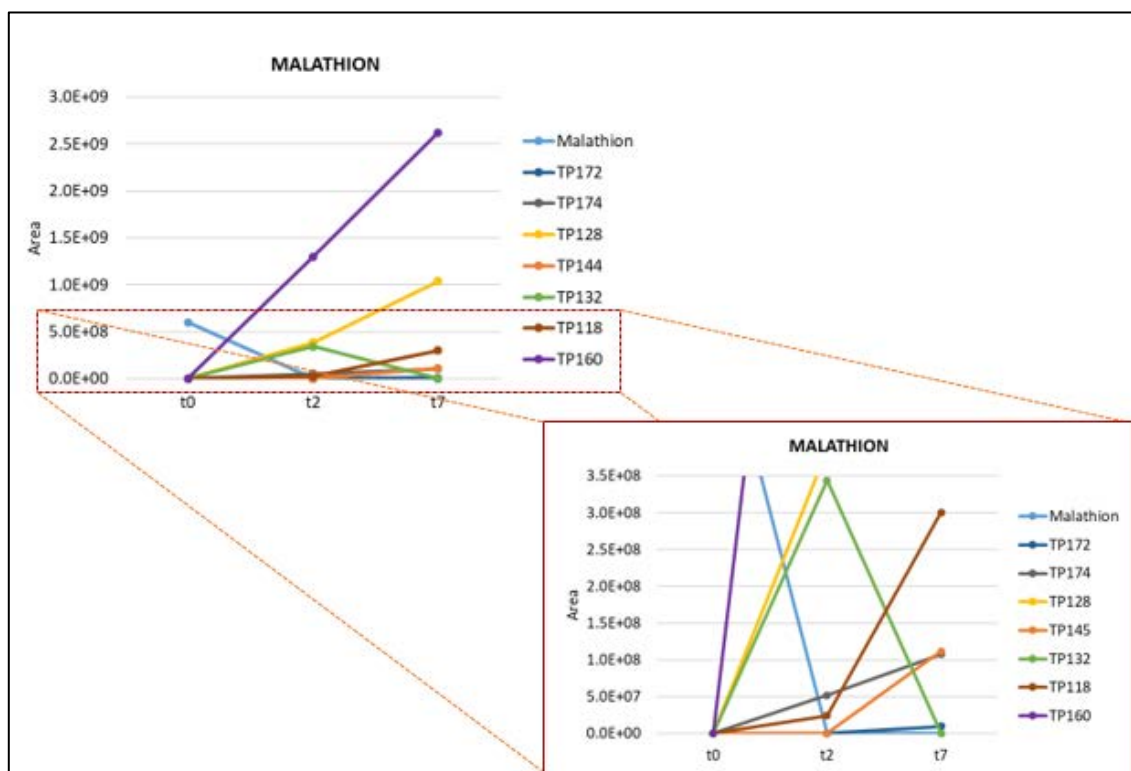
Annex B

Figure B.1 Evolution of the TPs identified during malathion degradation by *T. versicolor*.
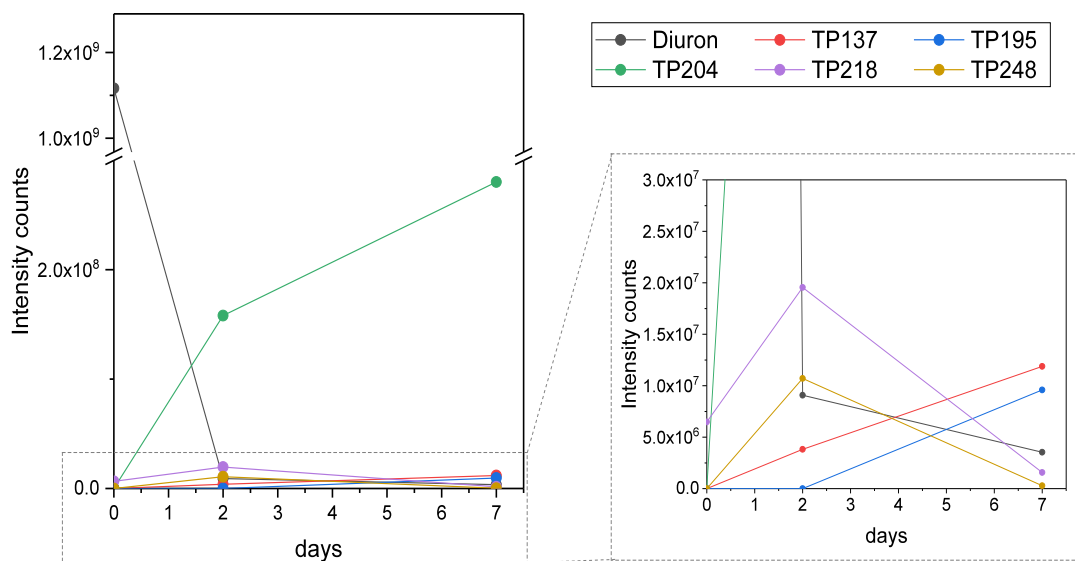
Figure B.2 Evolution of the TPs identified during diuron degradation by *T. versicolor*.
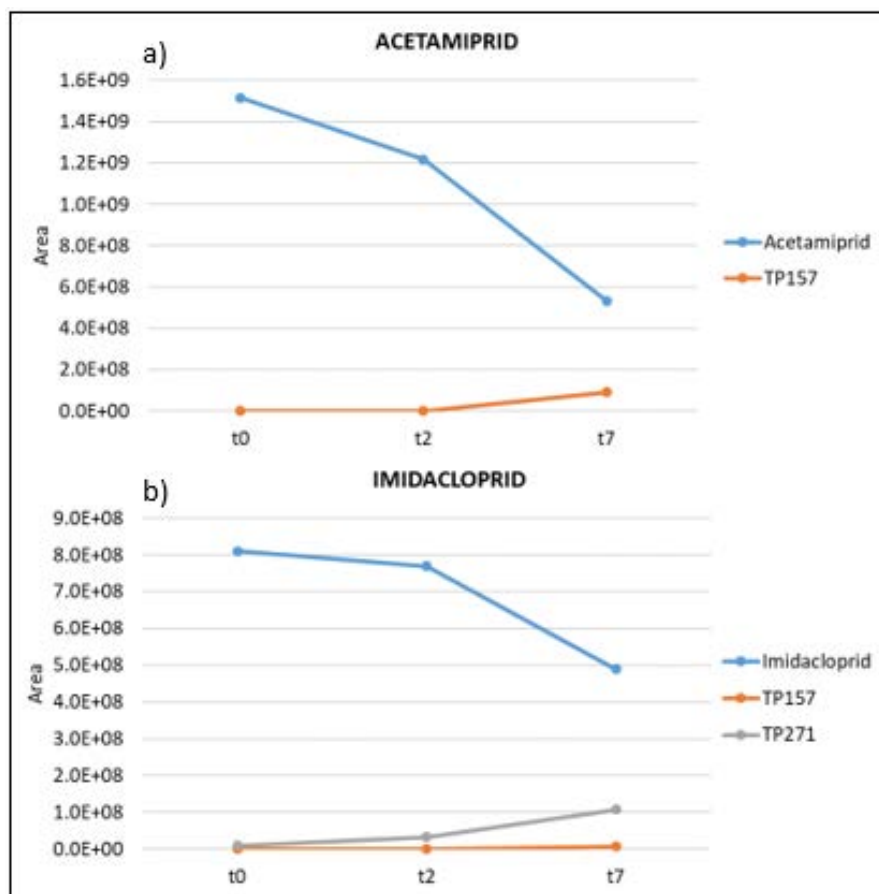
Figure B.3 Evolution of the TPs identified during a) acetamiprid and b) imidacloprid degradation by *T. versicolor*.

Table B.1 Transformation products identified through UPLC-(HESI-)-HRMS/MS during bentazon degradation by *T. versicolor* that lack of logical tentative structure.

Compound	t_R (min)	m/z measured [M − H]⁻	Formula	m/z theoretical [M − H]⁻	Δm (ppm)	RDB
TP438	5.55	437.0781*				
		239.0486	$C_{10}H_{11}N_2O_3S$	239.0496	0.651	6.5
		197.0012	$C_7H_5N_2O_3S$	197.0021	− 0.707	6.5
		175.0862	$C_{10}H11N_2O$	175.0877	− 1.654	6.5
TP344	5.96	343.0748*				
TP372	5.84	371.0913*				
		239.0487	$C_{10}H_{11}N_2O_3S$	239.0496	0.651	6.5
		197.0015	$C_7H_5N_2O_3S$	197.0021	− 0.707	6.5
		175.0863	$C_{10}H11N_2O$	175.0877	− 1.654	6.5
		160.0389				
		116.0489				
TP408	5.83	407.0676*				
		239.0488	$C_{10}H_{11}N_2O_3S$	239.0496	0.651	6.5
		175.0864	$C_{10}H11N_2O$	175.0877	− 1.654	6.5
		132.0312	$C_7H_4N_2O$	132.0329	− 3.895	7.0
TP435	5.85	434.0869*				
		241.0442				
		239.0487	$C_{10}H_{11}N_2O_3S$	239.0496	0.651	6.5
		198.9963				
		175.0866	$C_{10}H11N_2O$	175.0877	− 1.654	6.5
		116.0490				
		61.9867				
TP432	5.85	431.1922*				
		239.0488	$C_{10}H_{11}N_2O_3S$	239.0496	0.651	6.5
		175.0863	$C_{10}H11N_2O$	175.0877	− 1.654	6.5
		132.0312	$C_7H_4N_2O$	132.0329	− 3.895	7.0
		59.0122	$C_2H_3O_2$	59.0133		
TP430	5.92	429.2486*				
		239.0490	$C_{10}H_{11}N_2O_3S$	239.0496	0.651	6.5
		167.0308				
		59.0116	$C_2H_3O_2$	59.0133	− 20.435	1.5
TP220	3.15	219.0070*				
		191.0119				
		163.0168				
		121.9537				
		97.9866				
		77.9637	NO_2S	77.9650	− 8.729	1.5

Table B.3 (cont)

Compound	t_R (min)	m/z measured [M − H]$^-$	Formula	m/z theoretical [M − H]$^-$	Δm (ppm)	RDB
TP388	6.25	387.1225[*]				
		239.0489	$C_{10}H_{11}N_2O_3S$	239.0496	0.651	6.5
		141.0154				
		116.9710				
		59.0116	$C_2H_3O_2$	59.0133	− 20.604	1.5
TP518	5.85	517.1489[*]				
TP192	4.54	191.0119[*]				
		163.0168				
		121.9537				
		59.0121	$C_2H_3O_2$	59.0133	− 10.606	1.5

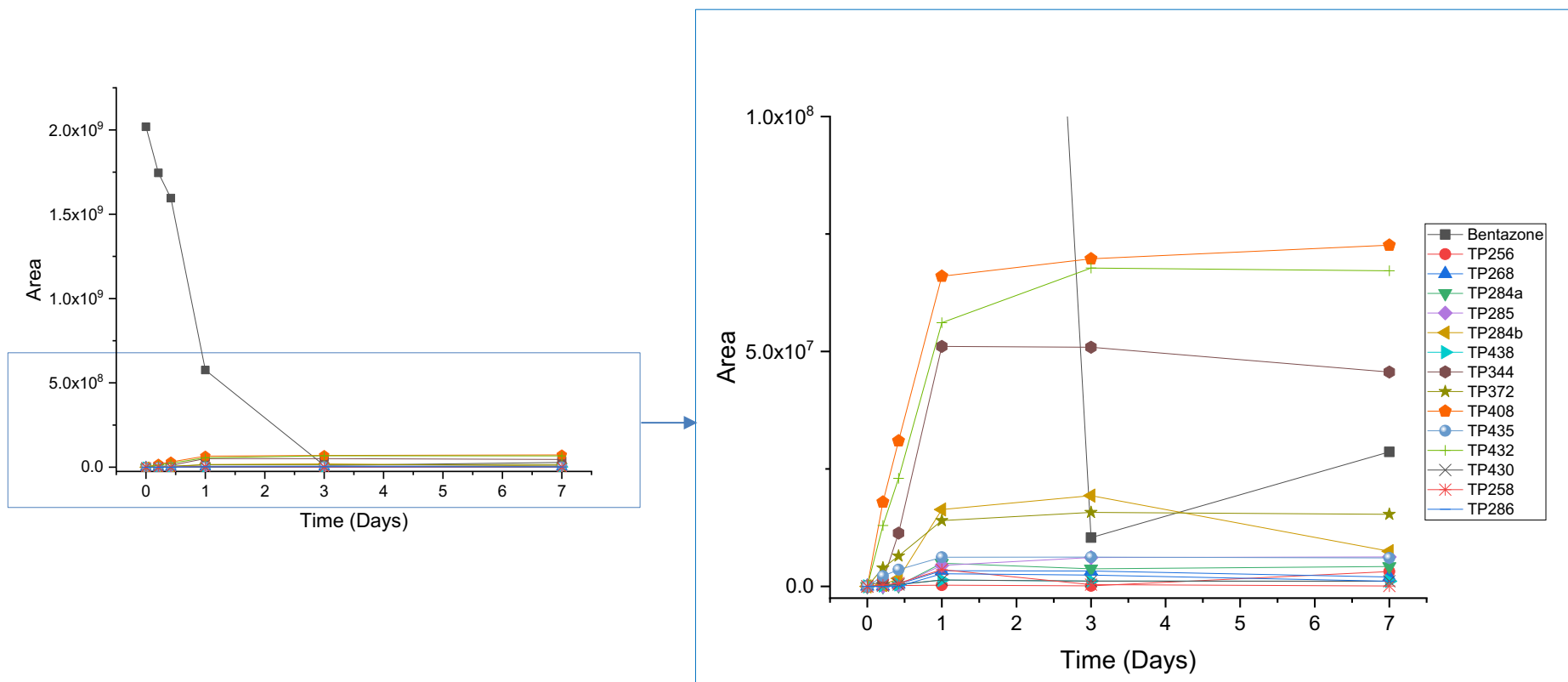Note: [*]corresponds to the precursor ion; Δm, mass measurement error.

Figure B.4 Evolution of the TPs identified during bentazon degradation by *T. versicolor*.

Annex C

Pesticide analysis for the real water

All the analytes were covered using an on-line solid-phase extraction-liquid chromatography-tandem mass spectrometry (on-line SPE-LC-MS/MS) method reported by Barbieri et al. (2020). Water sample was firstly fortified with the mixture of stable isotope-labeled analogs to a final concentration at 200 ng L^{-1} and centrifuged (3, 500 rpm, 10 min) at room temperature. 5 mL of the resultant supernatant was subsequently preconcentrated onto a previously conditioned CHROspe cartridge (divinylbenzene polymer, 10 mm × 2 mm, 25–35 μm) (Axel Semrau GmbH & Co. KG, Germany) using an automated on-line SPE sample processor Prospekt-2 (Spark Holland, The Netherlands) at a flow rate of 1 mL min^{-1}. After sample loading, the cartridge was washed with 1 mL of LC-grade water and the analytes were eluted with the LC mobile phase onto the chromatographic column. LC-MS/MS analysis was performed using a reversed-phase Purospher® STAR RP-18 end-capped column (100 mm × 2 mm, 5 μm) from Merck, a 1525 binary HPLC pump (Waters, Milford, MA, USA), and a TQD triple-quadrupole mass spectrometer (Waters) equipped with an electrospray ionization (ESI) source operated in both positive and negative modes. LC separation was carried out with a linear gradient of acetonitrile and water as mobile phase at a flow rate of 0.2 mL min^{-1}. The gradient started with 10% of acetonitrile that was increased to 50% in 5 min, to 80% in the next 20 min, and 100% in the following 6 min. Then, it dropped back to 10% in the following 9 min to meet equilibrium. Mass acquisition was accomplished in the selected reaction monitoring (SRM) mode. The ESI interface was operated in both positive (PI) and negative (NI) ionization modes. Other specific MS parameters were as follows: capillarity voltage, 3.5 kV; extractor voltage, 3 V; RF lens voltage, 1.8 V; source temperature, 150 °C; desolvation temperature, 450 °C. Nitrogen was used as cone gas (flow, 30 L Hr^{-1}) and desolvation gas (flow, 680 L Hr^{-1}); and argon was used as collision gas (flow, 0.19 mL min^{-1}). MassLynx 4.1 software from Waters was used to perform instrument control, data acquisition, and quantification.

Annex D

D.1 Sample pretreatment for SEM analysis

Samples were firstly fixed in 2.5% glutaraldehyde, which was prepared by 0.1M phosphate buffer (PB), and then washed in 0.1M PB. Afterward, a post-fixation was carried out overnight using vapors of 0.1M PB containing 1% osmium and 0.8% ferrocyanide. Then, they were washed with Mili-Q water and successively dehydrated in 50, 70, 90, 96 and 100% ethanol. Finally, they were further dried using a Bal-tec critical point dryer (CPD 030), followed by coating with AuPd, in order to improve the quality of images.

D.2 Fiber content analysis

Fiber content analysis was performed using Ankom200 Fiber Analyzer incubator (Ankom Technology, USA), during which neutral detergent solution (consists of SDS, disodium EDTA dihydrate, 10-hydrated sodium tetraborate, anhydrous dibasic sodium phosphate and triethylene glycol, pH 6.9–7.1), acid detergent solution (containing cetyltrimethylammonium bromide and sulfuric acid) and sulfuric acid (96%) were introduced successively. Ash was obtained after at least 3.5 h incineration in a muffle at 550 ℃.

The calculation follows the equations as below:

$$\text{Hemicellulose (\%)} = \text{NDF} - \text{ADF} \qquad \text{(D-1)}$$

$$\text{Cellulose (\%)} = \text{ADF} - \text{ADL} \qquad \text{(D-2)}$$

$$\text{Lignin (\%)} = \text{ADL} - \text{Ash} \qquad \text{(D-3)}$$

where NDF represents natural detergent fiber, ADF corresponds acid detergent fiber and ADL means acid detergent lignin.

D.3 Copper quantification

The copper concentration of the agricultural wastewater (AW) was determined through an inductively coupled plasma optical emission spectrometer (ICP-OES, Optima 4300DV, PerkinElmer, USA). Sample was acidified by HNO_3 to its concentration as 1% (v/v) prior to analysis.